UNIVERSITI TEKNOLOGI MARA

SUSTAINABLE DEVELOPMENT OF MORTAR WITH CARBON FIBRE REPAIR USING GRANITE DUST AND NANO-SILICA FOR MECHANICAL PROPERTIES IMPROVEMENT

NUR FATIN AMIRA BINTI MOHAMED YOSRI

MSc

March 2026

UNIVERSITI TEKNOLOGI MARA

SUSTAINABLE DEVELOPMENT OF MORTAR WITH CARBON FIBRE REPAIR USING GRANITE DUST AND NANO-SILICA FOR MECHANICAL PROPERTIES IMPROVEMENT

NUR FATIN AMIRA BINTI MOHAMED YOSRI

Thesis submitted in fulfilment
of the requirements for the degree of
Master of Science
(Mechanical Engineering)

Faculty of Mechanical Engineering

March 2026

CONFIRMATION BY PANEL OF EXAMINERS

I certify that a Panel of Examiners has met on 6th November 2025 to conduct the final examination of Nur Fatin Amira Binti Mohamed Yosri on her Master of Science Thesis entitled "Sustainable Development of Mortar with Carbon Fibre Repair using Granite Dust and Nano-Silica for Mechanical Properties Improvement" in accordance with Universiti Teknologi MARA Act 1976 (Akta 173). The Panel of Examiners recommends that the student be awarded the relevant degree. The Panel of Examiners was as follows:

Nik Normunira Mat Hassan, PhD
Associate Professor
Faculty of Mechanical Engineering
Universiti Teknologi MARA
(Chairman)

Natasha Ahmad Nawawi, PhD
Senior Lecturer
Faculty of Mechanical Engineering
Universiti Teknologi MARA
(Internal Examiner)

Aslina Anjang Ab Rahman, PhD
Senior Lecturer
School of Aerospace Engineering
Universiti Sains Malaysia
(External Examiner)

PROFESSOR DR HJH ZURAEDA IBRAHIM
Dean
Institute of Postgraduates Studies
Universiti Teknologi MARA

Date: 27 March 2026

AUTHOR'S DECLARATION

I declare that the work in this thesis was carried out in accordance with the regulations of Universiti Teknologi MARA. It is original and is the result of my own work, unless otherwise indicated or acknowledged as referenced work. This thesis has not been submitted to any other academic institution or non-academic institution for any degree or qualification.

I hereby, acknowledge that I have been supplied with the Academic Rules and Regulations for Post Graduate, Universiti Teknologi MARA, regulating the conduct of my study and research.

Name of Student	Nur Fatin Amira Binti Mohamed Yosri
Student ID. No.	2022108501
Programme	Master of Science (Mechanical Engineering) - EM750
Faculty	Mechanical Engineering
Thesis Title	Sustainable Development of Mortar with Carbon Fibre Repair using Granite Dust and Nano-Silica for Mechanical Properties Improvement

Signature of Student . . . . . .

Date March 2026

ABSTRACT

The Malaysian economy has experienced consistent annual growth, particularly in the construction sector, due to increasing demand for residential, commercial, and infrastructure developments. This demand has led to a significant rise in the consumption of concrete and mortar, thereby intensifying the use of essential raw materials such as sand and cement. However, the excessive exploitation of these natural resources has raised serious environmental concerns, including sand scarcity and elevated carbon dioxide emissions from cement production. In response to these challenges, this study aims to explore sustainable alternatives by incorporating granite dust (GD) as a partial sand replacement and nano-silica (NS) as a partial cement replacement in mortar mixtures, as well as evaluating the effectiveness of carbon fibre reinforced polymer (CFRP) wrapping for repair applications and mechanical performance improvement. The incorporation of GD offers cost efficiency and environmental benefits by reducing dependence on natural sand, while NS may contribute to strength development through packing and pozzolanic effects. Mortar specimens were prepared with GD and NS replacements ranging from 0% to 30% and 0% to 2.5%, respectively, and tested for compressive strength at 3, 7, and 28 days. Material characterization was conducted through X-ray fluorescence (XRF), particle size analysis using a Zetasizer, moisture content evaluation, and Scanning Electron Microscopy (SEM). The results indicate that the inclusion of GD and NS, both individually and in combination, generally improved the compressive and flexural strength of mortar compared to control specimens. The GD15+NS1 mixture exhibited the highest compressive strength of 52.63 MPa after 28 days of curing, which may be associated with densification and improved packing. It was found that a mortar mixture that contains 15wt.% granite dust and 1wt.% nano-silica (GD15+NS1) exhibited the highest compressive strength of 52.63 MPa at 28 days curing. Further investigation involving modified mortar patching and CFRP wrapping on cracked specimens demonstrated not only recovery of structural performance but also enhancements surpassing those of uncracked specimens. The results showed that the cracked specimen repaired with modified mortar patching and CFRP wrapping has flexural strength of 13.42 MPa when compared to the strength of undamaged mortar specimen of 3.20 MPa. These findings suggest that the combination of GD, NS and CFRP reinforcement offers potential for enhancing mortar properties and may present a potential approach for both new construction and rehabilitation projects, aligning with current efforts toward resource conservation and improved structural durability.

ACKNOWLEDGEMENT

All gratitude is directed towards Allah, and I acknowledge His blessings for successfully completing this extensive and demanding journey. I express my thanks to God for providing the opportunities, trials, and strength necessary to fulfil this research. Throughout this journey, I have gained valuable experiences. I extend my utmost gratitude to the revered Prophet Muhammad (Peace be upon him) whose exemplary life has consistently guided me.

My gratitude and thanks go to my supervisor, Prof Dr Aidah Jumahat and my co supervisor, Dr Muhd Norhasri Muhd Sidek. Thank you for the support, patience and ideas throughout the study, which has led to the smooth finishing of this study. I also would like to thank the staff of Makmal Konkrit (En. Muhammad Faiz Ahmad Zait and En. Muhammad Hazli Shariei), Institute for Infrastructure Engineering and Sustainable Material (IIESM) (Puan Nurliza Jasmi and En. Aliff), Makmal Sains Bahan (En. Mohd Rahimi Mohd Salleh) Makmal Penyelidikan BioRec (Cik Zalina), Makmal Pusat NanoElektrik (En. Asrul Mohamed and En. Muhamad Norsam Hashim).

My appreciation goes to my colleagues, Dr Mohd Afiq Mohd Fauzi, Dr Nuradilla Izzaty Halim and Dr Aidan Newman for helping me with this project.

Finally, this thesis is devoted to Ahmad Hafizuddin Luqman Anuar and my beloved family, Mohamed Yosri Ahmad, Hasniza Hassan, Nur Syafiqa Hanum and Nur Wafin Wardah the constant wellspring of inspiration and fortitude that has guided my education. This piece of victory is dedicated to all of you. Alhamdulillah.

TABLE OF CONTENTS

LIST OF TABLES

LIST OF FIGURES

LIST OF PLATES

LIST OF SYMBOLS

Symbols

%	Percentage
℃	Degree Celsius
cm	Centimetre
d	Particle diameter
g	Gram
K	Stress Intensity F
kN	Kilonewton
MPa	Kilopascal
mm	Millimetre
MPa	Megapascal
nm	Nanometre
µm	Micrometre
Gf	Fracture Energy
w/c	Water-to-cement
a/W	Notch depth-to-w

LIST OF ABBREVIATIONS

Abbreviations

3D	Three-Dimensional
AI2O3	Aluminium Oxide
Al(OH>	Aluminium Hydroxide
ASTM	American Society for Testing and Materials
BAGD	Bottom Ash Granite Dust
BSE-COMP	Backscattered Electron Composition
CAH	Calcium Aluminate Hydrate
CaO	Calcium Oxide
Ca(OH>	Calcium Hydroxide
CA(SH)	Calcium Alumino-Silicate Hydrate
CFRP	Carbon Fibre Reinforced Polymer
CO2	Carbon Dioxide
CSH	Calcium Silicate Hydrate
Cp	Control Mortar Patch
Cs	Control Mortar Bar
DFGD	Dry Fly Granite Dust
ECC	Engineered Cementitious Composites
EDX	Energy Dispersive X-ray Spectroscopy
FA	Fly Ash

$_2 0_3$	Ferric Oxide
FRP	Fibre Reinforced Polymer
GD	Granite Dust
GDNS	Granite Dust + Nano-Silica mix
GDNSs	Granite Dust filled Nano-silica Mortar Specimen
GDNSp	Modified Mortar Patch
GFRP	Glass Fibre Reinforced Polymer
ros	Industrialised Building System
ITZ	Interfacial Transition Zone
K	Potassium Aluminium Phosphate
K2O	Potassium Oxide
LC	Limestone-Cement
LGS	Larger Ground Sand Particles
LOI	Loss on Ignition
MgO	Magnesium Oxide
MGS	Medium Ground Sand Particles
$Na_2 0$	Sodium Oxide
NS	Nano-Silica
OPC	Ordinary Portland Cement
POFA	Palm Oil Fuel Ash
PSD	Particle Size Distribution
Q	Quartz

	Rice Husk Ash
RSM	Response Surface Methodology
S	Amorphous Silica
SCM	Supplementary Cementitious Materials
SDGs	Sustainable Development Goals
SEM	Scanning Electron Microscope
SiC-2	Silica Oxide
SO3	Sulfur Trioxide
UCS	Unconfined Compressive Strength
UTM	Universal Testing Machine
XRD	X-ray Diffraction
XRF	X-ray Fluorescence

LIST OF NOMENCLATURES

Nomenclatures

di	Lateral Dimensions of the Specimen (mm)
d2	Lateral Dimensions of the Specimen (mm)
Wi	Weight of the Empty Container (g)
W2	Weight of Container + Wet Specimen (g)
W3	Weight of Container + Dried Specimen (g)
p	Density of mortar (kg/m^3)
r	Flowability / Workability ((%)
L	Specimen length (mm)
h	Specimen height (mm)
P	Maximum load applied (kN)
TT	Logarithmic measure of hydrogen ion concentration, indicating acidity or alkalinity

CHAPTER 1
INTRODUCTION

1.1 Research Background

As the global community moves toward achieving net-zero carbon emissions by 2050, the construction industry faces increasing pressure to adopt more sustainable practices in both new construction and structural repair (Amran et al., 2021). Concrete and mortar, among the most widely used building materials, consume large quantities of natural resources such as cement and river sand, both of which contribute significantly to environmental degradation and carbon emissions. Cement manufacturing alone contributes approximately 8% of global CO_2 emissions due to the calcination of limestone and high-temperature furnace processes (Andrew, 2018). Similarly, uncontrolled river sand extraction has caused riverbank erosion, habitat destruction, reduced water quality, and increased flood risks, underscoring the urgent need for alternative fine aggregates (Ashraf et al., 2011; Pitchaiah, 2017).

Parallel to resource-based concerns, sustainability also demands attention toward the repair and rehabilitation of existing structures. Extending service life through effective repair minimizes demolition waste, reduces embodied carbon, and conserves materials (Nouri et al., 2025). Many structures experience deterioration from mechanical loading, environmental exposure, material degradation, or construction defects, making timely repair essential to maintain safety and durability. Common repair techniques include surface patching for minor cracks, resin injection for deeper fissures, and crack-filling for larger defects. Selection of an appropriate repair method depends on crack origin, structural function, and environmental conditions (Czarnecki et al., 2020). These practices highlight the need for repair materials that exhibit strong bonding performance, rapid strength gain, and long-term durability.

To address resource scarcity and environmental impacts, researchers have explored incorporating industrial by-products and advanced materials into mortar formulations. Granite dust (GD), a waste product from quarrying and stone-cutting operations, provides a promising partial sand replacement due to its fine particle size, micro-filling capacity, and potential pozzolanic activity (Wan Ahmad et al., 2020; Rahim et al., 2021). Utilizing GD helps reduce landfill disposal and decreases reliance

on natural sand. Likewise, nano-silica (NS) has gained significant attention as a highly reactive supplementary cementitious material. Its ultrafine particle size and large surface area improve hydration, refine the microstructure, and enhance the mechanical performance of mortar by producing additional calcium silicate hydrate (C-S-H) gel (Ghosal & Chakrabarti, 2022).

Beyond material substitution, modern repair technologies increasingly incorporate advanced composite materials. Carbon Fibre Reinforced Polymer (CFRP) has emerged as a high-performance strengthening system due to its exceptional tensile strength, corrosion resistance, and lightweight characteristics (Rajak et al., 2019). Its use in repair applications improves structural capacity, enhances crack resistance, and delays further deterioration, thereby extending the service life of repaired elements.

The integration of GD and NS in mortar, combined with CFRP wrapping for structural rehabilitation, aligns with global sustainability goals by reducing carbon emissions, conserving natural resources, and improving the performance of both new and repaired structures. This research contributes to this effort by evaluating sustainable GDNS mortar mixtures and assessing CFRP wrapping as an enhancement method for pre-cracked mortar elements.

1.2 Problem Statement

The sustainability of concrete structures throughout their construction and service lifespans has become a pressing concern in the global effort to reduce environmental impacts (Nouri et al., 2025). Cement concrete, the most widely used construction material in civil engineering, is extensively applied in infrastructure such as roads, bridges, tunnels, and ports. However, concrete structures are inherently susceptible to various forms of deterioration, including cracking and spalling, due to mechanical loading and environmental exposure. In addition, poor selection of raw materials, improper mix designs, and substandard construction practices can exacerbate these issues particularly in the concrete cover protecting reinforcement bars leading to diminished structural integrity and durability (Xuemin Song, 2022).

To address these challenges, timely and effective repair strategies are essential to restore both the functionality and safety of concrete structures and to extend their service life. Concrete repair and rehabilitation practices aim to correct defects, recover mechanical properties such as stiffness and strength, and ensure long-term durability

(Haroon & Bakar, 2021). In recent years, innovations in repair mortars and protective coatings with lower environmental impacts than conventional materials have emerged. For example, cementitious repair mortars are commonly used for crack patching; however, their production relies heavily on large quantities of cement and sand, contributing significantly to global sustainability concerns (Huseien et al., 2017; Xuemin Song, 2022).

The environmental impact of mortar production stems primarily from the overexploitation of natural resources. Sand, a primary component in mortar, is in critical demand. Excessive sand mining has been linked to severe environmental issues, including soil erosion, loss of biodiversity, and contamination of water bodies (Pitchaiah, 2017). In 2023, Malaysia's mining and quarrying sector contributed approximately RM 20 billion (around USD 4.5 billion) to the national GDP, while construction activities drove an annual demand of over 40 million cubic meters of sand (Ali et al., 2025). Yet, sand's role as a filler is often inefficient due to the potential for air voids within the mortar. Alternatively, granite dust (GD) a by-product of stone crushing offers promising potential as a sustainable partial substitute for sand. Studies have shown that GD contributes to enhanced durability and strength due to its micro-filling capacity and pozzolanic activity (Wan et al., 2021; N. Z. Rahim et al., 2021). Nevertheless, current mortar production still relies predominantly on natural sand, and the potential of quarry by-products such as granite dust remains insufficiently utilised in practice.

Cement, another major constituent of mortar, is the most widely used material globally after water. Its production is highly carbon-intensive and environmentally detrimental. The urgent need to decarbonize the construction industry has prompted researchers to seek alternative materials. Supplementary Cementitious Materials (SCMs) such as nano-silica (NS) offer a promising solution. Due to their high surface area and pozzolanic reactivity, nano-silica particles significantly enhance mortar properties such as strength, durability, and microstructure while reducing reliance on cement (Aggarwal et al., 2015; Ghosal & Chakrabarti, 2022). These advancements are crucial in reducing CO_2 emissions and aligning the industry with net-zero carbon targets (Amran et al., 2021). However, most existing studies have examined either GD or NS individually, and limited work has investigated their combined use within a single sustainable mortar system.

Beyond material substitution, modern rehabilitation techniques increasingly incorporate advanced composite materials. Fibre Reinforced Polymer (FRP) composites, particularly those reinforced with synthetic fibres have been widely adopted for strengthening concrete, steel, and composite structures due to their high tensile strength, corrosion resistance, and long-term durability (Rajak et al., 2019; Ortiz et al., 2023). While natural fibres such as coir and bamboo provide sustainable alternatives, they often exhibit variability in performance and durability limitations. Synthetic FRP systems, on the other hand, offer consistent material properties, lightweight installation, and superior strengthening performance. Although FRP systems are increasingly applied for strengthening, their integration with sustainable mortar alternatives has received limited scientific attention, particularly in relation to repair of damaged cementitious elements.

Given that structural damage in concrete elements is inevitable due to environmental degradation, weather events, impact loads, and aging (Scrivener et al. 2018), selecting an effective repair strategy is crucial. A repair system is considered successful when it restores functionality or slows the rate of deterioration (Czarnecki et al., 2020). Long-term structural reliability often depends on regular maintenance and repair, underscoring the need for durable, high-performance repair materials. However, despite the growing interest in sustainable mortars using GD and NS, limited studies have evaluated their combined performance in cracked mortar systems, particularly when subjected to repair and strengthening. In addition, the potential role of CFRP in enhancing the performance of modified sustainable mortars remains relatively underexplored in current research, creating a gap in knowledge regarding its suitability for repair of damaged cementitious elements.

In summary, current concrete repair practices are constrained by heavy dependence on non-renewable resources, rising environmental impacts, and the need for more durable repair solutions. Incorporating waste-based and high-performance materials presents a promising path forward. Therefore, this research investigates the use of granite dust and nano-silica as sustainable components in mortar production and evaluates the effectiveness of Carbon Fibre Reinforced Polymer (CFRP) wrapping in enhancing the structural performance of repaired mortar elements, contributing to broader goals of sustainability, durability, and carbon reduction in the construction industry.

1.3 Research Objectives

The main purpose of this research is to examine the impacts of using Granite Dust as a partial sand replacement and Nano-Silica as a partial cement replacement in the mortar and the mechanical properties effect of the Carbon Fibre patching on the modified mortar.

a) To evaluate the effect of granite dust and nano-silica content on the physical properties of mortar.
b) To determine the mechanical properties of various mixes for Granite Dust and nano-silica in mortar.
c) To assess the effect of carbon fibre wrapping on mechanical properties of nano-silica-filled granite dust mortar.

1.4 Research Question

i) How viable is the use of GD to be partially utilized as the sand replacement and Nano-silica as cement replacement to produce new development of modified mortar.
ii) What is the maximum strength of weight percentage of GD (sand replacement) and Nano-silica (cement replacement) that can influence the performance of mortars?
iii) How effective is carbon fibre patching on mechanical properties of the maximum strength of weight percentage of GD (sand replacement) and Nano-silica (cement replacement).

1.5 Significance of Study

This research contributes to the advancement of sustainable construction practices by promoting the partial replacement of natural resources namely sand and cement with environmentally friendly alternatives such as granite dust (GD) and nano-silica (NS). The overconsumption of sand and cement has led to significant ecological and economic concerns, including resource depletion, environmental degradation, and high carbon emissions. By utilizing GD, a widely available industrial by-product, and NS, a high-performance supplementary cementitious material, this study introduces a viable solution to mitigate the environmental footprint of the construction industry.

The integration of GD and NS in mortar mixes not only reduces the dependency on non-renewable resources but also supports effective waste management by diverting granite waste from landfills. This dual benefit aligns with national sustainability goals and offers a low-cost, eco-efficient alternative for conventional mortar production. Moreover, this study demonstrates the potential application of these modified mortars in infrastructure works, including road bases, drainage systems, and patch repairs, especially in lightweight or secondary structures.

Additionally, by incorporating CFRP (Carbon Fibre Reinforced Polymer) wrapping in the repair of damaged mortar specimens, this research presents a complete approach to structural rehabilitation. The enhancement of flexural strength and durability through CFRP wrapping showcases its effectiveness in extending the service life of repaired elements, minimizing the need for full structural replacement. Collectively, the outcomes of this study provide valuable insights for the development of sustainable repair materials and techniques, fostering long-term resilience, environmental responsibility, and economic efficiency in the Malaysian construction sector and beyond.

1.6 Scope of Study

This study investigates the potential of granite dust (GD), nano-silica (NS), and carbon fibre-reinforced polymer (CFRP) wrapping in enhancing the engineering properties of mortar, with a focus on both microstructural behaviour and mechanical performance. The research begins by analysing the physical and chemical characteristics of the materials used granite dust, nano-silica, cement, and sand through Particle Size Analysis (PSA), Moisture Content, X-Ray Fluorescence (XRF) and Scanning Electron Microscopy (SEM). These tests provide a foundational understanding of the morphology, particle distribution, elemental composition, and clear phases that influence the interaction of GD and NS within the mortar matrix, within the specific experimental conditions adopted in this study.

Twelve mortar mixes were prepared for this study. Six of these mixes involved partial sand replacement with granite dust at 5%, 10%, 15%, 20%, 25%, and 30%, while five mixes incorporated nano-silica as a partial cement replacement at 0.5%, 1.0%, 1.5%, 2.0%, and 2.5%. A control mix without any GD or NS known as Control Mortar (CM) was also included for baseline comparison. Mortar cubes (50 × 50 × 50 mm) were

cast and cured in water for 3, 7 and 28 days to evaluate compressive strength. In addition, mortar bars (160 × 40 × 40 mm) were cast and cured for 28 days for flexural strength testing. These mechanical tests were conducted to determine the maximum weight percentage of GD and NS that would yield the highest strength performance, within the replacement ranges specified.

After identifying the mixes with the maximum strength of weight percentage from both the GD and NS series, a new combination mix was developed by integrating both materials at their respective maximum strength of weight percentages. This maximum strength of weight percentage of GDNS modified mortar was then compared against the control mix by testing its flexural strength using standard-sized mortar bars. The final phase of the research involved assessing the role of CFRP wrapping in strengthening and rehabilitating mortar specimens. Pre cracked mortar bars were repaired using the control mix and the maximum strength of weight percentage of GDNS modified mortar and then externally wrapped with CFRP. Flexural testing was performed on six types of specimens, which demonstrated significant improvement in strength and crack resistances increasing the overall effectiveness of mortar repair and rehabilitation.

This study is limited to cementitious mortars incorporating GD and NS within the stated replacement ranges, laboratory curing conditions, and mechanical evaluation up to 28 days. Long-term exposure, large-scale structural behaviour and different CFRP configurations are beyond the scope of this research and are recommended for future research.

CHAPTER 2
LITERATURE REVIEW

2.1 Introduction

Numerous studies have been conducted to investigate the factors that influence the strength and performance of mortar and concrete specimens. A common approach among researchers involves the incorporation of waste materials as partial replacements for sand or cement within the mix. This strategy aims to reduce the reliance on natural resources while simultaneously addressing environmental concerns related to waste management and pollution. Concrete, as a widely used construction material, significantly contributes to global carbon dioxide (CO2) emissions, thereby playing a notable role in climate change. By substituting conventional materials such as sand and cement with sustainable alternatives, it is possible to mitigate environmental degradation and conserve finite resources. In this study, Granite Dust (GD), a byproduct of industrial processes, and Nano-Silica (NS), a high-reactivity pozzolanic material, are utilized as partial replacements for sand and cement in mortar mixtures. The study further evaluates the impact of these materials on the mechanical properties and overall effectiveness of the resulting mortar.

2.2 Mortar

Mortar is one of the most fundamental and historically significant materials used in masonry construction. It serves as a bonding agent between masonry units such as bricks, blocks, and stones, providing both structural cohesion and load transfer within the wall system. Mortar is primarily composed of cement (commonly Ordinary Portland Cement or OPC) as a binder, fine aggregates such as sand, and water. This mixture creates a workable paste that hardens over time, binding the construction units together. Portland cement mortar, also known as cement mortar, is the most widely used type in the building industry due to its availability and reasonable strength (Neville, 2011). Historically, lime-based mortars dominated until the development of OPC, which significantly improved the setting time and early strength.

Mortar consists of cement, sand and water are the main ingredients in mortar, an anisotropic composite material which is one of the construction elements of construction (Mollo et al., 2015). The type of mortar can be classified based on strength that is necessary for application, and the selection must be made among the specified proportions or the properties listed on ASTM C270. There are five types or mortar that had been specified based on ASTM C270 which are types M, N, O, S, and K. Table 2.1 indicates the types of mortar that are suitable for use based on location, technical requirements, and building area.

Table 2.1
Type of Mortar Depending on the Location & Building Segment

Location	**Building segment**	**Mortar**	
		Recommended	**Alternative**
Exterior, above grade	Load-bearing wall	N	S or M
	Non-load-bearing wall	O	N or S
	Parapet wall	N	S
Exterior, at or below grade	Foundation wall, retaining wall, manholes, sewers, pavements, walks and patios	S	M or N
Interior	Load-bearing wall	N	S or M
	Non-bearing partitions	O	N

According to table 2.2, the property specification of the mortar based on ASTM C270 was illustrated.

Table 2.2
Property Specification of Mortar

Mortar Type	**Average Compressive Strength at 28 Days (MPa)**	**Water Retention (min %)**	**Air Content (max %)**
M	17.2	75	12
S	12.4	75	12
N	5.2	75	14
O	2.4	75	14
K	0.7	75	14

Type M mortar is the strongest type of mortar. This application is ideal for below-grade applications and is suggested for heavy loads. It also has a compressive strength of 17.2 MPa, leading to perfect foundations, retaining walls, and roads. A type S mortar has a total strength of 10 MPa and is suitable for use at or below grade. The high-tensile bond strength of Type S allows it to function effectively against soil pressure and wind, and it is suitable for masonry foundations, manholes, and other applications. Type N mortar can be used and recommended for external and above-grade applications that are subjected to extreme heat and weather. The 5.2 MPa compressive strength is sufficient for everyday use. The type O mortar has a low compressive strength of 2.4MPa and is only suited for use in above-grade and non-load-bearing walls. This type of mortar is an alternative to type N, although it has limitations due to its low structural capability. Finally, type K mortar has the lowest compressive strength and can be utilised to rehabilitate outdated or historical buildings and masonry.

However, conventional mortar exhibits several mechanical limitations, especially in applications where higher compressive strength, durability, and resistance to environmental exposure are required. Mortar generally has a lower strength than concrete due to its lack of coarse aggregates and less dense internal structure. These limitations make it less suitable for structural elements subjected to high loads or severe weather conditions. Problems such as shrinkage cracks, reduced adhesion, water ingress, efflorescence, and long-term degradation are common in traditional mortar applications (Jahandari et al., 2023). Weak mortar joints can compromise the integrity of masonry walls, potentially causing delamination, moisture damage, and even partial structural failure under load or seismic events.

The usage of mortar in infrastructure may be seen in the drainage and curb system, which have a limited capacity and are of inferior strength. It is also visible through the Industrialised Building System (IBS). In modern construction practices, especially in systems like the Industrialised Building System (IBS), mortar plays a vital role not only in bonding masonry units but also as a filler in lightweight prefabricated components. Because it lacks coarse aggregates, mortar is lighter than concrete, making it suitable for use in wall panels, drains, pavements, and curb bedding systems. Despite this, the mechanical performance of traditional mortar remains inadequate for certain structural or high-performance applications, leading to the need for enhanced formulations.

To address these limitations, researchers have turned to modified mortars using additive, substitution, and replacement strategies. These approaches aim to enhance mechanical strength, durability, shrinkage control, and sustainability. Modifying mortar can involve the addition of chemical admixtures, pozzolanic materials, recycled waste, and nanomaterials. For example, pozzolanic materials such as fly ash, silica fume, nano-silica, and ground granulated blast furnace slag (GGBS) have been shown to improve the density and microstructure of mortar, contributing to higher strength and lower permeability (Khan et al., 2020). Industrial and agricultural wastes such as granite dust are increasingly used as partial replacements for fine aggregates, offering both performance enhancement and environmental benefits (Mhamal & Savoikar, 2023).

2.3 Constituent Materials in Mortar

2.3.1 Sand

Sand is one of the natural resources known as non-renewable resources that are widely used in the production of concrete or mortar. Thus, the usage of sand is very important in construction as it is used to build up buildings and infrastructures. According to Wan Ahmad et al. (2020), the data reported by the Unit of Minerals & Geosciences of Malaysia which is a sand mining operation has risen from 24,471 (2008) to 34,341 (2015) million tonnes in Malaysia. Hence, the high demand for sand consumption has resulted in the depletion of one of the natural resources. Sand mining operations can lead towards environmental problems (Ashraf et al., 2011). According to Tamanna et al. (2020), when higher extraction of sand occurred, it will not only result in depletion of sand but also damages the ecosystem of the marines, water and turbidity that resulted from the erosion of shoreline and riverbanks.

Finely split rock and mineral particles that make up and have a variety of compositions. The composition of the sand normally depends on the local rock sources and conditions. Sand can be categorized according to the grain size which is the grain of the sand is smaller than the rock fragments named gravel but coarser than silt. The diameter of the sand can be classified between 0.074 and 4.75 mm which contributes as a good filler in the concrete and mortar. In the production of concrete and mortar, not all types of sand are suitable for production. The physical characteristics and chemical characteristics of sand are shown in Tables 2.3 and 2.4 respectively.

Table 2.3
Chemical properties of Ground River Sand Adopted from (Akmal Zharif et al., 2021)

Chemical Composition (%)	Ground River Sand	Test Method
$Si0_2$	80.78	IS 4032-1968
AI2O3	10.52	
$Fe_2$03	1.75	
CaO	3.21	
MgO	0.77	
LOI	0.37	

Table 2.4
Physical properties of Ground River Sand Adopted from (Akmal Zharif et al., 2021)

Property	Ground River Sand	Test method
Specific gravity	2.60	IS2386(PartIII)-1963
Bulk Density (kg/m)	1460	
Absorption (%)	Nil	
Moisture Content (%)	15Q	
Fine particles less than 0.075mm (%)	6	
Sieve analysis	Zone-II	IS 383- 1970

High demand in building construction as the growing population has led to the rise of the usage of natural materials which is sand. Sand is the main ingredient for producing concrete as well as mortar. The elevation of sand usage that exceeds the production will lead to problems with the environment such as changing the river, and an increase in sediment that will cause the turbidity of water to be higher and cause erosion. Reducing the number of natural resources that humans use is one strategy to improve sustainability.

2.3.2 Cement

Cement, known as a binder due to its ability to bind with other materials, is an important material in the construction industry. Both mortar and concrete require cement to produce the mixture to build many structures. Based on their capacity to harden in the presence of water, construction cement may be divided into hydraulic and non-hydraulic categories. The difference between these two types is for hydraulic cement, it will set, and it will become hardened when reacting with water while non-hydraulic cement, it will not set under water. The most typical type of hydraulic cement is Portland cement which will be used in this study.

With an annual cement utilization of roughly 3.3 billion tonnes, cement can be categorized as the most extensively used paste material in concrete constructions (Amran et al., 2021). Moreover, Amran et al. (2021) stated that Ordinary Portland cement (OPC) output is growing by 9% per year, which raises serious environmental concerns since it produces a lot of CO2.

Cement consists of many ingredients such as limestone, shells, and other materials. Cement is a finely powdered mixture of calcium silicate, aluminates, and a small amount of gypsum that during mixing with water, it hardens into a hard stone-like mass. The most prevalent form of cement used in the building sector is OPC, sometimes referred to as form 1 cement. As a result, the proper ratio of components must be employed to manufacture cement that is acceptable for use. The chemical makeup of cement is shown below according to Table 2.5

Table 2.5
Chemical properties of Portland Cement Adopted from (Akmal Zharif et al., 2021)

Chemical Composition (%)	**Portland Cement**
Silicon Oxide ($Si0_2$)	22.4
Aluminium Oxide (AI2O3)	5.20
Ferric Oxide (FesOs)	3.80
Calcium Oxide (CaO)	61.6
Magnesium Oxide (MgO)	1.70
Loss on Ignition (LOI)	2.30

Cement is one of the essential materials in the industry sector to produce concrete and mortar. Cement is indispensable in concrete and mortar, as it acts as the binder that holds the mixture together. In this developing country, concrete and mortar production is very high and causing cement production to become high. Based on this, environmental pollution will become high due to carbon emissions, and this can be supported by Dunuweera & Rajapakse (2018) that mentioned that cement production is linked to large-scale emissions of greenhouse gases and pollutants into the environment. According to Gagg (2014), for a normal house building, 14 tonnes of cement will be needed, but 2,500 tonnes of cement will be needed to build a kilometre of roadway. Cement will make up 10 to 15% of the concrete mix by volume.

2.4 Modified Mortar Incorporating SCMs and Replacement Materials

In recent years, extensive research has been conducted on modifying traditional mortar compositions using additives, partial substitutions, or complete replacements of conventional materials to improve performance, durability, and sustainability. These modifications aim to enhance mechanical strength, reduce environmental impact, and address the limitations associated with conventional mortar ingredients such as cement and natural fine aggregates. Commonly studied materials include fly ash, silica fume, nano-silica, waste glass powder, rice husk ash, and various types of industrial by-products. For example, nano-silica (NS) has gained attention due to its high pozzolanic reactivity and particle fineness, which contributes to improved compressive strength, reduced porosity, and denser microstructure in mortar (Mydin et al., 2024). Similarly, granite dust (GD), an industrial by-product, has been investigated as a sand replacement to reduce resource depletion and enhance the mortar's mechanical and durability properties (Singh & Verma, 2016).

2.4.1 Pozzolanic Reaction Mechanisms in Supplementary Cementitious Materials

Pozzolanic reactions play a critical role in enhancing the mechanical and durability performance of mortar incorporating supplementary cementitious materials. A pozzolanic material reacts with calcium hydroxide (CH), a by-product of cement hydration, to form additional calcium silicate hydrate (C-S-H) gel, the primary strength-contributing compound in cementitious systems. This secondary C-S-H formation not only increases strength but also refines pore structure, reduces permeability, and enhances long-term durability (Thomas, 2013).

In the context of this study, nano-silica (NS) exhibits extremely high pozzolanic reactivity due to its ultrafine particle size and large specific surface area. NS reacts rapidly with CH, accelerating early hydration, increasing particle packing, and reducing porosity (Ghosal & Chakrabarti, 2022). Meanwhile, granite dust (GD) although less reactive than NS, contributes through micro-filling effects and, depending on its silica composition, may also participate in slow pozzolanic reactions at later ages (Sapiai et al., 2021).

2.4.2 Fly Ash (FA)

Fly ash is one of the most extensively utilized supplementary cementitious materials (SCMs) in concrete manufacturing, primarily due to its cost-effectiveness, consistent availability, and ability to enhance both the fresh and hardened properties of cementitious composites. It is a finely divided by-product resulting from the combustion of pulverized coal in thermal power plants. During combustion, inorganic mineral constituents within the coal undergo fusion and subsequently solidify into spherical glassy particles upon rapid cooling within the flue gas stream. These fine particulates are subsequently extracted from the exhaust gases through high-efficiency particulate collection systems, such as electrostatic precipitators or fabric filters (Chiang & Pan, 2017).

Improper disposal of fly ash poses serious environmental challenges, such as air and water pollution, as well as land degradation. However, incorporating fly ash into structural and pavement concrete mixes has emerged as an effective strategy to enhance

resource efficiency and reduce waste accumulation. A substantial body of research has explored the use of fly ash as a partial replacement for cement in both cement paste and concrete systems (Karim et al., 2025; Padavala et al., 2024; Moghaddam et al., 2019). Initially, fly ash was primarily applied in mass concrete projects, including dam construction, where it was valued for its cost efficiency and ability to reduce the heat of hydration (Nath et al., 2017). §ahin & Eker, (2024) emphasized the beneficial role of fly ash in improving the chemical resistance of concrete, particularly its durability against sulphate attack and alkali-silica reaction (ASR), through its pozzolanic reaction with calcium hydroxide which generates additional cementitious compounds, thereby enhancing strength development (Hefni et al., 2018).

Nayak et al., (2022) reported that for every 10% replacement of cement with fly ash, water demand could be reduced by approximately 2% to 3%. When used alongside other supplementary materials such as slag, calcined clay, and calcined shale, fly ash improves the workability of concrete without compromising slump performance. Combined with Portland cement, it contributes to enhanced mechanical strength and durability. Additionally, the use of fly ash as a supplementary cementitious material (SCM) offers economic advantages and modifies specific properties of both fresh and hardened concrete in a favourable manner (Li et al., 2022).

According to ASTM C618 specifications, fly ash qualifies as a Class F material based on its chemical composition. Table 2.6 presents the oxide composition, where the total content of reactive oxides SiCh, AI2O3, and Fe203 exceeds 70%, satisfying the pozzolanic criteria. Fly ash particles are predominantly spherical and exhibit a finer grain size compared to Portland cement and lime, typically ranging from below 1 um up to 150 um (Hardjito & Rangan, 2005). Sahin & Eker, (2024) noted that the spherical morphology of these particles facilitates improved flow characteristics during mixing and placing, acting as microscopic ball bearings that enhance workability. Plate 2.1 illustrates the scanning electron microscopy (SEM) image depicting the typical morphology of fly ash particles.

Table 2.6
Chemical Composition of Fly Ash (Balakrishnan et al., 2017)

CHEMICAL COMPOSITION	(%)
Silicon Oxide (SiOi)	49.97
Aluminium Oxide (AI2O3)	28.36
Ferric Oxide (FesOs)	7.04
Calcium Oxide (CaO)	5.17
Magnesium Oxide (MgO)	2.07
Sulphur Oxide (SO3)	0.46
Sodium Oxide (NaiO)	2.11
Potassium Oxide (K2O)	1.50
Loss on Ignition (LOI)	0.59

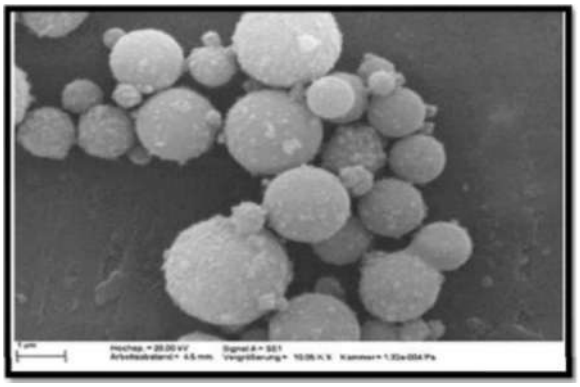

Plate 2.1 SEM of Fly Ash particles (Balakrishnan et al., 2017)

Extensive research has been carried out to evaluate the compressive strength performance of concrete incorporating fly ash as a partial cement replacement (Fantu et al., 2021). Gao et al., (2025) reported that substituting at least 50% of cement with fly ash as a supplementary cementitious material (SCM) leads to reductions in both cement and water content, resulting in a lower water-to-binder ratio (w/b). Despite these benefits, several challenges have limited the practical adoption of high-volume fly ash concrete. These include variability in fly ash quality and composition, delayed strength gains and stiffness development, extended setting times, and complications in construction practices (Gao et al., 2025). However, recent advancements in mix design and material optimization have facilitated cement replacement levels of up to 80% by mass in high-volume fly ash concrete systems. Strategies to address the limitations

include the selection of high-quality fly ash (Du et al., 2021), incorporation of finely ground limestone powder to accelerate early strength gain and control setting behavior (Mohammed & Al-Numan, 2024), and the application of internal curing techniques to enhance hydration (J. Du et al., 2021).

In addition, Wang and Park (2015) observed that while fly ash-modified concrete typically exhibits lower compressive strength at early ages compared to conventional Portland cement concrete, it surpasses the control concrete at later curing stages when fly ash is used in moderate amounts (15-25% replacement). This strength development is attributed to the higher silica (SiCh) content in fly ash, which contributes to extended pozzolanic reactions over time. Similarly, Hefni et al. (2018) found that replacing cement with fly ash at levels up to 40% initially reduced early-age strength; however, significant strength gains were noted between 56 and 180 days, underscoring the long-term performance benefits of fly ash incorporation.

2.4.3 Rice Husk Ash (RHA)

Rice Husk Ash (RHA) is a pozzolanic by-product derived from the controlled combustion of rice husks the protective outer shells of paddy grains (Park et al., 2015; Kudus, 2023). Globally, rice husk generation is substantial, with approximately 690 million metric tons of paddy rice produced annually, and RHA constituting nearly 4% of this volume (Van Tuan et al., 2011; Chatterjee & Tiwari, 2025). The incineration of rice husk yields RHA at about 20% of the original husk weight (Ahsan & Hossain, 2018), contributing to a significant quantity of agro-industrial waste. The pozzolanic performance of RHA is highly dependent on combustion conditions. Empirical studies have demonstrated that calcination temperatures below 700°C result in RHA with over 80%) amorphous silica content an essential criterion for pozzolanic reactivity (Ahsan & Hossain, 2018).

RHA shares several physicochemical characteristics with Ordinary Portland Cement (OPC), making it a viable candidate for use as a supplementary cementitious material (SCM) in cement and concrete composites (Bie et al., 2015; Fapohunda et al., 2017; Sandhu & Siddique, 2017). Notably, RHA is rich in silica, typically exceeding 80%), which underpins its pozzolanic functionality (Bie et al., 2015; Foong et al., 2015; Ahsan & Hossain, 2018). As indicated in Table 2.7, the RHA used in this study contains 96.7%o silicon dioxide (SiCh), while the combined content of reactive oxides (SiCh +

AI2O3 + Fe203) reaches 97.8%. These values satisfy the chemical criteria for Class N pozzolans, as stipulated by ASTM C618, which requires a minimum of 70% reactive oxide content and a maximum loss on ignition (LOI) of 6%.

Plate 2.2 presents a representative Scanning Electron Micrograph (SEM) of the RHA, illustrating its highly porous, irregularly shaped particles. The porous microstructure is a consequence of the thermal decomposition of organic matter during combustion, which in turn contributes to the relatively high LOI value observed for the RHA.

Table 2.7
Chemical Composition of RHA (Kartini, 2011)

CHEMICAL COMPOSITION	(%)
Silicon Oxide (SiOi)	96.7
Aluminium Oxide (AI2O3)	1.01
Ferric Oxide (FesOs)	0.05
Calcium Oxide (CaO)	0.49
Magnesium Oxide (MgO)	0.19
Titanium Dioxide (TiOi)	0.16
Sodium Oxide (NaiO)	0.26
Potassium Oxide (K2O)	0.91
Loss on Ignition (LOI)	4.81

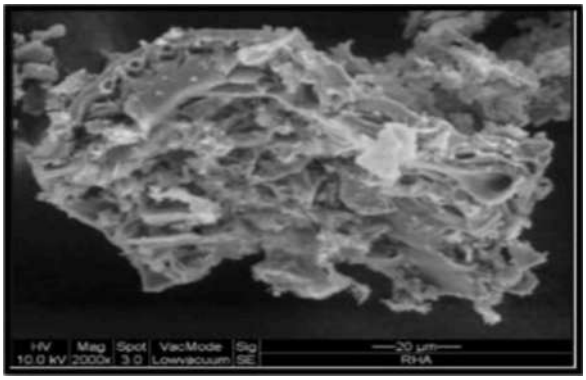

Plate 2.2 SEM of RHA particles (Foong et al., 2015)

Previous research has established the technical efficacy of Rice Husk Ash (RHA) as a supplementary cementitious material, particularly in enhancing the

durability performance of concrete beyond what can be achieved by Ordinary Portland Cement (OPC) alone (Jongpradist et al., 2018). The pozzolanic activity of RHA, which is characterized by the chemical interaction between amorphous silica, calcium hydroxide, and water, is a critical parameter influencing the formation of additional calcium silicate hydrate (C-S-H) phases, thereby contributing to the long-term strength development and microstructural densification of concrete. This reactivity is a prerequisite for RHA's application in structural-grade concretes. Extensive research indicates that the pozzolanic activity of rice husk ash (RHA) is significantly influenced by its content of amorphous silica, particle fineness, and specific surface area (Pinheiro et al., 2016). Nguyen (2011) further emphasized that increased pozzolanic activity is directly correlated with a higher degree of amorphousness, while larger particle sizes tend to diminish reactivity.

In terms of mechanical performance, various studies have investigated the compressive strength of concrete incorporating RHA as a partial cement replacement. Kudus, (2023) reported that a 10% replacement of cement with RHA consistently produced higher compressive strengths across all curing ages when compared to control OPC concrete. This enhancement was attributed to reductions in total porosity and calcium hydroxide content, along with a more refined interfacial transition zone (ITZ) between the cement paste and aggregates, which also contributed to reduced permeability. Similarly, Chindaprasirt et al. (2014) demonstrated that partial substitution of OPC Type I with finely ground RHA and Palm Oil Fuel Ash (POFA) at a 20%) replacement level by weight resulted in marked improvements in compressive strength, largely due to the finer particle size relative to OPC. Khan et al. (2018) observed that increasing RHA replacement up to 15%> led to enhanced compressive strength, although early-age strength was initially reduced. However, the long-term strength gains more than compensated for this initial decline. Moreover, Singh et al., (2020) reported that OPC could be effectively replaced with reburnt RHA up to 30%> by weight without compromising compressive strength or permeability performance.

2.4.4 Palm Oil Fuel Ash (POFA)

Palm Oil Fuel Ash (POFA) is an industrial by-product generated during the processing of fresh fruit bunches in palm oil mills. During this process, biomass waste materials such as fibres, shells, and empty fruit bunches are combusted to produce steam

for electricity generation. The combustion process results in the formation of POFA, which accounts for approximately 5% of the total biomass by weight (Hamada et al., 2018). Given the scale of palm oil production, the industry generates millions of tonnes of POFA annually, posing serious challenges in terms of waste management, land utilization, and associated transportation and maintenance costs for government agencies (Ahamed & Siddiraju, 2016).

Chemically, POFA contains a substantial amount of silica, typically ranging from 50‰ to 70%, contributing to its pozzolanic reactivity (Galau & Ismail, 2015). The physical appearance of POFA is generally grey, although its colour darkens with increasing levels of unburned carbon. Morphologically, POFA particles are heterogeneous in size but predominantly spherical, as illustrated in the microstructural image shown in Plate 2.3. Based on the chemical composition data presented in Table 2.8, POFA satisfies the pozzolanic criteria stipulated in ASTM C618-94a. Specifically, the combined percentage of the principal reactive oxides silicon dioxide (Si02), aluminium oxide (AI2O3), and iron oxide (Fe20s) amounts to 60.4%>, positioning POFA within the classification range of both Class C and Class F pozzolanic materials.

Table 2.8
Chemical Composition of POFA (Olivia et al., 2024)

CHEMICAL COMPOSITION	(%)
Silicon Oxide (SiCfe)	49.20
Aluminium Oxide (AI2O3)	5.45
Ferric Oxide (FesOs)	5.73
Calcium Oxide (CaO)	7.50
Magnesium Oxide (MgO)	3.93
Potassium Oxide (K2O)	5.30
Phosphorus Pent Oxide (P2O5)	6.41
Loss on Ignition (LOI)	13.85

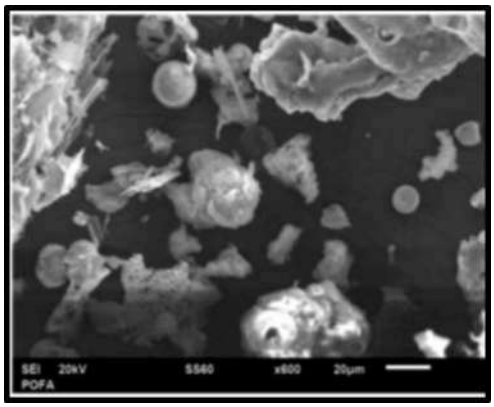

Plate 2.3 SEM of POFA particles (Mulizar et al., 2020)

The use of pozzolanic materials as partial replacements for Ordinary Portland Cement (OPC) signifies a key advancement in sustainable concrete technology (Olivia et al., 2024). Research conducted by Sofri et al., (2015), How et al., (2024) and Hamada et al., (2018) confirmed that only specific proportions of Palm Oil Fuel Ash (POFA) can be ideally used as cement replacements to develop modified concrete with superior performance characteristics. Khankhaje et al., (2015) and Hamada et al., (2024) demonstrated that ground POFA can effectively replace up to 30% of OPC by binder weight, highlighting its viability as a reactive pozzolan. Despite the inherently low pozzolanic reactivity of POFA attributable to its coarse particle size and porous morphology numerous studies have reported significant improvements in its reactivity following mechanical grinding (Galau & Ismail, 2015; Zeyad et al., 2017; Hamada et al., 2018). Hamada et al. (2018) emphasized POFA's potential as a supplementary cementitious material due to its appreciable silicon dioxide (Si02) content. During the pozzolanic reaction, this silica reacts with calcium hydroxide [Ca(OH>2], a by-product of cement hydration; to form additional calcium silicate hydrate (C-S-H) gel, which enhances the mechanical strength and durability of the concrete matrix. This transformation also reduces the content of Ca(OH>2, which is otherwise associated with the formation of deleterious compounds.

The mechanical performance of POFA-incorporated concrete has been widely investigated, particularly with respect to compressive strength. Islam et al. (2015) reported that the best compressive strength across various curing regimes was achieved with a 15%) POFA replacement. Similarly, Ahamed & Siddiraju (2016) found that a 12.5‰ replacement level yielded superior compressive strength relative to the control mix. Zeyad et al. (2017) further demonstrated that the compressive strength of concrete

incorporating ultrafine POFA could exceed 90 MPa at 28 days, outperforming conventional OPC concrete.

2.4.5 Granite Dust (GD)

Granite dust (GD) is a by-product generated in significant quantities during granite stone crushing, grinding, cutting, and polishing activities. These processes produce fine particles; commonly referred to as granite dust because of pulverizing, washing, and screening operations in quarries. Although the properties of GD can vary depending on the source, they tend to remain moderately consistent within a given location (Etim et al., 2021). GD poses substantial environmental concerns, particularly due to its disposal and accumulation in landfills. In Malaysia, mining and granite quarrying activities have also raised ecological and social issues, especially when conducted near ecologically sensitive areas (ESAs), where impacts on air, water, and noise levels are pronounced (DOE, 2016). Additionally, forest degradation and wildlife disturbances related to granite extraction further emphasize the need for sustainable waste management strategies.

Granite dust is commonly categorized based on how it is collected:

a) Dry Fly Granite Dust (DFGD) refers to the fine particles released into the air during crushing or polishing, captured by dry collection systems like bag filters or cyclone separators. This form is typically ultrafine (< 75 um), lightweight, and powdery, similar in texture to fly ash (Chajec, 2021).
b) Bottom Ash Granite Dust (BAGD) consists of coarser, heavier particles that settle at the bottom during granite slurry or water-based operations. These particles typically have a larger size distribution and are less reactive (Chajec, 2021).

One sustainable approach is the incorporation of GD as a supplementary cementitious material (SCM) or fine aggregate replacement in concrete and mortar. This not only mitigates waste disposal issues but also enhances the mechanical and durability performance of concrete (Ali et al., 2017). Chemically, granite dust is rich in silica (Si02), alumina (AI2O3), and iron oxides (Fe20s), which are essential for pozzolanic reactions. According to Kumar and Balamurugan (2013), the silica content in GD typically ranges between 50% and 70%, meeting the reactivity requirements outlined in

ASTM C618. The total reactive oxide content (SiCh + AI2O3 + Fe203) generally exceeds 66%, qualifying GD as a pozzolanic material.

Table 2.9
Chemical Composition of Granite Dust (Gudla Amulya et al. 2021)

CHEMICAL COMPOSITION	(%)
Silicon Oxide (SiCfe)	45-75
Aluminium Oxide (AI2O3)	15-19
Ferric Oxide (FesOs)	6-17
Calcium Oxide (CaO)	3-14
Magnesium Oxide (MgO)	1-3.6
Sulphur Oxide ($S0_3$)	0-2.65
Sodium Oxide (NaiO)	0-3.7
Potassium Oxide (K2O)	3-4.5

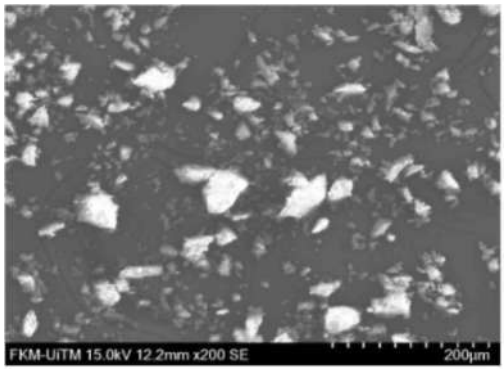

Plate 2.4 SEM of Granite Dust (Sapiai et al., 2021)

The physical characteristics of GD also contribute to its usefulness in cementitious systems. GD particles are generally finer than cement particles, enhancing the packing density of the composite and reducing porosity. Plate 2.4 Scanning Electron Microscopy (SEM) images, as presented by Sapiai et al. (2021), reveal that GD particles are irregular in shape, promoting mechanical interlocking and improved strength development. When used as a partial cement replacement, GD reacts with calcium hydroxide released during cement hydration to form additional calcium silicate hydrate (C-S-H) gel. This gel improves the microstructure and overall strength of the concrete (Singh &Verma, 2016).

Several studies have explored the mechanical performance of concrete incorporating GD. Research by Singh and Verma (2016) found that replacing cement with up to 25% GD resulted in increased compressive and flexural strength due to enhanced pozzolanic activity. Similarly, Patel et al. (2021) investigated the influence of GD particle size on mechanical performance and found that concrete containing ultrafine GD particles (<75 um) achieved significantly higher compressive strength at 28 and 90 days compared to control specimens. In contrast, coarse GD particles (>150 um) led to marginal strength reductions due to inadequate particle bonding with the cement paste. GD also contributes to the durability of concrete. Its fine particles reduce the pore structure and enhance densification, which in turn lowers water absorption and permeability. Furthermore, replacing up to 25% of sand and 15% of cement with GD can enhance the sustainability of concrete by reducing CO2 emissions and the consumption of natural resources (Raman & Nateriya, 2024)

Despite its advantages, GD affects the flowability of fresh concrete and mortar mixtures. Flowability refers to the ability of the mixture to spread and fill formwork under its own weight, which is crucial for achieving proper compaction and finish. GD's high surface area and angular particle shape increase inter-particle friction and water demand, leading to a noticeable decline in flowability at higher replacement levels (Kumar et al., 2016). Reddy et al. (2020) observed that increasing GD content from 5% to 30%) reduced the mortar flow spread from 11.0 cm to 7.0 cm. S. Singh et al., (2016) similarly noted that excessive fine content reduces mobility and mix consistency. However, at lower replacement levels (e.g., up to 10%>), GD may improve packing density without severely compromising flow. When higher amounts are used, the inclusion of superplasticizers or adjustments to the water cement ratio become necessary to maintain acceptable workability.

In addition to its role as a cement replacement, GD has been studied as a fine aggregate substitute. Amudhavalli et al. (2020) found that concrete made with GD as sand replacement had greater compressive strength than conventional concrete with river sand. GD's ability to act as a micro-filler improves the bonding between coarse aggregates and the cement matrix (Khan & Chandrakar, 2017). Research by Umamaheshwari et al. (2015) and Rahim et al. (2021) supports the feasibility of GD as a replacement for natural sand, remarking its similar gradation and mineralogical composition. The use of GD in this manner offers an additional sustainable option for reducing environmental degradation associated with sand mining.

In conclusion, granite dust presents a viable and eco-friendly alternative for use in cementitious systems. Its chemical and physical characteristics support improved mechanical strength, enhanced durability, and reduced environmental footprint when used as a partial replacement for cement or fine aggregates. However, the reduced flowability associated with higher GD content must be carefully addressed through mix design optimization. When appropriately managed, the integration of GD into concrete aligns with sustainable construction practices and effective waste valorisation.

2.4.6 **Nano-Silica** (NS)

Nano-silica (NS) is an advanced pozzolanic material that has garnered significant attention in mortar and concrete technology due to its ultrafine particle size, high reactivity, and exceptional ability to improve both mechanical and durability properties. Synthesized via sol-gel processing, precipitation, or vapor-phase reactions of silicon compounds, nano-silica generally appears as an amorphous white powder with an extremely high surface area. This characteristic significantly enhances its reactivity in cementitious systems and its capacity to influence the microstructure of the hardened matrix.

Chemically, nano-silica consists of over 99% silicon dioxide (SiCh) in amorphous form, contributing to its high pozzolanic activity. Compared to traditional pozzolanic materials like silica fume, nano-silica has a much higher surface area, allowing it to accelerate the hydration reaction of cement by serving as nucleation sites for calcium silicate hydrate (C-S-H) formation. This results in improved microstructural development, particularly in the interfacial transition zone (ITZ) between cement paste and aggregates, leading to a denser and more durable mortar matrix (Althoey et al., 2023)

According to ASTM C1240, nano-silica qualifies as a highly reactive pozzolan. Table 2.10 illustrates its typical chemical composition, highlighting its high purity and negligible impurity content. Its reactivity supports enhanced strength development, especially in early curing phases.

Table 2.10
Chemical Composition of Nano-Silica

CHEMICAL COMPOSITION	(%)
Silicon Oxide (SiCfe)	95
Aluminium Oxide (AI2O3)	1.08
Ferric Oxide (FesOs)	0.45
Calcium Oxide (CaO)	0.20
Magnesium Oxide (MgO)	1.06
Sulphur Oxide (SO3)	0.18
Sodium Oxide (NaiO)	0.68
Potassium Oxide (K2O)	0.12

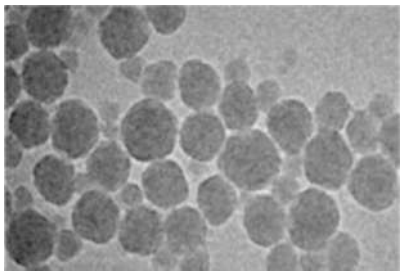

Plate 2.5 SEM of Nano-Silica (AlTawaiha et al., 2023)

Numerous studies have emphasized the importance of optimizing nano-silica dosage. Incorporating NS at low dosages (1%-5% by weight of cement) has been shown to significantly increase compressive and flexural strength (Labaran et al., 2024; AlTawaiha et al., 2023). The pozzolanic reaction between NS and calcium hydroxide [Ca(OH)2] a by-product of cement hydration leads to the formation of additional (C-S-H) gel, contributing to both early-age and long-term strength gains.

A study by Saleh et al., (2015) and K. Khan et al. (2023) explored the influence of nano-silica particle size on mortar performance. Three particle size ranges were examined: coarse (200-500 nm), medium (50-100 nm), and ultrafine (<50 nm). Mortars containing ultrafine NS (<50 nm) exhibited the highest compressive strength at 28 and 90 days, attributed to superior dispersion and reactivity within the matrix (Supit et al., 2013).

In terms of durability, nano-silica enhances the mortar's resistance to external chemical and environmental factors. By filling microvoids and refining pore structure, NS reduces porosity and lowers water permeability (AlTawaiha et al., 2023; Raveendran & Krishnan, 2025). NS also enhances performance under freeze-thaw cycles and mitigates alkali-silica reaction (ASR), thereby extending the service life of mortar and concrete structures (Zeidan & Said, 2015).

However, despite its beneficial effects on strength and durability, nano-silica poses challenges in fresh-state properties, especially workability. Due to its high surface area and fine particle size, NS exhibits a high-water demand, which can lead to reduced flowability and denser, more viscous mixtures. This behaviour has been widely documented in experimental studies. For instance, Mydin et al. (2024) found that increasing NS content reduced the spread diameter in flow table tests, indicating lower workability. The addition of 1-5% NS led to a progressive decline in flow spread, which necessitated the use of superplasticizers or water-reducing admixtures to maintain desired flowability without compromising strength (Suarez et al., 2018).

This inverse relationship between NS content and flowability is due to both the increased interparticle friction and the greater surface area requiring water for adequate dispersion. As such, the incorporation of NS demands careful mix design adjustments. Studies recommend pre-dispersion of NS in water or combining it with polycarboxylate-based superplasticizers to achieve a balance between workability and mechanical enhancement (Ren et al., 2020; Althoey et al. 2023).

In conclusion, nano-silica offers significant advantages in terms of strength development, microstructural improvement, and durability enhancement when used as a supplementary cementitious material in mortar. Nevertheless, its impact on flowability must not be overlooked. Effective utilization of NS in mortar requires careful optimization of dosage, water-to-cement ratio, and admixture selection to ensure workability is not compromised. As an innovative and sustainable material, nano-silica has the potential to elevate the performance of modern cementitious composites, though continued research is necessary to fine-tune its application under varying environmental and loading conditions.

Table 2.11
Summary of Properties and Performance of Supplementary Cementitious Materials in Mortar/Concrete

SCM Properties	RHA	FA	POFA	Granite Dust (GD)	Nano-Silica (NS)
Primary Source	Rice husk combustion residue	Coal combustion residue	Palm oil boiler ash	Granite quarrying/cutting waste	Synthetic amorphous silica (nanoscale)
Key SiCh Content (%)	85-95	35-60	49-70	45-75	>95
Pozzolanic Reactivity	Very High	Moderate-High	Moderate-High	Moderate (enhanced when ultrafine)	Very High (ASTM CI240 compliant)
Common Replacement (%)	5-15 (up to 25)	15-30	10-20	5-25	1-5
Compressive Strength	Up to 60 MPa (10-15% RHA)	40-55 MPa at 28 days (30% FA)	43-55 MPa at 28-90 days (15% POFA)	50-58 MPa (25% GD <75 urn)	Up to 65-75 MPa (2-3% NS)
Effect on Flowability	Slightly	Slight improvement (spherical)	Moderate (coarse, porous)	Significantly with higher content	Strongly reduces

Physical Form	Fine, porous powder	Spherical or irregular fine powder	Porous unless ground	Fine, angular	Ultrafine powder
Workability Adjustment	May need SP at high content	Often improves	Needs SP or water at >15%	SP needed at > 15-20%	Requires SP + dispersion methods
Environmental Benefit	Excellent (agricultural waste)	Excellent (industrial waste)	Excellent (biomass waste)	Excellent (mining waste reuse)	Excellent (reduced cement content)
Challenges	Burning control, fineness	Variability, slower strength gain	High LOI, low fineness	Poor flow, particle size variability	Water demand, dispersion, cost

Among the additional cementitious materials evaluated, nano-silica (NS) demonstrates the most significant enhancement in compressive strength, reaching up to 75 MPa, due to its ultrafine particle size and exceptionally high pozzolanic reactivity. Used in small dosages (typically 1-3%), NS not only improves early-age strength but also refines the microstructure of mortar and concrete. Rice husk ash (RHA) and granite dust (GD) also contribute to substantial strength improvements, with compressive strengths of up to 60 MPa, provided they are properly processed and incorporated at maximum strength of weight percentage replacement levels. Meanwhile, palm oil fuel ash (POFA) and fly ash (FA) are more effective in enhancing long-term strength and durability, although POFA often requires additional treatment, such as fine grinding, to increase its reactivity. Despite their benefits, the use of GD and NS can lead to reduced workability due to increased water demand, necessitating careful adjustments in mix design. Overall, all five materials present viable options for producing sustainable and high-performance mortar or concrete, provided their specific characteristics and limitations are properly addressed.

2.5 Rehabilitation Technique for Repairing Structure

Structural rehabilitation is a crucial aspect of civil engineering that aims to restore, strengthen, and extend the service life of deteriorated or damaged infrastructure. Various techniques have been developed and refined based on regional needs, material availability, and technological advancements. Traditional rehabilitation methods include surface patching, crack injection, jacketing, and section enlargement, while more advanced techniques incorporate externally bonded fibre-reinforced polymer (FRP) composites, prestressed strengthening, and self-healing materials (Baggio et al., 2014). Among these, carbon fibre-reinforced polymer (CFRP) wrapping has emerged as a highly effective solution due to its high strength-to-weight ratio, corrosion resistance, and ease of application, particularly for columns, beams, and slabs subjected to bending or axial loads (Donnini et al., 2018). In seismic regions, techniques such as base isolation, shotcreting, and seismic retrofitting using steel or FRP covers are commonly used to enhance ductility and resilience (Sohel & Karim, 2015). Cementitious repair mortars modified with nano-silica or pozzolanic materials such as fly ash and silica fume have also gained popularity due to their improved bond strength and durability (Quercia & Brouwers, 2014). Furthermore, electrochemical repair

methods, such as cathodic protection and re-alkalization, are employed for reinforced concrete structures affected by corrosion, particularly in coastal or industrial environments (Bertolini et al., 2013). As infrastructure continues to age globally, the selection of a suitable rehabilitation technique must consider not only the type and extent of damage but also the long-term performance, environmental impact, and economic feasibility of the solution.

In addition to conventional rehabilitation strategies, fracture mechanics-based approaches have become increasingly important in evaluating and improving the performance of repair materials. One widely adopted configuration is the Single Edge Notch (SEN) specimen, which has been extensively used to study crack initiation, propagation, and fracture resistance of cementitious composites (Aliha et al., 2012; Karihaloo, 2016). The SEN geometry provides a controlled stress concentration that simulates real-world fracture scenarios, making it a reliable method to evaluate the effectiveness of rehabilitation techniques. By introducing a sharp pre-notch of defined depth-to-width ratio, researchers can calculate critical fracture parameters such as stress intensity factors and fracture energy, which are key indicators of toughness and crack resistance. According to ASTM E399 and ASTM D5045, the notch depth-to-width ratio (a/W) in SEN specimens should range between 0.2 and 0.5, with notch widths of 2-3 mm to ensure sharp crack tips for accurate and reproducible fracture testing. SEN-based approaches have been applied to assess the contribution of supplementary cementitious materials, nano-additives, and fibre reinforcement in enhancing crack-bridging ability and durability (Zhang et al., 2019; Lv et al., 2020). More recently, the integration of SEN testing with rehabilitation methods such as GDNS modified mortars and CFRP wrapping has provided deeper insights into how these materials improve crack resistance, extend service life, and ensure long-term structural durability under realistic fracture conditions.

2.5.1 Glass Fibre

In the composite sector, glass fibres represent the largest segment, accounting for approximately 95% of the total use in reinforced plastics and composites (Zheng et al., 2022; Farinha et al., 2019). However, despite their widespread use, glass fibres contribute to a significant amount of waste due to their high scrap rates and frequent decommissioning, generating between 5% and 40% of waste (Zhou et al., 2021). The

management of this waste has become a major challenge, as reported by Zhou et al. (2021) and Lin et al. (2022), due to the non-degradable nature of glass fibres, which persist for 200 to 300 years due to their excellent corrosion resistance. Previous studies have indicated that landfills and incineration are the most common disposal methods for Glass Fibre Reinforced Polymer (GFRP). With the increasing demand for manufacturing, the volume of glass fibre waste is expected to rise, exacerbating the environmental impacts. It is crucial to address this issue to prevent further environmental damage, as emphasized by Heriyanto et al. (2018) and Delbari and Hof (2024).

Past studies have explored the potential of utilizing GFRP waste in the construction industry, with the aim of reducing the production of cement and minimizing its content in concrete and mortar. As the demand for materials that can improve the strength of concrete specimens grows, the use of waste materials has become an attractive option to mitigate environmental pollution. According to Farinha et al. (2019), waste from GFRP obtained during the cutting process of GFRP rebars can serve as a replacement for natural aggregates in mortar. Similarly, Zhou et al. (2021) investigated the use of GFRP waste as a substitute for natural sand in concrete and mortar, specifically to enhance flexural properties. These studies have shown positive results, indicating that the incorporation of GFRP waste as a sand replacement can effectively improve the mechanical properties of concrete and mortar (Zhou et al., 2021 and Farinha et al., 2019).

GFRP is a composite material widely used in industries such as construction, automotive, and aerospace due to its exceptional strength-to-weight ratio, corrosion resistance, and the ability to be tailored for specific applications (Meira Castro et al., 2013; Ribeiro et al., 2013). Additionally, the use of GFRP rebars in concrete and mortar has been explored by several researchers. As a significant advancement in concrete reinforcement technology, GFRP rebars offer several advantages over steel rebars, such as non-corrosive properties and excellent mechanical performance, making them an effective alternative for traditional steel reinforcement (Jabbar & Farid, 2018).

GFRP has emerged as one of the most promising materials in recent research, as highlighted in Table 2.9. This is primarily due to its superior corrosion resistance compared to traditional steel, along with its lower cost, while still offering significant improvements in strength. Furthermore, GFRP can be used effectively in damage repair applications. According to Abdulsalam et al. (2021), the use of GFRP as an anchoring

method has proven to be highly effective in reducing peeling and increasing the flexural strength of reinforced concrete slabs. Additionally, Corradi et al. (2014) noted that specimens that were retrofitted or repaired with GFRP grids performed well, demonstrating the material's effectiveness in enhancing the structural integrity of concrete.

Zaki et al. (2024), Losaria et al. (2022) and Raza et al. (2019) further highlighted the innovation of integrating GFRP grids into low cement content mortar jacketing, which addressed several issues associated with traditional methods, such as corrosion of steel rebars, excessive reinforcement stiffness, and the limited reversibility of the repairs. Besides, Bitouri et al. (2024) emphasized that the use of GFRP waste as a partial replacement for sand not only improved flexural strength but also compressive strength, confirming its potential as a sustainable alternative in construction materials. This claim was further supported by Tao et al. (2023), who attributed the strength enhancement to the filler effect of the GFRP waste, which helped improve the overall performance of the mix.

2.5.2 Basalt Fibre

In the composite sector, basalt fibres have gained increasing attention as an alternative to glass fibres due to their superior mechanical properties, cost-effectiveness, and environmental benefits. Basalt fibres are produced from naturally occurring volcanic rock, making them a sustainable and eco-friendly reinforcement material (Vatin et al., 2024). Unlike glass fibres, basalt fibres exhibit excellent thermal stability, high chemical resistance, and superior mechanical performance, which contribute to their growing application in construction, automotive, and aerospace industries (Fiore et al., 2015; Zhang et al., 2020).

Basalt fiber-reinforced polymer (BFRP) composites are highlighted for their exceptional durability and corrosion resistance in structural applications, as demonstrated in recent studies (Mohamed et al., 2021; Lu et al., 2022). One of the key advantages of basalt fibres over traditional glass fibres is their higher tensile strength, estimated to be around 4,000 MPa, compared to 3,500 MPa for E-glass fibres (Asmatulu et al., 2013). Additionally, basalt fibres possess excellent alkali resistance, making them an ideal choice for reinforcing concrete and mortar exposed to aggressive environments (Vatin et al., 2024; Hamada et al., 2025).

The disposal of basalt fibre waste is a critical issue that has been explored in recent studies. Unlike glass fibres, basalt fibres are biodegradable over time and do not pose long-term environmental concerns (Zhang et al., 2020). Moreover, basalt fibres exhibit lower energy consumption during production, making them a more sustainable alternative to synthetic fibres (Wei et al., 2019).

Past studies have investigated the incorporation of basalt fibre waste in mortar and concrete to enhance mechanical properties and sustainability. Zhang et al. (2020) demonstrated that basalt fibre waste could replace fine aggregates in mortar, leading to increased flexural strength and durability. Similarly, Wu et al. (2021) reported that incorporating basalt fibres as reinforcement in cementitious materials significantly improved impact resistance and crack control. These findings align with the studies of Y. Zheng et al. (2022), which highlighted the benefits of basalt fibre reinforcement in increasing the tensile and flexural strength of cement-based composites.

Basalt fibre-reinforced mortar has also shown promising results in reducing shrinkage and enhancing fracture toughness. According to Fiore et al. (2015), the inclusion of 1% basalt fibres by volume led to a 25% increase in compressive strength and a 30% enhancement in flexural strength compared to control specimens. Additionally, basalt fibres have been found to improve the bonding characteristics between cement paste and aggregate, leading to a more cohesive microstructure (Zhang et al., 2020).

In terms of fire resistance, basalt fibres outperform glass fibres due to their higher melting point of approximately 1,450°C, compared to 1,100°C for glass fibres (Wei et al., 2019). This makes basalt fibres a preferred choice for fire-resistant applications in buildings and infrastructure. Furthermore, basalt fibres contribute to better energy absorption in impact-prone structures, such as bridge decks and earthquake-resistant constructions (Wu et al., 2021).

Despite these advantages, the application of basalt fibres in mortar and concrete requires further optimization in mix design. Studies have shown that excessive basalt fibre content may lead to fibre clustering, reducing workability and mechanical performance (Fiore et al., 2015). To mitigate this issue, proper dispersion techniques and the use of admixtures, such as superplasticizers, are recommended to enhance fibre distribution and improve mechanical properties (Zhang et al., 2020).

Overall, the integration of basalt fibres into mortar and concrete offers a sustainable and high-performance alternative to traditional fibre reinforcements. Their

superior mechanical properties, durability, and environmental benefits make them a valuable material for modern construction applications. Future research should focus on optimizing basalt fibre dosage and exploring hybrid reinforcement strategies to further enhance the performance of cementitious composites.

2.5.3 Kevlar Fibre

Kevlar fibre, a type of aramid fibre, is widely recognized for its outstanding mechanical properties, including high tensile strength, excellent impact resistance, and thermal stability. Due to these characteristics, Kevlar fibre-reinforced composites have been extensively used in the aerospace, automotive, and defence industries (Natrayan et al., 2023). In the construction sector, Kevlar fibre has gained attention as a reinforcement material in mortar and concrete to improve mechanical performance and durability (Al-Daraji & Aljalawi, 2024). Compared to conventional reinforcement materials such as steel, Kevlar fibres exhibit superior resistance to corrosion, making them particularly suitable for harsh environments (Gao et al., 2020).

The inclusion of Kevlar fibres in mortar and concrete has been shown to enhance tensile strength, flexural strength, and impact resistance. According to research by Gholampour and Ozbakkaloglu (2020), the incorporation of short Kevlar fibres improves crack resistance and fracture toughness, resulting in a more durable cementitious matrix. Similar studies have demonstrated that Kevlar fibre reinforcement significantly enhances energy absorption capacity, making it suitable for applications requiring high impact resistance, such as blast-resistant structures (Zhang et al., 2019). Additionally, Kevlar fibre-reinforced mortar exhibits improved ductility, which is crucial for minimizing sudden failure in structural applications. Studies by Li et al. (2018) reported that mortar specimens containing Kevlar fibres maintained structural integrity even under high loading conditions, reducing the risk of catastrophic failure. Furthermore, Kevlar fibres contribute to reducing shrinkage-induced cracking by acting as a bridging mechanism between cracks (Gao et al., 2020).

Kevlar fibre-reinforced composites are widely used for structural strengthening and repair applications. Kevlar Fibre Reinforced Polymer (KFRP) sheets and wraps have been employed for retrofitting damaged concrete structures, providing an effective alternative to steel plate bonding (Chawla, 2012). Experimental studies by Zhang et al. (2019) demonstrated that Kevlar fibre wraps significantly improved the load-carrying

capacity and ductility of reinforced concrete beams subjected to flexural and shear forces. Additionally, Kevlar fibre-reinforced mortar has been utilized in repair applications to enhance the bond strength between new and existing concrete. The use of short Kevlar fibres at the interface of repair materials improves adhesion and mechanical interlocking, leading to a more durable repair solution (Gholampour & Ozbakkaloglu, 2020).

Compared to steel and other synthetic fibres, Kevlar offers several advantages. Firstly, Kevlar fibres possess a high strength-to-weight ratio, making them significantly lighter than steel while providing comparable tensile strength (Li et al., 2018). Secondly, Kevlar fibres are non-corrosive, unlike steel reinforcement, which makes them ideal for applications in aggressive environments (Gao et al., 2020). Thirdly, Kevlar fibres exhibit superior impact and fatigue resistance, enhancing the toughness of mortar and improving its performance under repeated loading conditions (Zhang et al., 2019). These benefits make Kevlar fibres an attractive alternative for specialized structural applications.

Despite its advantages, Kevlar fibre reinforcement faces some challenges, including higher costs and difficulties in achieving uniform dispersion within the cementitious matrix. Studies suggest that surface modifications and the use of superplasticizers can improve the bonding between Kevlar fibres and the mortar matrix, ensuring better stress transfer and mechanical performance (Gholampour & Ozbakkaloglu, 2020). Future research should focus on optimizing fibre dosage and hybrid reinforcement strategies to maximize the benefits of Kevlar fibre in construction materials.

Kevlar fibre is a high-performance reinforcement material that significantly enhances the mechanical properties, durability, and impact resistance of mortar and concrete. Its non-corrosive nature, lightweight properties, and superior toughness make it a promising alternative to traditional reinforcement materials. While cost remains a limitation, ongoing research and advancements in fibre technology are expected to expand the applications of Kevlar fibre in structural repair, rehabilitation, and high-performance cementitious composites.

2.5.4 Carbon Fibre

Carbon fibre (CF) is a high-performance material composed of extremely thin filaments of carbon atoms, known for its exceptional tensile strength, low density, chemical inertness, and high durability. When used in its raw form, carbon fibre can be directly incorporated into mortar or concrete mixtures as internal reinforcement. Numerous studies have demonstrated that adding short carbon fibres to cementitious matrices enhances mechanical performance by improving tensile strength, flexural strength, fracture toughness, and post-cracking behaviour (Donnini et al., 2018; Biscaia et al., 2018). Carbon fibre-reinforced polymer (CFRP) composites have become increasingly important in civil, aerospace, and automotive industries due to their exceptional tensile strength, stiffness, corrosion resistance, and lightweight nature (Vijayan et al., 2023). In the construction sector, CFRP is employed in two primary ways: (i) as an internal reinforcement material by dispersing carbon fibres within cementitious composites, and (ii) as an external strengthening solution through surface patching or wrapping techniques. Both approaches significantly enhance structural performance, but their mechanisms and applications differ.

a. Internal Reinforcement (Fibre Inclusion in Cementitious Matrix)

In internal reinforcement applications, short carbon fibres are incorporated directly into mortar or concrete mixtures to improve their mechanical and durability properties. This method enhances tensile strength, flexural capacity, and fracture toughness by bridging microcracks and delaying their propagation (Donnini et al., 2018). Biscaia et al. (2018) reported that adding short carbon fibres improved impact resistance and crack control, while Zhang et al. (2023) noted that the resulting denser microstructure reduced porosity and enhanced durability.

The performance of carbon fibre-reinforced mortar depends on fibre dosage, length, and dispersion quality. Poor dispersion can lead to agglomeration, reducing efficiency and creating weak zones. To address this, superplasticizers and fibre surface treatments are often used to improve workability and fibre-matrix bonding (H. Gao & Xia, 2023). While internal fibre reinforcement improves the overall toughness of the mix, it does not provide the same degree of confinement or crack-closing capability as external patching.

b. External Strengthening (CFRP Wrapping)

CFRP external strengthening involves bonding sheets, plates, or fabrics to the surface of structural elements using high-performance epoxy adhesives. This technique significantly increases flexural, tensile, and shear capacity by externally confining the substrate and carrying tensile loads (Maseer & Abdulridha, 2025). Unlike internal reinforcement, which is embedded during casting, external wrapping is applied post-construction, making it ideal for repair and rehabilitation of damaged structures.

Studies have shown that externally bonded CFRP can restore and even exceed the original load-bearing capacity of deteriorated members (Kopiika et al., 2024). Its main strengthening mechanisms include increasing tensile strength in the tension zone, restraining crack opening, and enhancing ductility (Alsuhaibani, 2024). (Jue-Ding et al., 2024) demonstrated that CFRP patching improved fracture toughness and energy absorption in cracked beams, while Tafsirojjaman et al. (2021) confirmed improved cyclic loading resistance.

CFRP wrapping is especially effective in mortar and concrete repairs. When applied over cracked surfaces, it bridges the damaged areas, distributes stresses more evenly, and limits crack widening. Naderi and Rahbari (2021) also found that CFRP confinement reduced permeability and improved durability against aggressive environments. However, its performance depends heavily on surface preparation, adhesive quality, fibre orientation, and anchorage to prevent premature debonding (Mohamed et al., 2018).

Meanwhile CFRP is more expensive than conventional reinforcement, advances in manufacturing and recycling have begun to reduce costs, and the reuse of reclaimed carbon fibres is emerging as an eco-friendly alternative (Chen et al., 2023; Yuan et al., 2024). Hybrid strengthening strategies, where sustainable mortar modifications are combined with external CFRP confinement, offer a promising approach for long-term durability and environmental benefits.

Overall, whether used internally or externally; significantly enhances the mechanical performance and service life of mortar and concrete structures. Internal reinforcement primarily improves the material's intrinsic toughness, while external patching offers superior crack control and load restoration capabilities, making it particularly valuable for structural repair applications.

Table 2.12
Summary of Rehabilitation Technique

SCM	Glass Fibre	Basalt Fibre	Kevlar Fibre	Carbon Fibre
Source	Manufactured from silica-based materials	Volcanic rock (natural source)	Synthetic aramid polymer	Combination of carbon fibres (virgin or recycled) embedded in a polymer matrix
Form Used	Short chopped fibres	Short chopped fibres	Short fibres or wraps	Short fibres, pre-cured sheets or Wraps bonded to surface
Mechanical Strength Improvements	Increases tensile and flexural strength; improves impact resistance	Enhances compressive, tensile, and flexural strength; superior fire and crack resistance	Significantly improves tensile, flexural, and impact resistance; enhances ductility and energy absorption	Improves tensile, flexural strength, and crack resistance; Provides significant load-bearing enhancement, structural stiffness, and crack closure
Compressive Strength (MPa)	50-60	60-65	55-65	60-70
Tensile & Flexural Strength	Moderate improvement	Higher than glass; good crack resistance	Excellent tensile and flexural gains; improved post-cracking performance	Internal: High tensile and flexural gains; External: Outstanding strength enhancement, fatigue resistance, and stiffness recovery
Impact Resistance	Improved compared to plain mortar	Good impact strength; fire resistant	High impact resistance; energy absorption	Very high impact strength: External patching can prevent crack propagation and enhance impact resilience
Ductility	Slight improvement	Moderate improvement	High ductility; resists sudden failure	Moderate ductility; better post-crack performance

Durability	Non-corrosive, long-lasting, resistant to chemicals	Excellent in thermal, alkali, and chemical resistance	Corrosion-resistant, fatigue and impact-resistant	Internal: High durability, corrosion and fatigue-resistant, External patching offers environmental protection to substrate
Workability & Dispersion	Good if fibres are uniformly distributed; risk of fibre clumping	May reduce workability if overdose; improved with admixtures	Difficult to disperse; benefits from surface treatment	Internal: Challenging to disperse evenly, requires superplasticizers; External: Requires surface preparation, adhesive application, and curing control
Environmental Impact	Non-biodegradable; recyclable; moderate energy production	Sustainable, biodegradable, low energy production	Lightweight, durable, but high cost and non-biodegradable	High embodied energy: environmentally concerned waste, external patching extends service life, reducing demolition waste
Application	General-purpose applications; economical choice	Sustainable alternative with better thermal/fire performance	Specialized infrastructure, high-security or high-impact zones	Internal reinforcement for crack control and strength gain; External patching for retrofitting, strengthening, and repairing structural elements

Externally bonded Carbon Fibre Reinforced Polymer (CFRP) is widely recognised as an effective technique for repairing and strengthening mortar and concrete structures. Applied as surface-bonded sheets, plates, or wraps, CFRP significantly improves flexural strength, crack resistance, and fatigue performance while adding minimal weight to the structure (Alsuhaibani, 2024; Z. Liu et al., 2024). Its high tensile strength and strong adhesive bond with cementitious substrates enable efficient stress transfer, effective crack bridging, and enhanced post-cracking behaviour (Juon et al., 2021).

Beyond mechanical enhancement, CFRP serves as a protective barrier against moisture ingress, chemical attack, and environmental degradation, extending service life. Compared to alternative fibres such as Kevlar, basalt, or glass, CFRP offers a superior balance of strength, stiffness, and durability, making it the preferred choice for high-performance retrofitting and repair application.

2.5.5 Carbon-Fibre Based Strengthening Mechanisms in Concrete and Mortar

In recent decades, Fibre Reinforced Polymer (FRP) composites have become one of the most effective materials for structural strengthening, particularly in elements experiencing flexural and shear deficiencies. Among all FRP types, Carbon Fibre Reinforced Polymer (CFRP) has emerged as the preferred external reinforcement due to its exceptionally high tensile strength, lightweight characteristics, corrosion resistance, and ease of installation (Rajak et al., 2019). CFRP systems are typically applied using externally bonded laminates, sheets, or wraps, enabling significant performance improvements in both reinforced concrete and unreinforced mortar elements.

The effectiveness of CFRP strengthening is attributed to its ability to provide external confinement and additional tensile capacity along the tension zone of flexural members. Numerous studies have demonstrated that CFRP wrapping increases flexural strength, stiffness, and crack resistance by delaying crack propagation and redistributing stresses away from weakened regions (Ortiz et al., 2023; Deng et al., 2020). When applied to cracked or repaired specimens, CFRP not only restores the lost mechanical capacity but can also provide strength enhancement beyond the original uncracked state, making it a highly efficient rehabilitation technique for deteriorated structures.

In mortar-based repairs, CFRP is especially beneficial because mortar inherently lacks coarse aggregates, resulting in lower tensile strength and a higher likelihood of crack initiation. External CFRP confinement improves bonding, reduces stress concentrations along repaired zones, and enhances the overall integrity of the retrofitted element. These characteristics make CFRP a promising solution for extending the lifespan of repaired mortar structures, particularly in applications involving patch repair of pre-cracked elements.

Table 2.13
Summary of Literature Findings and Gaps on GD, NS, and CFRP in Mortar/Concrete Performance

Author(s) & Year	Materials Studied	Focus Area	Key Findings	Identified Gap
Safing et al. (2025)	Granite dust	Stress strain of residual soil (soil stabilization)	8% GD gave highest peak deviator stress (690 MPa) after 7 days curing; GD is an eco-friendly alternative to cement	Focused on geotechnical applications, not cementitious mortar/concrete
Raman & Nateriya (2024)	Granite waste powder	Comprehensive review on utilization in concrete and moisture correction	Replacement: 20-25% (sand) and 10-15% (cement) improves mechanical properties (compressive strength up to 66-72 MPa)	Limited long-term durability studies; lacks evaluation of synergy with other SCMs like nano-silica
Pateletal. (2021)	Granite Dust particle sizes	Particle size influence on compressive strength	Ultrafine GD (<75 um) improve mechanical properties (gave best strength outcomes)	Limited application of blended systems dual combination (GD + NS)
Jain et al. (2020)	Waste granite powder (GrP) and waste glass powder (GP)	Durability performance of blended concrete mixes	15% GP (cement replacement) + 30% GrP (sand replacement) significantly improved water absorption	Did not explore mechanical strength in depth or assess combined performance with nano-silica
Amudhavalli et al. (2020)	Granite dust + manufactured sand (M-sand)	Mechanical properties of concrete (M30) with partial cement replacement and M-sand as fine aggregate	Replacing cement with 5-20% GD and river sand with 50% M-sand improved compressive, split tensile, and flexural strength at 7 and 28 days	Did not examine microstructural properties; no synergy explored with nano-silica or other SCMs
Singh & Verma (2016)	Granite Dust	Pozzolanic activity & strength	Up to 25% granite dust as fine aggregate partial replacement can enhance compressive and flexural strength	Did not examine microstructure or combine with nano-silica

Raveendran & Krishnan (2025)	Nano-silica (NS) and metakaolin (MK)	Engineering performance, durability, microstructure, and environmental impact of concrete	Hybrid mix (12.5% MK + 2% NS) showed highest strength and eco-strength efficiency (0.15 MPa/kg $C0_2/m^3$ at 28 days); MK-only mix had lowest embodied CO2; NS + MK reduced porosity, improved durability, and densified microstructure	Did not investigate synergy with granite dust; limited long-term performance data under field conditions
Labaran et al. (2024)	Nano-silica	Study on strength, durability, and cost efficiency of nano-silica concrete	3% NS significantly improved compressive strength; increased drying shrinkage; even 1% NS raised production costs, highlighting trade-off between performance and cost	Limited cost-benefit optimization for large-scale applications; no evaluation of combined use with other SCMs like granite dust
Althoey et al. (2023)	Nano-silica	Review on hydration, strength, durability, and microstructure of cement-based concrete	NS (2-4%) improves mechanical, durability, and microstructural properties by enhancing C-S-H gel formation and densifying the matrix	Did not investigate combined effects with other SCMs like granite dust
AlTawaiha et al. (2023)	Nano-silica	Review on mechanical, durability, and microstructural properties of cementitious composites	NS enhances compressive, split tensile, and flexural strengths; supports microstructural densification. The recommended replacement dose of nano-silica varies between 2 and 3%, according to the kind of cement used	Limitation exploration of synergy with other SCMs like granite dust
Carneiro et al. (2022)	Nano-silica (with/without other supplementary admixtures)	Review on effects of NS on cement-based materials	NS (<5%, surface area <300 m^2/g) improves early-age strength and pore refinement; proper dispersion with superplasticizers essential; excessive surface area or dosage reduces workability and strength; synergy with other nanomaterials possible	Limited consensus on ideal dosage; few evaluations combining NS with granite dust or similar fine waste materials

Ren et al. (2020)	Nano-silica-doped polycarboxylate superplasticizer (NS/PCE)	Workability, mechanical properties, and microstructure of cement pastes/mortars	NS grafted onto PCE improved dispersion, adsorption, and reduced Ca(0Ff)2 crystal content; refined microstructure and enhanced mechanical performance	Focused on modified superplasticizer systems; no evaluation of synergy with granite dust or other SCMs; lacks long-term durability assessment
Suarez et al. (2018)	Nano-silica (low dosage, limited dispersal)	Fresh and early-age mechanical properties of pastes and mortars without plasticizers	Larger NS particle size increased flowability; smaller particles reduced it; no significant gain in early compressive strength; dispersion quality critical for performance	Did not explore long-term strength; no synergy with other SCMs like granite dust;
Yuan et al. (2024)	Carbon Fiber Reinforced Polymer (CFRP)	Recycling technologies and sustainability	Reviewed four main CFRP recycling methods (incineration, physical, chemical, thermal); thermal recycling showed best balance between recovery and fiber quality; called for greener solvents, optimized thermal processes, and better standards	No direct experimental work; lacks performance data for recycled fibers in structural applications; limited integration with mortar/concrete repair studies
Kopiika et al. (2024)	CFRP-bonded tapes for RC beams with corroded rebar	Flexural strengthening and performance monitoring	CFRP repair restored 95% of original bearing capacity in beams with 50% rebar damage; increased strains and deflections compared to control	Limited understanding of CFRP long-term performance in corroded RC elements under varying environmental & loading conditions
Jue-Ding et al. (2024)	Concrete beams with cracks strengthened using different CFRP bonding layers	Influence of strengthening methods on fracture parameters and crack behavior	Single-layer prestressed CFRP provided the best crack resistance and fracture performance; 3-4 bonding layers led to over-reinforced failure modes	Lack of evaluation on performance under varying environmental or service conditions

Vijayan et al. (2023)	Carbon Fibre Reinforced Polymer (CFRP)	Structural applications in civil engineering	CFRP offers high modulus, superior strength-to-weight ratio, fatigue and tensile strength; improves ductility and flexural strength in concrete members; excellent fire and chemical resistance; promotes durability and sustainability	Lacks quantitative comparison with other strengthening materials in specific repair scenarios; no life-cycle cost analysis or integration with mortar repair studies
Naderi & Rahbari (2021)	CFRP-strengthened concrete with various protective coatings	Durability enhancement under extreme environmental conditions	Protective layers (cement-based mortars, polymer waterproof mortar) reduced permeability by up to 36% and increased bond strength by up to 32% under wet-dry, freeze-thaw, and temperature change cycles	Focused on environmental durability; did not examine structural performance improvements (e.g., flexural or shear capacity) under service loads
Tafsirojjaman et al. (2021)	CFRP-strengthened welded beam-column connections	Performance under monotonic and cyclic loading	CFRP improved ultimate moment capacity, stiffness, ductility, and energy dissipation in welded connections; enhanced hysteresis behavior under cyclic loading; experimental results aligned with theoretical predictions	Focused on steel welded connections; did not assess applicability to concrete or long-term performance under environmental exposure
Donnini et al. (2018)	Concrete members strengthened with CFRP	Mechanical behavior under flexural and compressive loading (experimental + analytical study)	CFRP strengthening significantly enhanced load-carrying capacity, stiffness, and ductility; CFRP delayed failure and improved crack distribution	Only focus on internal reinforcement applications

2.6 Summary

Extensive research has been conducted on the use of nano-silica (NS), granite dust (GD), and carbon fibre-reinforced polymer (CFRP) in enhancing the performance of cementitious materials. Nano-silica, with its ultrafine particle size and high pozzolanic activity, has been consistently shown to refine pore structure, accelerate hydration, densify the microstructure, and significantly improve compressive strength and durability of mortar (Khaloo et al., 2016). Similarly, granite dust a silica-rich by-product of stone crushing has been widely explored as a sustainable fine aggregate replacement due to its micro-filling capability and potential late-age pozzolanic reactivity. Incorporation of GD contributes to improved packing density, reduced void content, enhanced strength, and reduced environmental impact associated with natural sand extraction (Singh & Verma, 2016; Rahim et al., 2021).

In parallel, CFRP has gained prominence as an external reinforcement material due to its exceptional tensile strength, corrosion resistance, and crack-bridging capacity. Numerous studies have demonstrated that CFRP wrapping enhances flexural strength, stiffness, and crack resistance in both concrete and mortar-based elements (Donnini et al., 2018; Biscaia et al., 2018). CFRP has also been increasingly investigated for multifunctional applications, such as self-sensing capabilities for structural health monitoring (Roopa & Hunashyal, 2021).

Despite clear benefits, most existing studies investigate NS, GD, and CFRP individually, leaving a significant gap in understanding their combined behavior within a single mortar system. Limited research has examined how NS (as a cement replacement) and GD (as a sand replacement) interact synergistically to influence strength, flowability, microstructure, and chemical composition. Even fewer studies have explored how the combined GDNS mortar performs when integrated with CFRP strengthening, particularly in repairing pre-cracked mortar elements. Although flowability reduction is a common challenge associated with NS and GD addition, almost no studies address how this issue interacts with CFRP reinforcement or how combined effects influence the interfacial transition zone (ITZ), crack-bridging behavior, and long-term performance.

Furthermore, much of the literature relies on bottom granite dust collected during grinding or cutting processes. In contrast, this study utilizes dry fly granite dust (DFGD), a fine waste material captured from dust filters in quarry plants after drying,

blowing, and heating processes at approximately 200 °C. The use of DFGD is advantageous not only because it is a freely available industrial by-product, but also because it mitigates disposal and environmental management challenges associated with quarry waste. This positions DFGD as a promising component in sustainable mortar formulations.

A critical research gap also exists in structural rehabilitation, particularly for Objective 3. While CFRP strengthening has been extensively studied in reinforced concrete beams and slabs, its use on mortar specimens, especially mortar modified with GD and NS remains underexplored. Importantly, no existing studies have evaluated the flexural behaviour of pre-cracked mortar repaired using the best GDNS mortar patch and subsequently strengthened with CFRP wrapping. This gap is significant, as effective repair of cracked elements is essential for improving structural lifespan, reducing carbon footprint, and supporting sustainable infrastructure development.

Therefore, this research aims to address these gaps by investigating the combined influence of NS as a cement replacement, GD (specifically DFGD) as a partial sand replacement, and CFRP as external reinforcement in mortar. The study evaluates their effects on compressive strength, flowability, microstructure, chemical composition, and particularly the flexural performance of repaired, pre-cracked mortar elements. This integrated approach not only advances sustainable construction through the reuse of industrial waste and high-performance composites but also contributes to the development of durable, multifunctional mortar systems for future repair, strengthening, and smart infrastructure applications.

CHAPTER 3
RESEARCH METHODOLOGY

3.1 Introduction

This chapter highlighted the details of the processes involved in achieving the objectives of this research. The objectives included the formulation of the mix design, the selection of the materials used for preparation, such as granite dust, nano-silica, and carbon fibre reinforced polymer (CFRP), and the procedures for mixing, casting, curing, cracking, patching, and wrapping. Additionally, the physical and mechanical testing methods were discussed to obtain the maximum strength of weight percentage results of mortar mixtures containing granite dust (GD) as a partial sand replacement, nano-silica as a partial cement replacement, and the combination of both mixtures, with nano-silica as a partial cement replacement and GD as a partial sand replacement.

The main objective of this study was to identify the morphological properties of the materials and specimens, to assess the strength of hardened mortar incorporating granite dust and nano-silica as partial replacements for sand and cement, respectively, and to evaluate the effect of carbon fibre patching on the mechanical properties of nano-silica—filled granite dust mortar. The flowchart below described the procedures for preparing the mixture specimens of mortar, consisting of GD as partial sand replacement and nano-silica as partial cement replacement. The maximum strength of weight percentage of the mortar bars obtained from both mixtures was determined, and the bars were prepared with CFRP wrapping accordingly. Figure 3.1 illustrated the overall flowchart of the study.

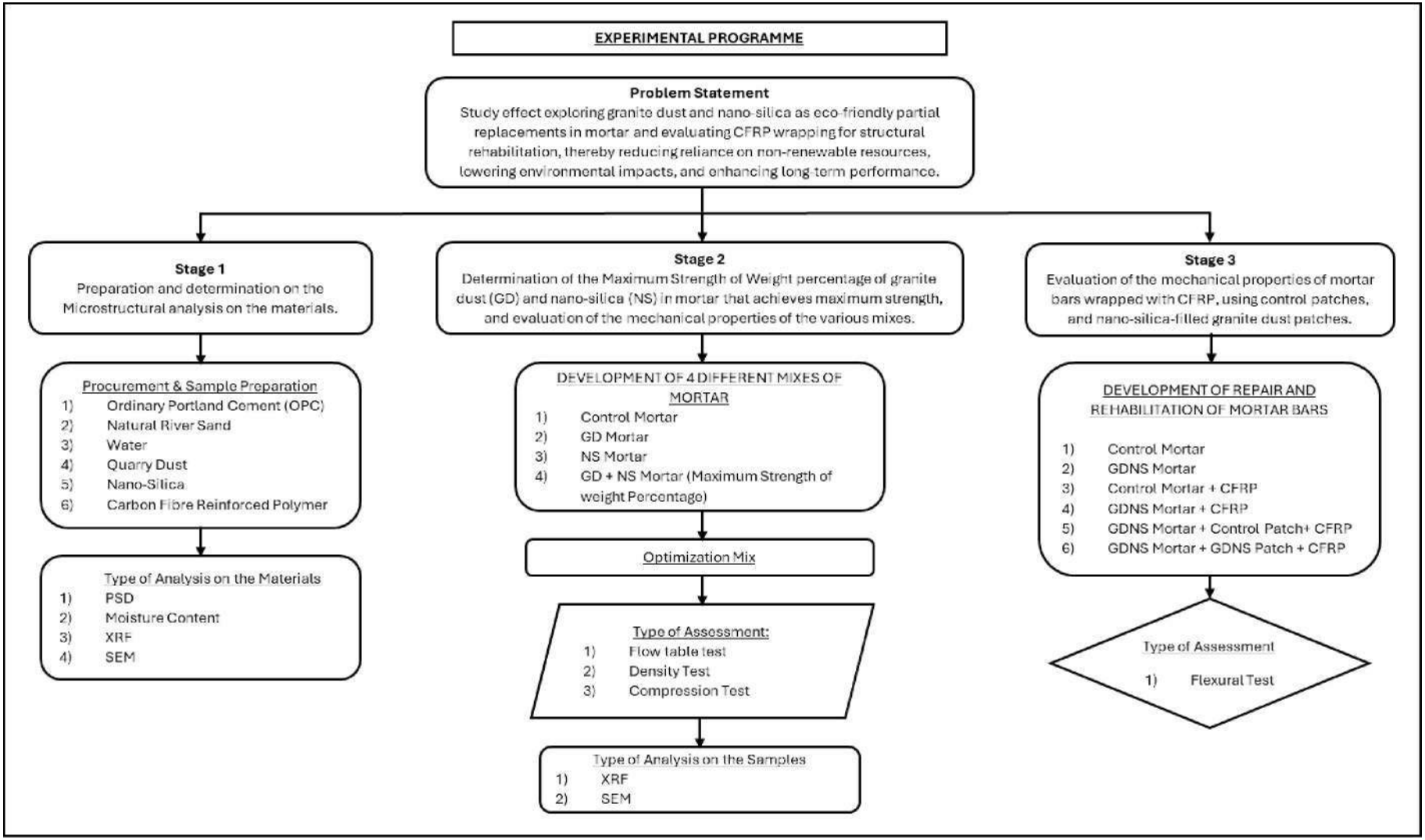

Figure 3.1 Flow of Experimental Programme

3.2 Preparation of Raw Materials

The materials selected for preparing the mortar specimens with granite dust (GD) and nano-silica (NS) as partial sand and cement replacements were sand, cement, granite dust, nano-silica, water, and carbon fibre (CF). The proportions of these materials were determined according to their respective mix design form, which was explained in detail in the sub-sections below.

3.2.1 Sand

A mortar mixture was produced using only fine sand. To remove its moisture content, the sand was placed in an oven and was exposed to a temperature of 100 °C for at least 24 hours. After drying, the sand was sieved to a size of 2 mm, and the resulting product was used for the casting process, as shown in Plate 3.1.

Plate 3.1 Sand

3.2.2 Ordinary Portland Cement (OPC)

A common type of cement, Ordinary Portland Cement (OPC), was used throughout this study, as shown in Plate 3.2. Technically, the cement acted as a binder when mixed with sand, nano-silica (NS), and granite dust (GD) in the mortar mixture. Additionally, the OPC, which was produced by YTL Cement (M) Sdn. Bhd. was stored in an airtight container to prevent direct contact with moisture in the air.

3.2.3 Water

In the production of mortar and concrete, water was one of the main materials used. For this research, tap water was collected for the mixing phase to ensure that the mixture was thoroughly blended. The agitation of the mixture resulted in a reaction between the cement and water, forming a paste that bonded with the sand. As a result, during the hydration process, the water caused the mortar and concrete to solidify. To avoid undesirable effects, such as the weakening of concrete and mortar, it was crucial to ensure the water source remained as clean as possible. Furthermore, the water-to-cement ratio was an important factor to consider, as the strength of the mortar would significantly decrease if the water volume was too high. The water-to-cement (w/c) ratio used in all mortar mixes was fixed at 0.50, in accordance with ASTM C305 requirements for laboratory-prepared mortar. This ratio was selected to ensure adequate workability while allowing meaningful comparison across mixes containing varying GD and NS replacement levels. On the other hand, if the water volume was too low, the workability of the mortar could also be compromised. Therefore, the water-to-cement ratio had to be balanced to produce mortar and concrete that were both workable and high-strength. Plate 3.3 showed the water that was used in this study.

Plate 3.3 Water

3.2.4 Granite Dust

Granite Dust (GD) was known as a type of waste in landfills, which needed to be properly managed to prevent environmental issues. In this study, the GD used was in the form of Dry Fly Granite Dust, a much finer material that was produced and captured during air-blowing, drying, and heating processes (approximately 200 °C) in quarry plants. This dust was collected directly from filtration systems such as bag filters or cyclone separators.

The GD used was obtained from JKR Bukit Buloh, Kelantan, Malaysia. The collected dust, typically less than 75 um, was oven-dried at 100 °C for 24 hours. Following drying, the material was sieved through a 212 um mesh using a manual shaker for 10-15 minutes. The prepared GD, shown in Plate 3.4, was used as a partial sand replacement in the mortar mixtures.

\

Plate 3.4 Granite Dust

3.2.5 Nano-silica

Plate 3.5 showed the nano-silica (NS) used in this study, which was sourced from SkySpring Nanomaterials, USA. According to the manufacturer, the product consists of high-purity amorphous silicon dioxide (SiCh) nanoparticles synthesised via the sol-gel method, a technique widely recognized for producing uniformly sized nanomaterials with high specific surface area and strong pozzolanic reactivity.

The NS used in this research exhibits the following typical properties (SkySpring Nanomaterials, 2024):

a. Chemical composition: >99.5% SiCh
b. Particle size: 20 nm
c. Surface area: -160-200 m^2/g
d. Appearance: White, amorphous nanopowder
e. Density: -2.2 g/cm^3

The ultrafine size and high surface area of NS enhanced the pozzolanic reaction by consuming calcium hydroxide (CH) released during cement hydration and forming additional C-S-H gel. This mechanism was essential for improving microstructural density, early-age strength, and durability of the mortar mixes tested.

Plate 3.5 Nano-silica

3.2.6 Carbon fibre

The woven carbon fibre fabric used in this study, as shown in Plate 3.6, was supplied by Innovative Pultrusion Sdn. Bhd., Seremban, Negeri Sembilan. The product is a bidirectional (0790°) woven carbon fibre sheet designed for structural strengthening applications.

Based on manufacturer documentation, the carbon fibre fabric possessed the following typical properties:

a. Fibre type: High-strength PAN-based carbon fibre
b. Weave type: Plain/bidirectional weave
c. Orientation: 0°/90°
d. Tensile strength: ~3,500-4,000 MPa
e. Elastic modulus: ~230-240 GPa
f. Areal density: ~200-300 g/m²
g. Nominal thickness: 0.167-0.200 mm per layer
h. Ultimate elongation: ~1.5-2.0%
i. Density: ~1.75-1.8 g/cm³

The bidirectional carbon fibre sheet was chosen due to its high tensile capacity, corrosion resistance, lightweight character, and suitability for external bonding to brittle cementitious substrates. These material characteristics allowed efficient stress redistribution, crack bridging, and confinement when applied as a strengthening layer on repaired mortar specimens.

Plate 3.6 Carbon Fibre

3.2.7 Willkat Resin

The epoxy resin system used to bond the CFRP sheets to the mortar surface was WILLKAT® PL 2K WINTER, as shown in Plate 3.7. This product was supplied by T & I Avenue (M) Sdn. Bhd., Subang Jaya, Selangor, and is commonly used as an adhesive and structural bonding agent in FRP strengthening applications.

According to product data provided by the supplier and typical epoxy resin system specifications, WILLKAT® PL 2K WINTER exhibited the following characteristics:

a. Type: Two-component epoxy resin (resin + hardener)
b. Mix ratio: 2:1 by weight
c. Viscosity: Medium to high (suitable for wet lay-up application)
d. Tensile strength: ~30-40 MPa
e. Elastic modulus: ~2.5-3.5 GPa
f. Full curing time: ~24 hours

This resin system was selected due to its strong adhesion to cementitious substrates, chemical stability, and compatibility with carbon fibre sheets. Its mechanical properties ensured effective load transfer between the CFRP laminate and the mortar surface, which is essential for reliable strengthening performance.

Plate 3.7 WILLKAT® PL 2K WINTER

3.3 Characterization of Raw Materials

Waste material used in this study which was granite dust, Nano-silica, sand, and cement underwent four (4) types of testing to determine the material characterization.

3.3.1 Particle Size Distribution (PSD)

The first characterization test conducted for the NSGD mortar formulation was the particle size distribution (PSD) analysis using a Malvern Zetasizer Nano ZS Particle Size Analyzer (Malvern Panalytical, UK), as shown in Plate 3.8(a). The test was performed at the Environmental Research Laboratory (Makmal Alam Sekitar

Penyelidikan BioRec), College of Civil Engineering, Universiti Teknologi MARA (UiTM), Shah Alam, Selangor.

This test aimed to determine the particle size distribution of sand, granite dust (GD), ordinary Portland cement (OPC), and nano-silica (NS). Prior to testing, all materials were oven-dried at 105 °C for 24 hours to remove residual moisture. Sand, GD, and cement were sieved to remove oversized particles, while NS being a nanopowder was handled using a micro-spatula to prevent agglomeration.

For analysis, samples were dispersed in pure distilled water and subjected to ultrasonication for approximately 5 minutes to break up agglomerates and ensure uniform dispersion before measurement, as shown in Plate 3.8(b). The Zetasizer was used:

a. Laser diffraction for micro-sized particles such as sand, GD, and cement (1-500 µm range), and
b. Dynamic Light Scattering (DLS) for nano-sized particles, especially NS (in the 10-100 nm range).

The instrument produced PSD parameters including D10, D50 (median particle size), and D90, which indicated the distribution and fineness of each material. These parameters were essential to evaluate packing density, surface area, and their influence on workability and mechanical performance of the mortar. To ensure consistency and accuracy, the instrument was calibrated prior to testing, and three repeated measurements were conducted for each sample. The average values were used for analysis in Chapter 4.

Plate 3.8 (a) Zeta Potential Analyzer and (b) Sample prepared for PSD analysis

3.3.2 Moisture Content

The moisture content of the raw materials was a critical factor affecting the properties of mortar, particularly its workability and strength. This test was conducted in accordance with ASTM D2216 at the Concrete Laboratory (Makmal Konkrit), College of Civil Engineering, Universiti Teknologi MARA.

The procedure began by weighing a clean, dry, and empty container, and recording its weight as Wi. A known weight of the specimen (150 g each of granite dust, sand, and cement, and 50 g of nano-silica) was then placed into the container. The combined weight of the container and the wet specimen was recorded as W2.

The container with the specimen was placed in a drying oven maintained at 110 ± 5°C for approximately 24 hours. After drying, the specimen was cooled to room temperature in a desiccator and then reweighed to obtain the final weight, W3.

The moisture content (%) was calculated using the following formula:

Moisture Content (%) = (W2 -W3/W3-W1) x 100

Where:

a. *Wi* = Weight of the empty container (g)
b. *W2* = Weight of container + wet specimen (g)
c. *W3* = Weight of container + dried specimen (g)

This procedure was repeated for each raw material to determine its individual moisture content. Plate 3.9 illustrated the oven used in this analysis.

Plate 3.9 Oven Dried Specimens

3.3.3 X-Ray **Fluorescence** (XRF)

The chemical composition of the raw materials used in the NSGD mortar specifically granite dust (GD), nano-silica (NS), sand, and ordinary Portland cement

(OPC) was determined using X-Ray Fluorescence (XRF) analysis. This test was performed using the SI TITAN Handheld XRF Analyzer (Bruker Elemental, USA), as shown in Plate 3.12. The instrument was designed for rapid, non-destructive elemental analysis and was widely used for characterising geological, mineral, and cementitious materials.

The SI TITAN employed an X-ray tube and silicon drift detector (SDD) to quantify elemental composition, particularly the major oxides relevant to cementitious systems, such as SiCh, CaO, AI2O3, Fe203, MgO, and various trace elements. The handheld unit operated with an excitation voltage up to 50 kV and is equipped with advanced fundamental parameter (FP) calibration software to generate accurate oxide results.

Prior to analysis, all raw materials were oven-dried at 105 °C to remove moisture and then finely ground to improve homogeneity. The powder samples were placed in XRF sample cups sealed with polypropylene film to ensure consistent testing conditions and to prevent contamination. Each sample was scanned for 60-90 seconds, allowing sufficient acquisition time for stable signal detection. The analyzer was operated in Mining and Minerals Mode, which is optimized for oxide-based materials commonly found in cementitious systems. Three readings were taken for each material to ensure repeatability and accuracy, and the average values were reported.

This chemical characterization is essential for understanding the role of GD and NS in hydration, microstructure development, and performance enhancement of the modified mortar mixtures.

Plate 3.10 SI TITAN Handheld XRF Analyzer

3.3.4 Scanning Electronic Microstructure (SEM)

SEM analysis was conducted to examine the morphological characteristics of granite dust, nano-silica, sand, and cement, focusing on particle shape, surface texture, fineness, and the presence of angular or rounded features that influence the packing density and microstructure of mortar.

A Hitachi SU3500 Scanning Electron Microscope was used for this analysis. The specimens were mounted on aluminium SEM stubs using conductive carbon tape to ensure mechanical stability. Since the raw materials are non-conductive, the samples were coated with a thin layer of gold in a Quorum SC7620 Sputter Coater for approximately 90 seconds. The gold coating prevents electron charging on the sample surface and ensures clear, high-resolution imaging.

SEM imaging was performed:

a. under high vacuum,
b. at an accelerating voltage of 10-15 kV,
c. in Backscattered Electron (BSE-COMP) mode,
d. at magnifications up to 5000x, as shown in Plate 3.11.

This imaging mode emphasizes contrast between particles based on atomic number differences, making it suitable for visualizing cement phases, roughness of GD particles, and the ultrafine morphology of NS. These microstructural observations provided essential insights when correlating PSD, pozzolanic activity, and mechanical performance of GDNS modified mortar.

Plate 3.11 Gold Coating Machine

Plate 3.12 Hitachi SU3500 SEM Analyzer

3.4 Preparation of Mortar Mixtures, Mortar Patching and Fibre Wrapping

In this section, four (4) different mixtures were produced. The first mixture consists of mortar without any inclusion of waste materials known as a control specimen. For the second mixture, Nano-silica was used as partial cement replacement and granite dust as partial sand replacement for the third mixture. The fourth mixture was the combination of the maximum strength of weight percentage between a Nano-silica as a partial cement replacement with granite dust as a partial sand replacement in one mortar mix. Compressive strength was conducted to determine the strength of each mixture followed by the study on the characterization of the mixtures had been verified and a flexural test was conducted to determine the flexural strength of specimens between the maximum strength of weight percentage GDNS modified mortar mixture with control mortar wrapped with CFRP. The details of the mix proportion for the preparation of mortar had been discussed in the sub-section below.

3.4.1 Mix Proportions

Mortar specimens in this study were prepared according to the stage. The presences of waste material used in this study which was single granite dust as a partial sand replacement ranged from 0% as a control specimen, 5%, 10%, 15%, 20, 25%, and 30%, and single Nano-silica as a partial cement replacement ranged from 0.5%, 1.0%, 1.5%, 2.0% and 2.5% respectively. The GD replacement levels (5-30%) were selected based on prior studies showing that workability decreases significantly beyond 30%,

while compressive strength typically increases up to a 15-25% range (Singh & Verma, 2016; Rahim et al., 2021). Nano-silica replacement levels (0.5-2.5%) were chosen in alignment with previous research demonstrating ideal pozzolanic activation and strength gain within this small-percentage range, whereas higher NS dosages introduce severe agglomeration and workability issues (Ghosal & Chakrabarti, 2022; Khaloo et al., 2016). Four different types of mixture proportions were prepared in this study as already mentioned in section 3.3.

The first mixture will be labelled as the control specimen. The second mixture was the mortar with the inclusion of granite dust, which was designated as GD5, GD10, GD15, GD20, GD25, and GD30 while the third mixture was the mortar with Nano-silica which was designated as NS0.5, NS1.0, NS1.5, NS2.0, and NS2.5. The last mixtures, contained the maximum strength of weight percentage of single Nano-silica as a partial cement replacement and the inclusion of granite dust as a partial sand replacement in mortar to obtain the maximum strength of weight percentage with combination mixtures of granite dust as a partial sand replacement and Nano-silica as partial cement replacement in one mortar mixture was designated as NS1GD5, NS1GD10, NS1GD15, NS1GD20, NS1GD25 and NS1GD30.

All specimens were water-cured for 3, 7, and 28 days prior to compressive strength testing. The details of the mix proportions utilised in this study are presented in Table 3.1. The values listed in Table 3.1 refer to the actual mass of constituent materials measured using a laboratory weighing scale during the batching process for each mixture configuration. These values were recorded to ensure accurate mass proportioning for specimens. The table indicated the measured material quantities used in each mix.

Table 3.1
Summary of Mix Proportion

MORTAR: NANOSILICA AS A PARTIALLY CEMENT REPLACEMENT & GRANITE DUST AS A PARTIALLY SAND REPLACEMENT

Mixture	Sand (kg/m³)	Granite Dust (kg/	Cement (kg/m³)	Nano-silica (kg/m³)	Water (kg/m³)
Control	1600	0	533.33	0	266.67
GD5	1520	80	533.33	0	266.67
GD10	1440	160	533.33	0	266.67
GD15	1360	240	533.33	0	266.67
GD20	1280	320	533.33	0	266.67
GD25	1200	400	533.33	0	266.67
GD30	1120	480	533.33	0	266.67
NSO.l	1600	0	530.66	2.67	266.67
NS1.0	1600	0	528	5.33	266.67
NS1.5	1600	0	525.33	8	266.67
NS2.0	1600	0	522.66	10.67	266.67
NS2.5	1600	0	520	13.33	266.67
NS1GD5	1520	80	528	5.33	266.67
NS1GD10	1440	160	528	5.33	266.67
NS1GD15	1360	240	528	5.33	266.67
NS1GD20	1280	320	528	5.33	266.67
NS1GD25	1200	400	528	5.33	266.67
NS1GD30	1120	480	528	5.33	266.67

3.4.2 Casting Process

Prior to the casting process, all raw materials, including cement, sand, granite dust (GD), nano-silica (NS), and water; were accurately weighed according to the designated mix proportions.

For the control mix, cement and sand were combined and mixed in a mechanical mixer for 60 seconds to ensure uniformity. Water was then gradually added to the dry mixture and mixed until a consistent, homogeneous mortar was obtained. In mixes incorporating granite dust, the sand and GD were first dry mixed to achieve an even distribution. Cement was then added to the mixture, followed by the gradual addition of water. For mortar containing nano-silica, the NS was pre-mixed with cement to promote even dispersion. This cement and NS blend were then introduced into the mixer containing pre-mixed sand and water. In mixes combining both GD and NS, the sand was first mixed with granite dust, while the cement was separately mixed with nano-silica. These two dry mixtures were then combined and mixed thoroughly before water was added gradually.

This systematic mixing approach ensured uniform dispersion of materials and contributed to the consistency and performance of the mortar mixes. The mixer used in this casting process is shown in Plate 3.13 below.

Plate 3.13 Mixer Used for Preparation of Mortar Cubes

The casting of twelves (12) different type of mortar specimens was conducted using standard 50 mm cube molds. Proper preparation of the molds was essential to ensure high-quality specimens. Each mold was thoroughly cleaned, dried, and uniformly lubricated with a release agent to facilitate the smooth removal of the hardened mortar.

The freshly mixed mortar, prepared to the desired consistency, was placed into the molds using a scoop in two layers. Care was taken to fill each mold evenly to avoid the formation of air pockets or voids. Each layer was compacted by gently tapping the sides of the mold or using a vibrating table to ensure proper consolidation and eliminate entrapped air. After the final layer was placed, the surface was leveled with a trowel or straight edge to achieve a smooth and uniform finish, with attention given to the edges and corners for well-defined specimen geometry.

The filled molds were then left undisturbed in a controlled environment to cure under standard conditions as shown in Plate 3.14, in accordance with relevant standards ASTM C109, maintaining appropriate temperature and humidity levels.

Plate 3.14 Specimens of 50 mm Cubes for Each Different Percentages

Following the determination of the maximum strength of weight percentage for individual mixes of granite dust (GD) as a partial sand replacement and nano-silica (NS) as a partial cement replacement, a subsequent casting was performed to evaluate their combined effect. In this phase, the maximum strength of weight percentage of GD and NS was incorporated simultaneously into the mortar mixture. The GDNS modified mortar was then cast into 160 × 40 × 40 mm prism molds, along with control specimens for comparison as shown in Plate 3.15 below.

These prism specimens were intended for application-based testing. Specifically, they were used as patching materials in pre-wrapped damaged bars to assess the rehabilitation performance of the GDNS modified mortar. The results were compared with control mortar used under the same conditions. This application test aimed to evaluate the effectiveness of the newly developed mortar in structural repair and maintenance within the construction industry.

Plate 3.15 Three (3) Specimens of 160 x 40 x 40 mm Bar for Each Different Percentages

3.4.3 Curing Process of Mortar Cube and Bar

Curing is a critical phase in mortar specimen preparation, as it directly influences the development of mechanical strength by promoting adequate hydration and reducing the risk of shrinkage cracking. Proper curing also contributes significantly to the long-term durability and performance of cement-based materials.

In this study, all mortar specimens were subjected to water curing as shown in Plate 3.16. After 24 hours of initial setting in the molds, the specimens were carefully demolded and immersed in a water tank maintained at ambient laboratory conditions. The water curing process was sustained for designated periods of 3, 7 and 28 days to monitor the progressive strength development of each mortar mixture.

This curing method ensured consistent moisture availability, facilitating continuous hydration and enabling the specimens to achieve their full-strength potential. The strength evolution over time was subsequently evaluated through compressive and flexural testing. The rigorous curing regime adopted in this study was essential to ensure the reliability, repeatability, and validity of the test results, ultimately supporting data-driven conclusions regarding the performance and structural suitability of the modified mortar mixtures.

Plate 3.16 Specimens Immersed in a Water Tank of Lab

3.4.4 Single Edge Notch Bar Specimen Preparation

To prepare a mortar bar for the patching process, a damaged fracture or crack was created. In general, the type of cracks may be listed as shrinkage cracks, settlement cracks as well as structural cracks. The Single Edge Notch (SEN) specimen is a standard configuration in fracture mechanics studies, designed to evaluate crack propagation and fracture resistance of materials. In this research, the SEN specimens were prepared from mortar bars with precise dimensions of 160 mm in length, 40 mm in width, and 40 mm in height to facilitate the testing process. A sharp, single-edge notch was introduced at the midpoint of the specimen, extending from one face toward the centre to create a localized stress concentration.

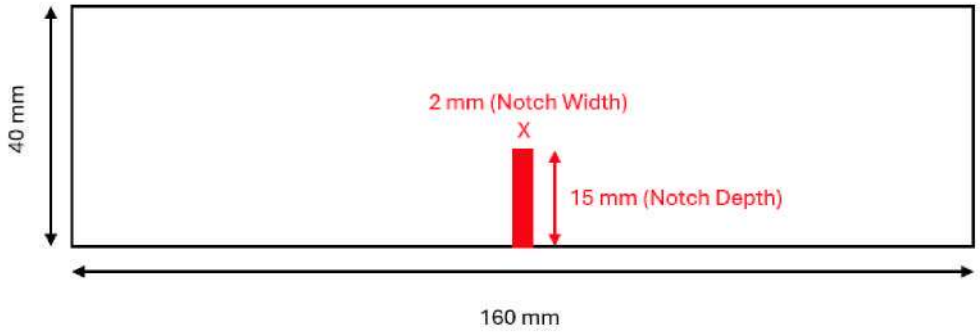

Figure 3.2 Geometry of Single Edge Notch (SEN) specimen used for fracture testing

The SEN preparation followed fracture mechanics recommendations in ASTM E399 and ASTM D5045, where the notch depth-to-width ratio (a/W) is typically between 0.2 and 0.5 and the notch width between 2-3 mm. Accordingly, the specimens in this study were notched to a depth of 15 mm (a/W = 0.375) with a width of 2 mm, as shown in Figure 3.2 and Plate 3.17. This notch served as a pre-crack to simulate real-world fracture scenarios under controlled loading conditions. The notching process was

performed with precision using fine cutting tools to maintain sharpness and consistency, which are essential for reproducible results.

After the 28th day of the curing process, the mortar specimens with the maximum strength of weight percentage combination of GD and NS and the control mortar were thoroughly cleaned to remove any surface contaminants such as dust. The location for inducing the crack was determined at the middle of the mortar bar, where external stress was applied using a laboratory grinding machine from Makmal Batu. This step was crucial for simulating real-world damage scenarios and evaluating the effectiveness of patching materials or techniques.

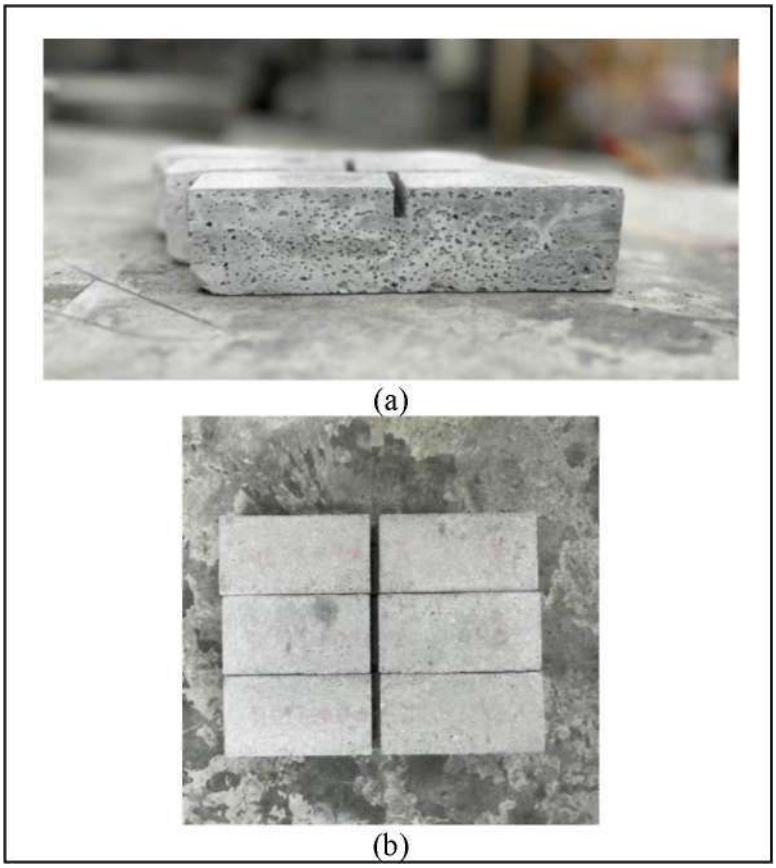

Plate 3.17 Single Edge Notch (SEN) specimens (a) Side View (b) Top View

3.4.5 NS-GD Mortar Patching Process

The patching process began when visual inspection of the structure takes place. This can be identified by assessment of severity, width, depth, and location. The process of patching fracture damage on 160 x 40 x 40 mm mortar bars using the maximum strength of weight percentage combination of granite dust (GD) and nano-silica (NS) and control mortar involves several important steps for effective repair and restoration

of structural integrity. Initially, the damaged area undergoes meticulous cleaning to remove loose debris, dust, or contaminants, ensuring a clean and sound substrate.

Next, two different patching mortars were prepared which are the best mix proportion of GD and NS obtained from maximum strength of weight percentage and control mortars as shown in Plate 3.18. This material is then carefully applied on the cracked area of the mortar bar, ensuring complete coverage and uniform surface as shown in Plate 3.18. Following application, the patched area is allowed to be cured under appropriate conditions to facilitate strength development.

Plate 3.18 Patched Fracture Damage of Specimens on Different Type of Mortar Bars

3.4.6 Fibre Wrapping Process

Carbon Fibre Reinforced Polymer is a composite material characterized by carbon fibres interwoven into a fabric and infused with a polymer resin matrix. Willkat was used as a polymer serving to unite the fibres, safeguard the CFRP against environmental elements, and facilitate load transfer among the fibres. The CFRP wrapping process begins with the specimens' surface undergoing thorough preparation. This includes cleaning to remove any contaminants and repairing any cracks with the patching procedure to ensure a smooth and uniform substrate for the application of CFRP on the specimens. Following surface preparation, the CF was cut into 160 x 40 x 40 mm dimensions to suit the size of mortar bar.

Subsequently, the CF was impregnated with the mixed resin using brushes to ensure that the CF was fully covered with resin, facilitating strong bonding between the CFRP and the mortar bars. Pressure was applied to prevent air bubbles trapped to ensure fully contact between the CFRP and the treated specimens. After that, the CFRP wrapping underwent a curing process for a minimum of 60 seconds, allowing the resin to harden and form a durable bond with the specimens as shown in Plate 3.19

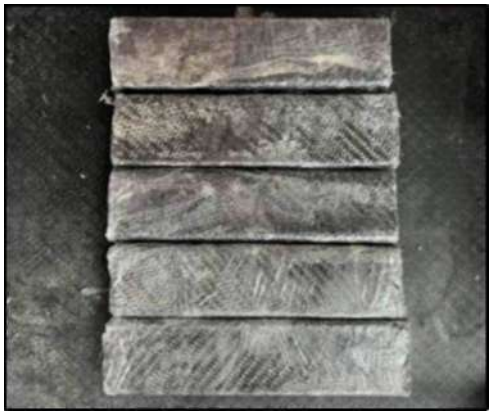

Plate 3.19 CFRP Wrapped on Patched Fracture Damage on Different Type of Mortar Bars

3.5 Physical Properties Testing of Mortar

3.5.1 Flow-Table Test

Flowability was evaluated according to ASTM C1437, using a standard flow-table and 25 drop cycles in 15 seconds. The procedure begins with the meticulous preparation of the apparatus, ensuring compliance with the specifications detailed in the ASTM standard. This involves verifying dimensions, construction, and surface finishing to ensure accurate and reliable test results. Once the apparatus was set up on a stable and level surface, fresh mortar with different weight percentages of GD and NS was carefully prepared according to specified mix proportions used in this.

Firstly, flow table mold is positioned centrally on the apparatus, and the prepared mortar specimen is filled, levelled, and compared to eliminate voids or air pockets as shown in Plate 3.20 (b) below. Excess mortar is then removed, and the flow table mechanism is released, allowing the mortar to spread freely. After the flow table drops continuously 25 times, the diameter of the mortar spread is measured, providing a quantitative flow value in millimetres. The diameter of the mortar was measured spread using a calibrated ruler or measuring tape. Ensure that the measurement is taken perpendicular to the centre of the flow table mold. The flow table apparatus used in this testing is shown in Plate 3.20(a).

Calculate the flow value (F) using the following formula:

$F = (Di+D_2)/2$

Where:

Di = the diameter of the mortar spread measured in one direction

D2 = the diameter of the mortar spread measured in the perpendicular direction

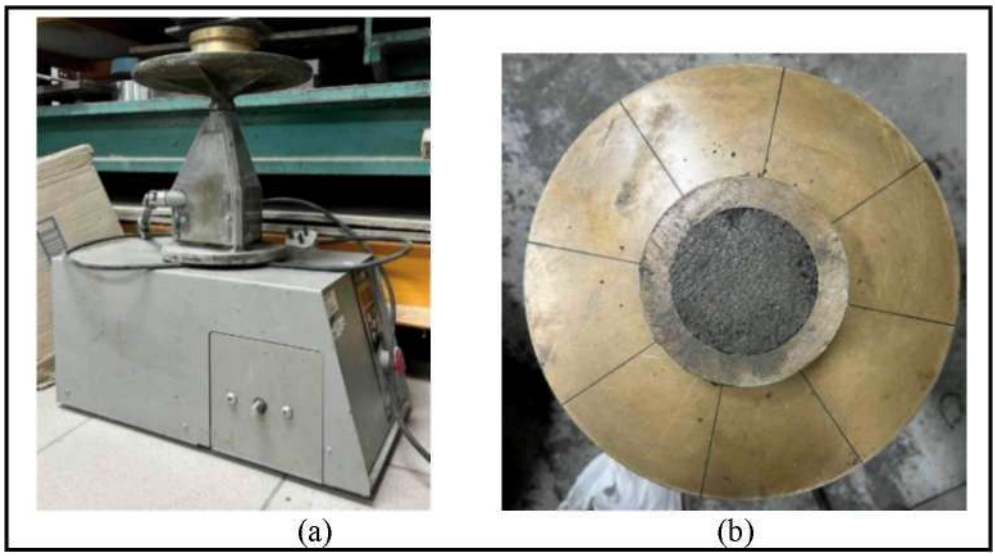

Plate 3.20 (a) Flow Table Apparatus (b) Fresh Mortar Prepared for Testing

3.5.2 Density Test

The density of mortar specimens is an important indicator of material compactness, homogeneity, and overall quality. In this study, density measurements were conducted after the specimens had undergone the full curing period, following the procedure outlined in BS EN 12390-7:2009.

To determine the density, each cured specimen was first weighed using a precision digital scale to obtain its mass (in grams). The volume of the specimen was calculated based on its measured dimensions length (L), width (W), and height (H) using the formula:

$$\text{Volume} = L \times W \times H$$

where:

a. L = length of the specimen (cm)
b. W = width of the specimen (cm)
c. H = height of the specimen (cm)

The density was then calculated using the following formula:

$$\text{Density} = \text{Volume/Mass}\ (\text{kg/m}^3 \text{ or } \text{g/cm}^3)$$

This measurement provided valuable information about the degree of compaction and void content within the hardened mortar. The results were used to assess the quality and consistency of different mortar mixes in the study.

3.6 Mechanical Properties Testing of Mortar

3.6.1 Compression Test

The term hardened mortar refers to mortar that has undergone the curing process and subsequently developed strength over time. In this study, compressive strength tests were performed on mortar specimens at curing ages of 3, 7 and 28 days. The test was conducted on 50 mm × 50 mm × 50 mm cube specimens for the following three mortar mix types:

a) Mortar with weight percentages of granite dust (GD) as partial sand replacement,

b) Mortar with weight percentages of nano-silica (NS) as partial cement replacement, and

c) Mortar with a combination of the maximum strength of weight percentages of GD and NS as partial sand and cement replacement, respectively.

The objective of this test was to evaluate and compare the strength development of each mix over time. The compressive strength of 50 mm cubes was tested according to ASTM C109, using a 1000 kN Universal Testing Machine (UTM). Prior to testing, specimens were removed from the curing tank and dried to eliminate surface moisture. The UTM was inspected and cleaned to ensure that the loading surface was free from dust or debris.

Each specimen was carefully positioned at the centre of the testing platform, ensuring its loading face was perpendicular to the applied load. Input parameters such as specimen weight, density, and age were recorded. A constant loading rate of 0.90 kN/s was applied axially until failure occurred. The average compressive strength was calculated from three specimens for each mix and curing age, ensuring test reliability and accuracy.

In addition, post-failure fragments from the tested cubes were collected for further microstructural analysis. These fragments were stored in airtight containers to prevent moisture ingress and preserve their condition for subsequent Scanning Electron Microscopy (SEM) evaluation. Plate 3.21 illustrated the Universal Testing Machine (UTM) used for compressive strength testing in this study.

Plate 3.21 Universal Testing Machine (UTM)

Plate 3.22 Specimens of 50 mm Cubes for Each Different Percentages for Compression Test

3.6.2 Flexural Test

Following the identification of the maximum compressive strength across twelve mortar mix variations, the maximum strength of weight percentages of granite dust (GD) and nano-silica (NS) were selected. These values were then utilized to produce a newly GDNS modified mortar bar incorporating both GD (as partial sand replacement) and NS (as partial cement replacement). This combination mortar bar was compared against a control mortar bar of the same dimensions (160 mm × 40 mm × 40 mm) to assess improvements in structural performance as shown in Plate 3.23 below.

The flexural strength test was conducted in accordance with ASTM C348, utilizing a Universal Testing Machine (UTM) under a three-point bending configuration. The mortar bars were placed on two supporting rollers, and a central load was applied perpendicular to the longitudinal axis of the specimen. The loading rate was maintained at 0.03 kN/s until failure.

Prior to testing, the dimensions of each specimen; namely, width (di and d2) and span length (1); were measured. As illustrated in Plate 3.23, the span-to-depth ratio was maintained at 4:1, with a span length of 160 mm, adhering to ASTM standards.

To ensure statistical reliability, the average flexural strength was calculated based on three replicate specimens for each mortar mix. This study aimed to evaluate the structural performance and repair potential of mortar modified with granite dust (GD) and nano-silica (NS), particularly when used with CFRP wrapping. By comparing the GDNS modified mortar to control specimens through flexural tests, the study provided a reliable assessment of the mechanical strength and durability of these sustainable materials for real-world structural maintenance and rehabilitation applications.

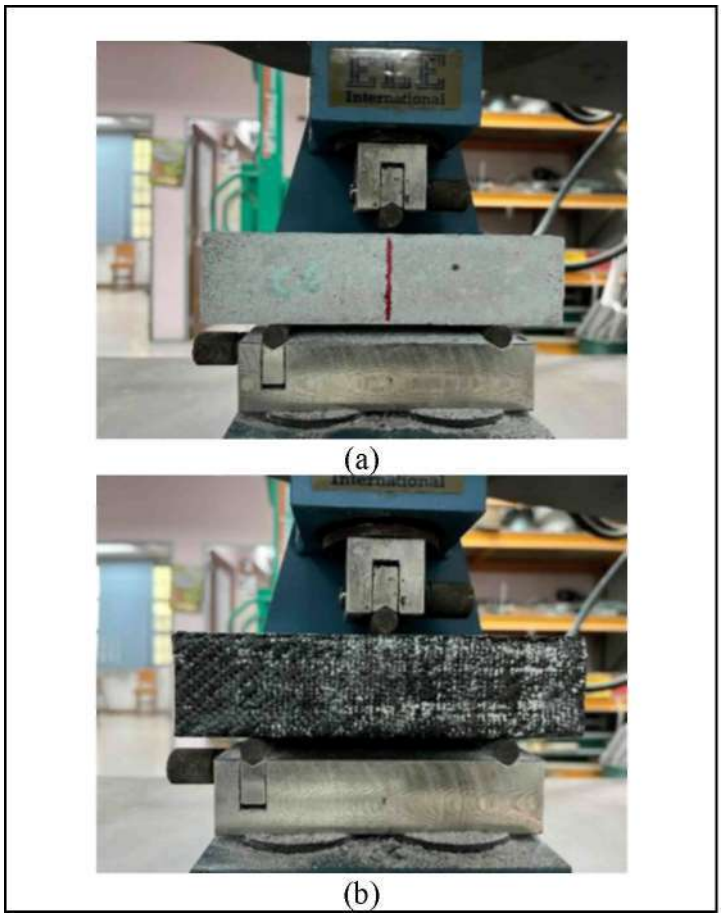

Plate 3.23 Flexural Strength Test of (a) Mortar Bar and (b) Pre-Cracked Mortar Bars Repaired and Wrapped with CFRP

3.7 Fractographic and Chemical Characterization of Mortar

This section outlined the characterization techniques used to analyse the microstructure and chemical composition of mortar specimens prepared with various mixtures. Two key tests were conducted on specimens with the highest compressive strength from each mix: Scanning Electron Microscopy (SEM) and X-ray Fluorescence (XRF) analysis.

3.7.1 Chemical Composition Analysis via XRF

To determine the chemical composition of the mortar materials, XRF testing was conducted in accordance with ISO 29581-2:2010. The analysis was performed at the Advanced Material Laboratory, Institute for Infrastructure Engineering and Sustainable Management (IIESM), UiTM Shah Alam. The XRF device used in this test is shown in Plate 3.10. This test helped identify the elemental composition of the materials used, supporting the interpretation of performance results based on their chemical characteristics.

3.7.2 Microstructural and Fractographic Analysis via SEM

SEM was employed to observe the microstructural morphology of mortar specimens incorporating the maximum strength of weight percentage of granite dust (GD) and nano-silica (NS), both individually and in combination, as partial sand and cement replacements. A control mortar specimen was also analysed for comparison.

Crushed specimens from the 50 mm cube specimens retrieved after the compression test were used for SEM imaging. These fragments were stored in airtight containers to prevent moisture contamination. All SEM images were captured using the BSE-COMP setting at a magnification of 5000×. This analysis provided insight into surface texture, particle distribution, and matrix compactness, which contribute to the mechanical behaviour of the mortar.

CHAPTER 4
RESULTS AND DISCUSSION

4.1 Introduction

This chapter focused on the characterization of raw materials and mortar mixtures used in the study, followed by the evaluation of the physical and mechanical properties. The chemical composition, particle distribution, moisture content, and microstructure of the materials, including granite dust (GD) and nano-silica (NS), were analysed using XRF, SEM, and particle size analysis. The study examined the effects of GD and NS on the compressive strength, flexural properties, and water absorption of the mortar. Additionally, the combined effects of GD and NS in the mortar mix were explored. This chapter also investigated the application of the maximum strength of weight percentage mix through mortar patching and CFRP wrapping, assessing the repair performance and the enhancement of the mortar's mechanical properties. The findings were summarized, offering insights into the best use of GD and NS for improved performance and durability in mortar formulations.

4.2 Characterization of Raw Material

A comprehensive understanding of the influence of granite dust (GD) and nano-silica (NS) on mortar performance needs a thorough study of the fundamental properties of the raw materials used in this study. The characterization of these materials is critical in assessing the physical and chemical behaviour, as well as the interactions within the mortar matrix. This section presents the findings derived from various analytical techniques conducted on GD, NS, cement, and sand. These analyses assist to determine a foundational understanding of each material's properties and the potential contribution to the overall performance of the mortar.

4.2.1 Particle Distribution Analysis

Particle Size Distribution (PSD) analysis is a crucial technique for characterizing the size range of materials and the impact on the properties of

cementitious mixtures. The diameter values at peak intensity (%) indicate the most dominant particle sizes detected by the analyser, which helps determine the average particle size of each material. In this study, PSD analysis was conducted on sand, granite dust, nano-silica, and cement to evaluate their suitability as partial replacements for cement and sand in mortar production. The analysis provides insight into how these materials interact in a mixture, influencing the workability, strength, and durability of mortar.

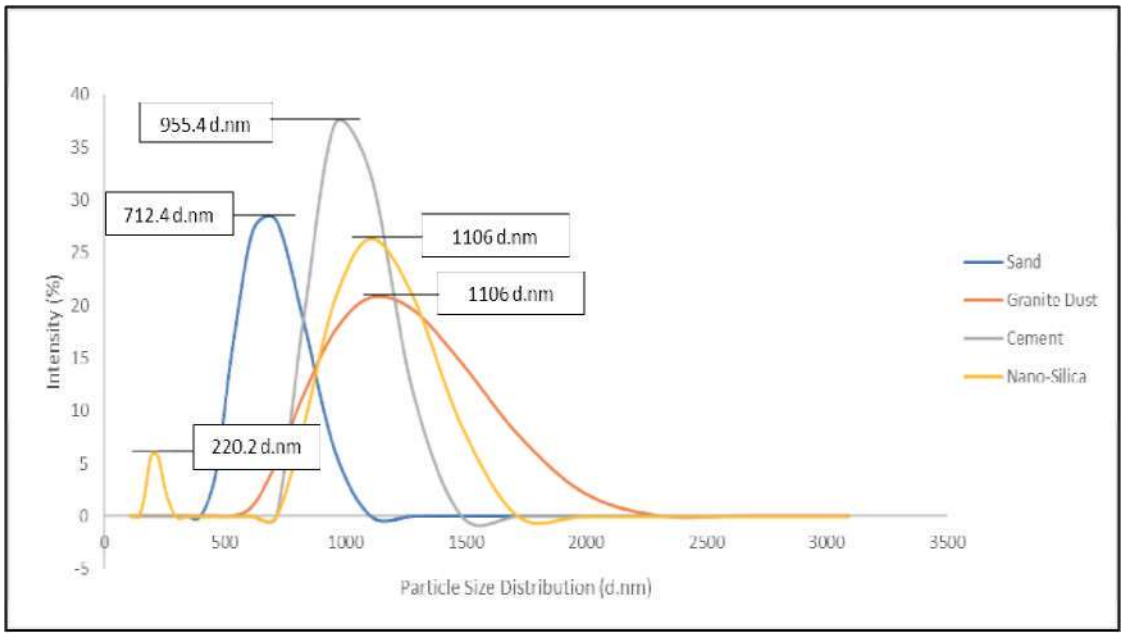

Figure 4.1 PSD Curves of Materials Used in The Present Study

Figure 4.1 illustrates the PSD curves of the four materials. Sand, GD, and OPC exhibited particle sizes within the micron (µm) range, consistent with their natural or manufactured origins. Sand displayed the coarsest distribution owing to its natural gradation, providing the primary thin structure within the mortar matrix. GD showed a finer profile due to quarry processing and dry fly dust collection methods. The smaller particle size of GD enables it to act as a microfiller, improving particle packing and reducing interstitial voids within the mortar a behaviour also reported by Singh and Verma (2016). OPC particles appeared in a slightly finer but narrower distribution range, supporting efficient hydration and early strength development through the formation of a dense cementitious matrix.

In contrast, NS exhibited particle sizes in the nanometer (nm) range, which aligns with its sol gel synthesis method. The PSD curve displayed two distinct peaks which were the first peak (10-20 nm) corresponds to primary nano-sized silica particles,

while the second broader peak is attributed to agglomeration, a common phenomenon in nano powders resulting from high surface energy and particle clustering during dispersion. This secondary peak does not represent actual particle growth but reflects temporary clustering in the aqueous medium used during analysis.

The PSD characteristics of these materials are strongly connected to their performance in fresh and hardened states. The ultra-fine NS particles provide a high specific surface area that accelerates cement hydration, promotes pozzolanic reactions, and refines the pore structure. These effects enhance matrix densification and contribute to early strength development (Derrouiche et al., 2025). Meanwhile, GD's finer micron-scale particles improve grading continuity and packing density, reducing void content and supporting a more compact mortar structure. When used together, NS and GD complement each other by enhancing both micro-filling (GD) and nano-filling/pozzolanic (NS) mechanisms, contributing to improved mechanical and microstructural performance.

Overall, the PSD analysis shows that each material possesses a particle size distribution suitable for its intended role within the mortar system. Cement remains the primary binder due to its fine, reactive particle size; sand provides structural stability through its coarse distribution; GD enhances fine aggregate gradation and packing; and NS improves hydration kinetics and pore refinement. These combined characteristics demonstrate the viability of GD and NS as sustainable partial replacements for sand and cement, respectively, contributing to denser, stronger, and more durable mortar mixtures.

4.2.2 Moisture Content Analysis

The moisture content of materials used in concrete plays an important role in determining the overall quality and performance of the mix. In this study, the moisture content of cement, sand, Nano-silica, and Granite Dust were analysed, with a focus on their potential impact when used as partial replacements for sand and cement as shown in Table 4.1 below.

Table 4.1
Moisture Content of Cement, Sand, Nano-Silica & Granite Dust

Weight	Moisture Content			
	Cement	**Sand**	**Nano-silica**	**Granite Dust**
C (g)	30.2	119.8	27.5	117.1
(BT) C+M (g)	134.6	885.4	38.5	728.6
(AT) C+M (g)	134	884	37.8	726.4
Percentage (%)	0.44	0.16	1.85	0.30

Cement exhibited a very low moisture content of 0.44%, which is typical for this material. Cement is hygroscopic in nature and readily absorbs moisture from the air. However, it is generally stored in dry, sealed environments to prevent premature hydration. Maintaining a low moisture content in cement ensures predictable performance in mortar mixtures and supports proper hydration without unexpected interference (Nguyen et al., 2024). Given this minimal moisture level, the incorporation of nano-silica as a partial cement replacement is unlikely to introduce major complications. However, adjustments to the water-to-cement (w/c) ratio may still be necessary due to the differing moisture properties of NS.

Sand recorded a moisture content of 0.16%, which is very low and consistent with well-dried sand typically used in laboratory conditions. As a key aggregate component, sand contributes to the volume and workability of the mortar mix. Its low moisture content means it does not significantly alter the overall water balance in the mixture. However, replacing sand with GD is essential to monitor and control the moisture levels. Although GD is compositionally like sand, it displayed a higher moisture content of 1.88%, which could lead to a wetter mix and may influence setting time and final strength if not properly adjusted (Safing et al., 2025).

Nano-silica showed a moisture content of 1.85%, which is notably higher than that of cement and sand. Due to its fine particle size and high surface area, NS tends to retain more moisture. While NS is known for improving the mechanical properties and durability of mortar by accelerating the hydration process and enhancing the microstructure, the excess moisture it introduces can affect the mix's water demand. Without proper adjustments, this can negatively impact strength development or lead to segregation issues in fresh mortar (Sikora et al., 2020).

Granite dust, with a moisture content of 1.88%, exhibited similar moisture characteristics to NS. As a partial sand replacement, GD contributes to improved packing density and sustainability of the mortar mix. However, its higher moisture content requires careful consideration in mix design. Failure to account for this additional moisture may result in a mix that is too fluid, potentially compromising setting behaviour and mechanical integrity (Osman et al., 2024).

In conclusion, accurate moisture content control of all raw materials is crucial when incorporating supplementary materials such as nano-silica and granite dust. The low moisture content in cement and sand supports consistency and hydration reliability, while the relatively higher moisture levels in NS and GD necessitate proportion adjustments in the w/c ratio. Proper monitoring and correction ensure that the final mortar achieves the desired strength, durability, and workability.

4.2.3 Chemical Composition Analysis via XRF

The chemical composition of natural sand and granite dust was analysed using X-ray fluorescence (XRF) spectroscopy to determine their suitability for use in mortar mixtures. This analysis provides insight into the potential of granite dust (GD) as a partial replacement for sand based on its oxide composition. The major oxides detected include silicon dioxide (SiCh), aluminium oxide (AI2O3), iron oxide (FeiCb), and calcium oxide (CaO), which are essential for influencing the hydration reactions and strength development in cementitious systems. The XRF results are summarized in Table 4.2

Table 4.2
Chemical Composition of Sand and Granite Dust

Material	**Sand (%)**	**Granite Dust** (%)
$Si0_2$	89.168	79.504
AI2O3	5.423	10.889
Fe_20_3	0.586	1.672
CaO	0.566	1.966

Silicon dioxide (SiCh) was the main oxide in both sand and granite dust. Sand exhibited a higher SiCh content at 89.17%, while granite dust recorded a slightly lower

value of 79.50%. Despite this difference, the high silica content in granite dust remains beneficial, as SiCh plays a critical role in the formation of calcium silicate hydrate (C-S-H) gel during cement hydration, which significantly contributes to strength, durability, and long-term stability in mortar systems (Moolchandani, 2025). The slightly reduced silica content in granite dust does not compromise its function as a filler and reactive pozzolanic material, especially when used in controlled proportions.

Aluminum oxide (AI2O3) content was substantially higher in granite dust (10.89%) compared to sand (5.42%). This elevated alumina content suggests the presence of alumina-rich minerals in granite dust, which may contribute to secondary hydration reactions and potentially influence the early setting and hardening behavior of the mortar. Although AI2O3 contributes less directly to compressive strength, it is essential in forming ettringite and other hydration products that impact workability and early age performance (Zhang et al., 2024).

Iron oxide (Fe20s) was also leading in granite dust (1.67%) than in sand (0.59%)). Although Fe203 has minimal direct impact on mechanical strength, its presence can improve the density of the mortar mix. Additionally, it may act as a catalyst in early hydration, leading to slight improvements in initial strength development. The increased Fe203 content in granite dust suggests the potential for enhanced microstructural densification and improved resistance to environmental degradation.

Calcium oxide (CaO) content in granite dust (1.97%) was significantly higher than in sand (0.57%), indicating the potential for some fundamental cementitious behaviour. CaO is a important compound in cement chemistry, reacting with water to form calcium hydroxide, which further reacts with pozzolanic materials such as Si02 to produce additional (C-S-H) gel (Tural et al., 2023). The presence of CaO in granite dust supports its ability to participate in hydration processes, thus enhancing the strength and structural performance of mortar when used as a partial sand replacement.

In conclusion, the XRF analysis supports the chemical suitability of granite dust as a partial replacement for sand in mortar applications. Its substantial Si02 content supports the formation of strength-contributing hydration products, while the elevated levels of AI2O3, Fe203, and CaO provide additional pozzolanic and filler effects. These characteristics suggest that granite dust not only reduces dependency on natural sand but also enhances the mechanical performance and durability of mortar, contributing to more sustainable and resource-efficient construction practices.

Table 4.3
Chemical Composition of Cement and Nano-Silica

Material	**Cement OPC (%)**	**Nano-Silica** (%)
$Si0_2$	25.897	99.0857
AI2O3	4.2142	<LOD
Fe_20_3	3.7554	0.1313
CaO	60.155	0.132

The chemical composition of Ordinary Portland Cement (OPC) and nano-silica (NS) was evaluated using X-ray fluorescence (XRF) spectroscopy to assess their suitability for use in mortar production. The results, shown in Table 4.3 above, provide valuable insights into the roles of each material in cementitious systems, particularly when nano-silica is utilized as a partial replacement for cement.

One of the most significant findings is the remarkably high silicon dioxide (Si02) content in nano-silica, recorded at 99.09%, compared to only 25.90% in OPC. This proves nano-silica's ultra-pure siliceous nature and high surface reactivity, establishing it as a highly effective pozzolanic additive. In cement systems, silica reacts with calcium hydroxide [Ca(OH)2], a byproduct of cement hydration, to form additional calcium silicate hydrate (C-S-H) gel. This reaction enhances the microstructural density, improves the interfacial transition zone (ITZ), and ultimately increases the mechanical strength and durability of the mortar (Moolchandani, 2025). The high Si02 content in nano-silica not only accelerates early-age hydration but also reduces porosity, contributing to improved durability.

In contrast, OPC displayed a significantly higher calcium oxide (CaO) content at 60.15%), while nano-silica contained only 0.13% CaO. This is consistent with the composition of OPC, where CaO plays a central role in hydration reactions and the formation of the cement paste matrix. The low CaO content in nano-silica shows that its contribution to hydration is primarily through pozzolanic activity. As such, nano-silica is best used as a supplementary cementitious material (SCM) to improve microstructural properties and long-term performance, instead of as a standalone binder (Labaran et al., 2024).

Further analysis showed that OPC contains 4.21% aluminium oxide (AI2O3) and 3.76%) iron oxide (Fe20s), while these oxides are below detection limits in nano-silica

(with Fe203 at 0.13%). These oxides in OPC are essential for forming calcium aluminates and ferrites, which influence hydration kinetics and setting time (Mache et al., 2025). The absence of these oxides in nano-silica highlights its role as a pure pozzolanic filler. While nano-silica may not influence setting time significantly, it densifies the matrix and improves resistance to permeability and microcracking (Verma et al., 2025).

In summary, the XRF analysis strengthens that nano-silica is a high-purity, silica-rich material with minimal impurities, making it an ideal pozzolanic additive for mortar production. Its fine particle size and high reactivity support it to enhance the formation of C-S-H gel, improve compressive strength, and reduce permeability when used in small dosages and typically 1-5% by weight of cement. Although it lacks calcium and alumina-based compounds necessary for direct hydration and structural development, nano-silica's role in secondary hydration makes it a powerful SCM for sustainable and high-performance cementitious applications. These findings align with previous studies emphasizing its effectiveness in refining microstructure, improving strength, and contributing to environmental sustainability in concrete and mortar systems (Khan et al., 2023).

4.2.4 Microstructure Analysis via SEM

SEM analysis was conducted to examine the morphological characteristics of sand, granite dust (GD), nano-silica (NS), and ordinary Portland cement (OPC). Understanding the surface texture, angularity, and fineness of these materials is essential because these features influence packing density, hydration behaviour, and the overall microstructural development of mortar. The first SEM image represented the surface morphology of sand, while the second SEM image showed the surface morphology of Granite Dust.

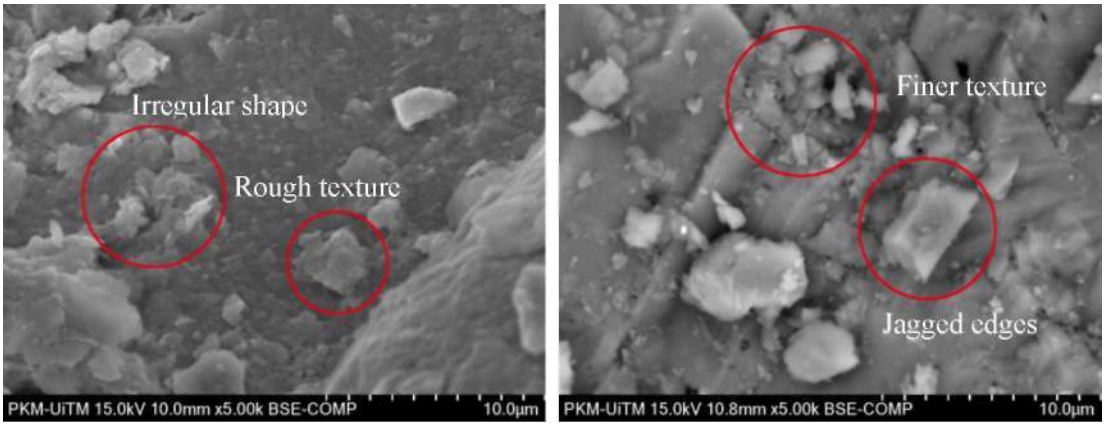

I_____(a)_____(b)_____

Plate 4.1 SEM Microstructures; (a) Sand - Irregular, angular, rough texture and (b) Granite Dust - Finer, more angular

Plate 4.1(a) shows that sand particles are predominantly angular and irregular in shape with a rough surface profile. This texture is characteristic of natural sand subjected to mechanical weathering or crushing (Daghistani & Abuel-Naga, 2023). The angularity and surface roughness contribute to good mechanical interlocking with the cement paste, which enhances the physical bond within the mortar matrix (Sharma et al., 2021). The relatively large particle size and visible micro-pores on the sand surface indicate an ability to hold limited amounts of water, which may slightly influence workability, density, and hydration conditions during mixing. These features are consistent with the XRF results in Table 4.2, which showed that sand is dominated by Si02, commonly present in the form of quartz. This chemically inert nature aligns with the SEM observation that sand primarily contributes physically to the mortar structure.

In contrast, Plate 4.1(b) reveals that GD particles are much finer and more angular than sand. The crushed, jagged edges and fractured surfaces indicate that the material has undergone mechanical processing, producing a higher specific surface area (Serelis et al., 2018). While some particles appear smoother, the morphology is dominated by sharp and irregular textures that enhance physical interlock but also increase water demand due to their fineness and angularity (Clement et al., 2025). This behaviour can reduce workability unless properly compensated during mixing. Despite this, the fine particles of GD can improve packing density and reduce pore volume in the mortar when used in the best proportion, contributing to a denser hardened matrix (Yosri et al., 2024).

In conclusion, SEM analysis visually proves clear morphological differences between sand and GD. Sand has a coarser, rough texture that provides reliable structural

interlocking, while GD offers finer angular particles that can enhance packing density and reduce voids. Although GD increases water demand, it also improves matrix compactness when used in best proportions. These complementary characteristics support the suitability of GD as a partial sand replacement in mortar mixtures.

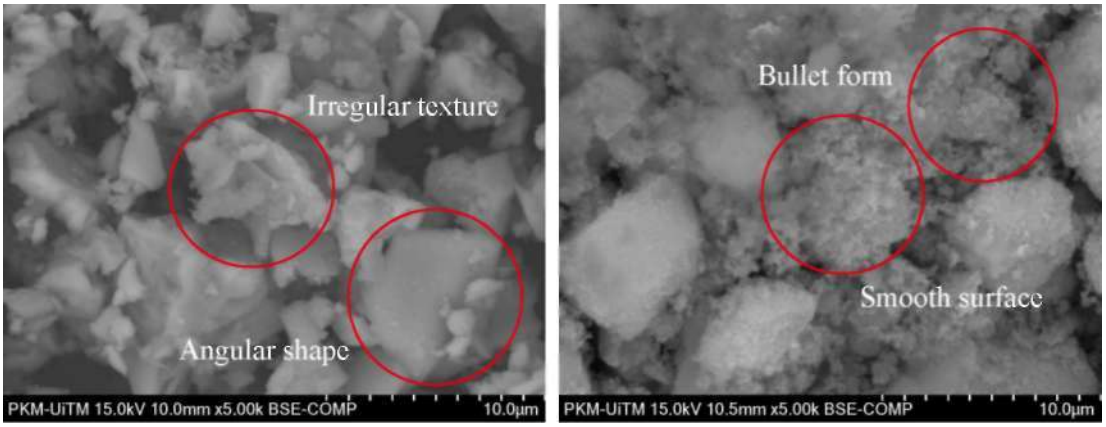

(a) (b)

Plate 4.2 SEM Microstructures; (a) Cement - Coarse, angular with rough surface and (b) Nano-Silica - Spherical, bullet form particle and smooth

The SEM image of cement in Plate 4.2(a) shows particles with angular, irregular shapes and fractured surfaces, typical of ground Ordinary Portland Cement (OPC). This morphology results from the clinker grinding process, which produces particles with relatively high surface roughness and reactivity (Qing et al., 2017). The irregular texture increases the available surface area for hydration, promoting faster initial reaction rates when water is added. The visible pores and micro-cracks within some particles indicate internal porosity, which can influence water absorption, early hydration behaviour, and workability during mixing (Zheng et al., 2021). These observations are consistent with the XRF results in Table 4.3, which show that cement contains high CaO and SiCh contents associated with calcium silicate phases such as C3S and C2S.

Plate 4.2(b) shows that nano-silica consists of ultrafine particles that appear as soft clusters or agglomerates under SEM. Due to their extremely fine particle size (10-20 nm), individual NS particles cannot be distinguished at this magnification and instead present as agglomerated groups with smooth, rounded morphologies. (Samani et al., 2024). Agglomeration is a known behaviour of nano powders due to the high surface energy and strong tendency to form bonds during handling and dispersion. Despite this, NS remains highly effective in modifying microstructure because its

ultrafine size increases surface area and enables it to fill voids within the cement matrix when well dispersed.

The XRF results show that NS consists almost entirely of SiO_2 with only trace amounts of other oxides. Although SEM primarily provides morphological instead of chemical information, the presence of fine agglomerated clusters is consistent with the behaviour of highly reactive pozzolanic materials. In cementitious systems, NS contributes to microstructural densification primarily through nano-filling and secondary hydration reactions that consume calcium hydroxide. These chemical processes cannot be directly observed in SEM, but the refined particle size and smooth morphology support improved packing and better integration within the cement paste (AlTawaiha et al., 2023).

In summary, the SEM images highlight the different morphological characteristics between cement and nano-silica. Cement's angular particles promote mechanical interlocking and support primary hydration, while nano-silica's ultrafine, rounded clusters enhance packing and contribute indirectly to microstructural refinement when dispersed in the matrix. Together, these materials complement each other, with cement providing the base hydration framework and nano-silica improving density and durability when ideally incorporated into mortar.

4.3 Determination of The Most Effective Formulation of Mortar Mix

4.3.1 Physical Properties

4.3.1.1 Flowability Analysis

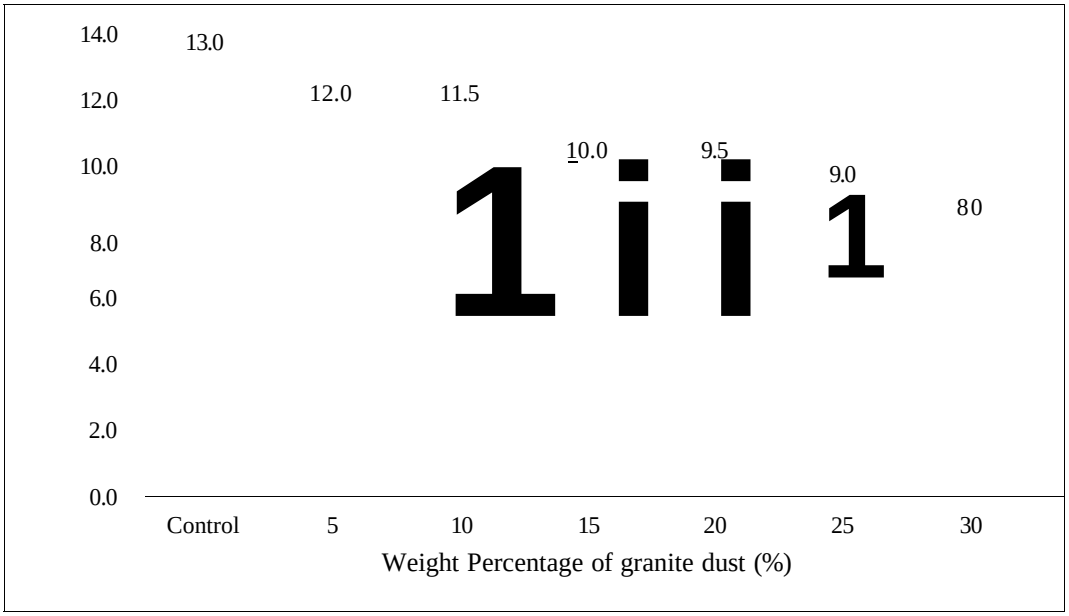

Figure 4.2 Flow table diameter of Different Weight Percentage of Granite Dust (cm)

The effect of granite dust (GD) as a partial sand replacement on mortar workability was assessed using the flow table diameter, with results shown in Figure 4.2. The flow table diameter represents the spreadability and rheological behaviour of the fresh mix. A constant water-cement (w/c) ratio of 0.5 was maintained for all mixes to differentiate the influence of GD content.

At low replacement levels (0 to 5% GD), the flow values remained close to the control (13.0 cm to 12.0 cm), and all values fell within the acceptable workability range recommended by ASTM C1437 (100-150 mm). This indicates that small additions of GD do not compromise practical flowability. This minor change suggests that the fine GD particles improved particle packing by filling voids between sand grains without substantially increasing water demand. As a result, the mortar maintained good workability, consistent with findings that low percentages of mineral fines can enhance mix cohesiveness without compromising flow (Benli et al., 2019).

As GD content increased to 10% and 15%, the flow diameter declined more clearly, from 12.0 cm to 9.5 cm. This trend exhibits increased water demand due to the higher specific surface area and angularity of GD particles, which require more water

for wetting and reduce the free water available for lubrication (Al-Kharabsheh et al., 2022). Under a constant w/c ratio, this leads to reduced spreadability and a stiffer fresh mix.

At higher replacement levels (20 to 30% GD), the flow diameter dropped significantly to 8.0 cm and 7.0 cm, respectively. This substantial reduction is attributed to several combined mechanisms which were GD's angular particles increase interparticle friction, reducing ease of flow; the high fines content increases the viscosity of the paste; and the greater surface area absorbs more water, leaving insufficient free water to maintain fluidity (Mansor et al., 2018; Tanikawa et al., 2025).

The general reduction in workability with increasing GD content is thus regulated by increased water demand and changes in mixture rheology. While GD offers beneficial micro-filling effects at lower dosages, excessive fines at higher replacement levels disrupt the fluid matrix and result in poor flow characteristics (Prokopski et al., 2021; Serelis et al., 2018).

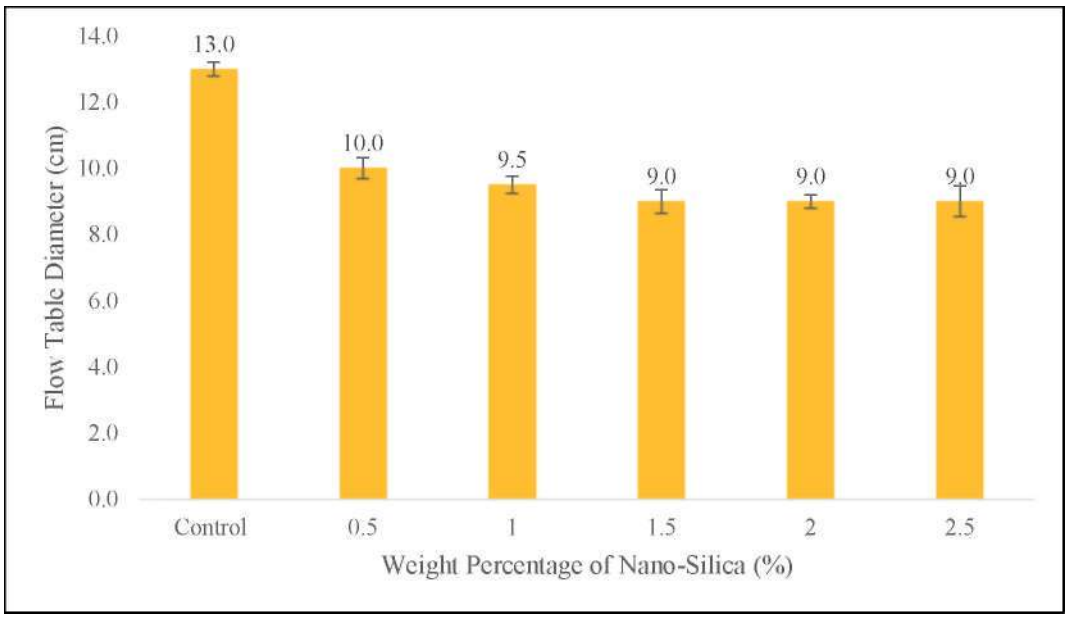

Figure 4.3 Flow table diameter of Different Weight Percentage of Nano-Silica (cm)

The influence of nano-silica (NS) as a partial cement replacement on mortar workability was evaluated using the flow table diameter, with results depicted in Figure 4.3. NS contents ranged from 0.5% to 2.5% by weight of cement, while the water-cement ratio remained fixed at 0.5 to isolate the effect of NS fineness.

At the lowest replacement level (0.5% NS), the mortar exhibited the highest flowability (10.0 cm), which falls within the ASTM C1437 acceptable range, indicating

that small NS dosages maintain practical workability. At such low dosages, the small quantity of NS is insufficient to significantly alter the mixture's surface area or frictional resistance, allowing the mix to behave similarly to the control (Nithiyanantham et al., 2022; P. Zhang etal., 2021).

As NS content increased to 1.0% and 1.5%, the flow diameter gradually reduced to 9.5 cm and 9.0 cm. This decline is attributed to NS's ultrafine particle size, which introduces substantial surface area and leads to increased water adsorption. These nanoscale particles also promote interparticle friction and cohesion within the paste, resulting in lower spreadability (Althoey et al., 2023).

At higher NS dosages of 2.0% and 2.5%, the flow diameter stabilised at 9.0 cm, showing no further significant reduction. This stage effect suggests that past a threshold concentration, additional NS does not proportionally increase water demand. It may indicate that the mix reaches a dispersion equilibrium, where additional NS contributes minimally to rheological resistance under fixed water conditions.

The observed reductions in flowability with increasing NS content align with existing literature emphasising the sensitivity of mortar rheology to nanoparticle fineness (Salman et al., 2024). Despite this, NS up to 1% provides an acceptable balance between workability and performance benefits.

In summary, NS can be incorporated as a partial cement replacement up to 1% without severely compromising workability. Beyond this level, flowability decreases but stabilises due to possible dispersion and particle packing effects. These findings showed the need to optimise NS dosage to achieve enhanced microstructure while maintaining workable mortar (Priya & Vanitha, 2021; Gayathiri & Praveenkumar, 2022; Meeravali et al., 2025).

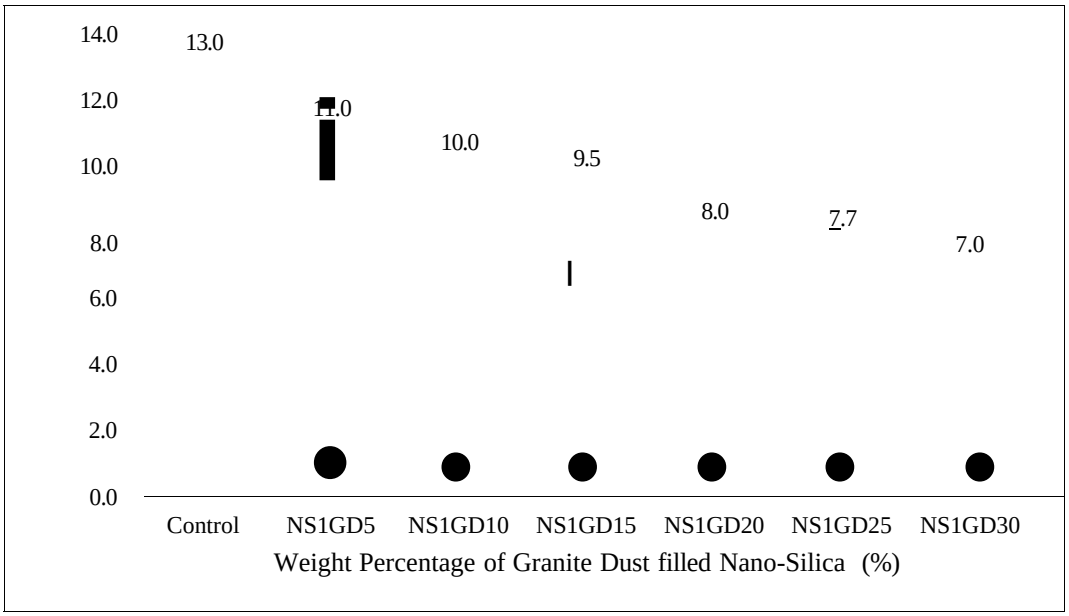

Figure 4.4 Flow table diameter of Different Weight Percentage of Granite Dust filled Nano-Silica (cm)

The combined effect of granite dust (GD) as a fine aggregate replacement and nano-silica (NS) as a cement replacement on mortar workability was evaluated using the flow table diameter test, with results shown in Figure 4.4. All mixes were prepared with a constant w/c ratio of 0.5.

The results indicate that increasing GD content consistently reduces flowability, with low to moderate GD levels (5 to 15%), the flow diameters ranged between 11.0 cm and 9.5 cm. These values remain within the ASTM C1437 acceptable range, showing that moderate GDNS combinations still maintain workable consistency. At these levels, the filler effect of GD improves particle packing without significantly increasing water demand (Reddy et al., 2020). Once GD content reached 20% and 30%, flow values dropped sharply to 8.0 cm and 7.0 cm, reflecting the substantial impact of GD fineness, angularity, and surface area on mixture viscosity and frictional resistance (Senff et al., 2012).

The presence of NS further emphasized this reduction in flowability. NS, being an ultrafine and highly reactive powder, increases water demand due to its large surface area. When combined with GD, the mix contains high quantities of fines at both micro and nano scales, increasing internal friction and reducing free water availability. This results in a denser, more cohesive mix with reduced mobility (Ashokan et al., 2023; Haque et al., 2024).

Although GD and NS contribute significantly to improved mechanical and microstructural properties in hardened mortar, their combined fineness poses challenges

for fresh-state workability. Excessive fines disrupt the fluid mortar matrix and require either water adjustments or the use of superplasticizers to maintain adequate flow during casting.

In conclusion, the combined incorporation of GD and NS results in a clear reduction in flowability, particularly at higher replacement levels. While low to moderate levels (<15% GD and <1% NS) maintain acceptable workability, higher dosages substantially decrease spreadability due to increased water absorption, particle interaction, and mix viscosity. Therefore, careful optimisation of GD and NS contents is necessary to balance fresh-state workability with the improved performance benefits these materials provide in the hardened state.

4.3.1.2 Density Analysis

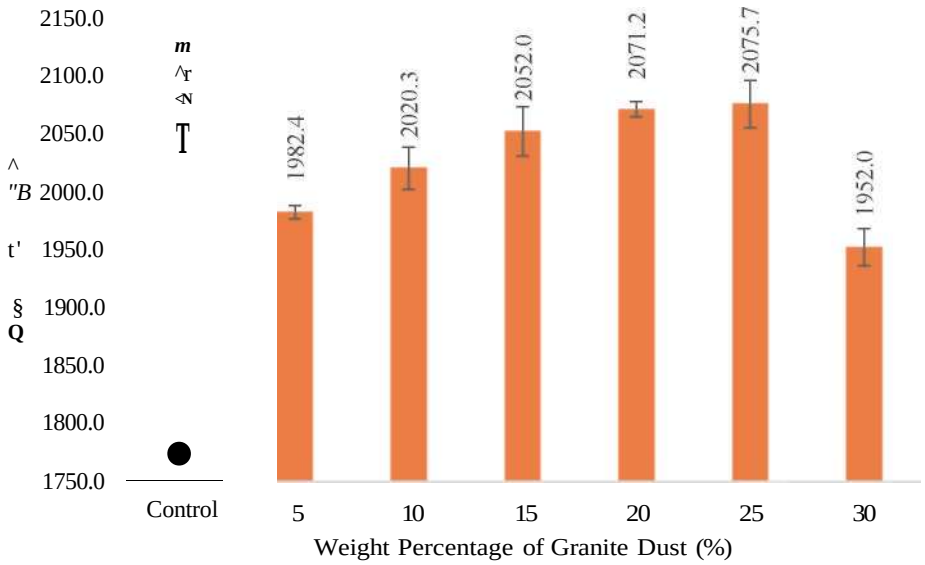

Figure 4.5 Density of Granite dust mortar (kg/m^3)

Figure 4.5 presents the effect of granite dust (GD) incorporation on density. The control mix recorded an average density of 2048 kg/m^3. When GD was incorporated from 5 to 25%, density gradually increased from 1982.4 to 2075.7 kg/m^3, reflecting an overall densification trend at moderate replacement levels. This behaviour is consistent with the filler concept, in which finer particles occupy void spaces between larger aggregates and cement grains, resulting in improved packing and reduced entrapped air (Zain et al., 2018; Safiuddin et al., 2020). Several studies on quarry dust and granite fines also demonstrated similar densification due to finer particle morphology and

angular texture improving interlocking within the matrix (Chandana et al., 2021; Singh & Verma, 2016; Adesina, 2022). The micro-filling mechanism aligns with the particle packing principles advanced by Brouwers (2006), who explained that particle size distribution closer to ideal logarithmic grading produces higher packing density and lower void volume.

The maximum densification observed at 25% GD corresponds to the best size distribution between coarse sand and cement, forming a multiscale packing system in which GD fills intermediate voids and enhances matrix compactness. This effect has been well-predictable in blended aggregate studies where fine by-product powders replace sand or filler fractions (Ali & Al-Tersawy, 2012; Jayasri et al., 2022). Furthermore, GD's angular shape promotes mechanical interlocking between particles, reducing microstructural discontinuities and contributing indirectly to densification, although without necessarily altering hydration behaviour directly (Neville, 2011; Kannan & Ganesan, 2016).

However, the density sharply declined to 1952 kg/m^3 at 30% GD. This decrease is a remarkable reversal of the expected trend and is primarily attributed to excessive fines content exceeding best packing proportions. Higher fines increase surface area and water demand, and under a constant water-cement ratio the available water becomes insufficient to lubricate particles, reducing flowability and preventing proper compaction (Prokopski et al., 2020; Yang et al., 2019). The loss of workability leads to entrapped air and uncontrolled pore formation, which has been widely reported in mixes incorporating ultra-fine materials at high proportions (Dinh et al., 2022; Dilek et al., 2018). Reduced particle mobility during casting also contributes to internal voids, impairing the density of hardened mortar.

Hence, granite dust improves particle packing and density up to 25%, but excessive replacement generates mixing and rheology challenges that result in adverse effects. These observations align with previous reports strengthening that best densification depends on the balance between fines content, workable water availability, and overall packing efficiency (Sharma et al., 2020; Hooton & Thomas, 2020).

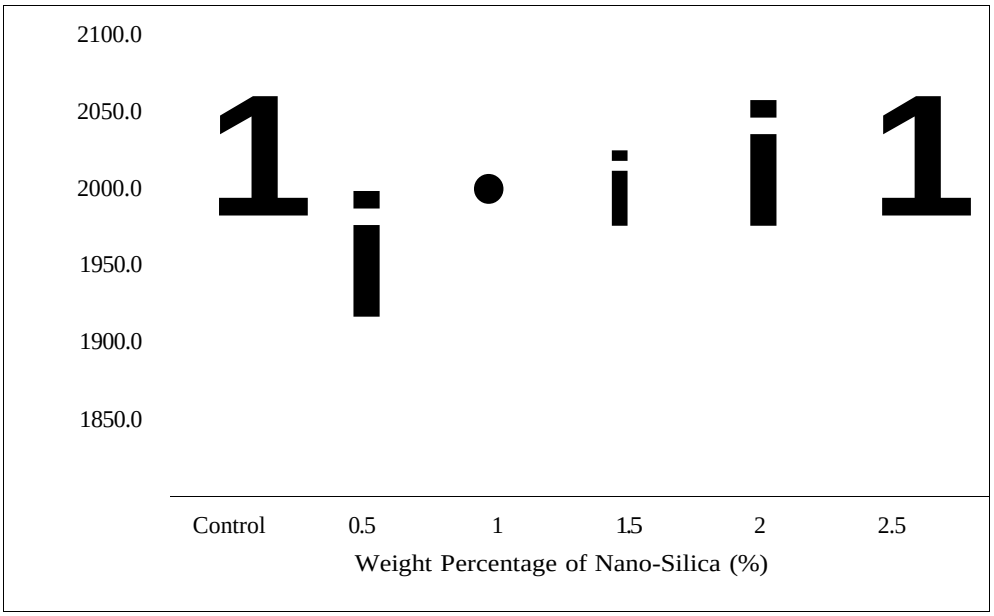

Figure 4.6 Density of Nano-silica mortar (kg/m³)

Figure 4.6 presents the effect of nano-silica (NS) incorporation on density. The control mortar recorded 2048 kg/m³ while the introduction of 0.5% NS resulted in a lower density of 1971.5 kg/m³. This initial decrease is commonly attributed to insufficient dispersion of nanosilica particles which agglomerate at low dosages due to their high surface energy and hydrophilic nature (Senff et al., 2012; Zaki et al., 2021). Agglomerated nanoparticles act as clusters rather than fillers, creating weak areas and potentially increasing microvoids instead of refining them (Li et al., 2015). This behaviour is typical during early incorporation of nanomaterials without adequate dispersive energy or chemical dispersant systems.

As the nano-silica content increased to 1.0-2.5%, density progressively improved, culminating at 2048.8 kg/m³ at 2.5% NS. This trend corresponds with the nano-filler theory, where ultrafine particles enter microvoids and reduce pore volume, leading to better packing and reduced porosity (Ghafari et al., 2014; Le & Ludwig, 2016). Numerous studies reported that nanosilica enhances packing and overall compactness by filling gel-sized voids and acting as nucleation sites for hydration product precipitation (Madandoust et al., 2015; Quercia & Brouwers, 2014). The increase in density observed in this study is interpreted primarily as a physical packing enhancement, in line with literature recommendations indicating that density measurements alone are insufficient for confirming hydration changes but may correlate with microstructural refinement (Mukharjee & Barai, 2020; Ghobadi et al., 2018).The improved density at higher NS levels aligns with the multiscale densification concept,

where nano-scale particles complement the fine cement fraction by bridging capillary voids and assisting physical filling rather than reacting chemically at the macro scale (Beigi et al., 2013; Rath et al., 2025). The magnitude of improvement in this study falls within values commonly observed for nano-silica-modified cementitious systems between 1-3% (Salman et al., 2024; Gholampour et al., 2020), confirming that higher dosages promote meaningful void refinement, whereas very low contents risk agglomeration and lower packing efficiency.

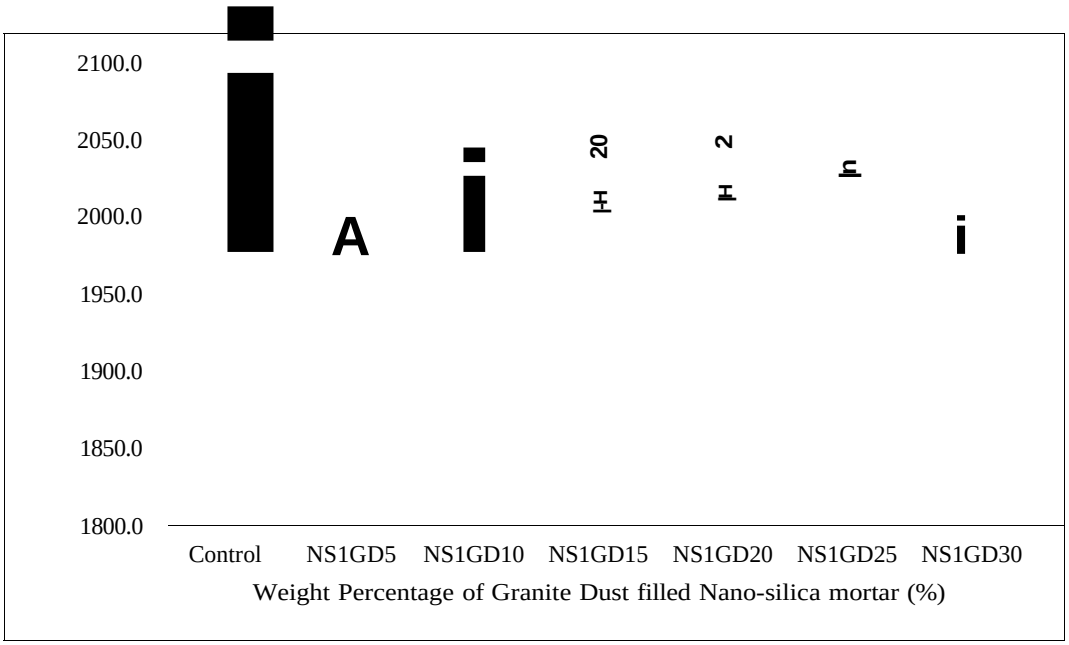

Figure 4.7 Density of Granite Dust filled Nano-silica mortar (kg/m³)

Figure 4.7 demonstrates the combined effect of granite dust (GD) and 1% nano-silica (NS) on mortar density. The control specimen exhibited the highest density (2048.3 kg/m³). However, inclusion of 5 to 10% GD led to initial reductions (1989 to 1997 kg/m³). These decreases coincide with earlier observations for individual materials, where insufficient water availability and limited dispersion of both NS and GD particles resulted in incomplete packing and possible particle clustering (Hadi et al., 2022; Lu et al., 2023). The combination of two fine materials increases surface area, potentially enhancing agglomeration and microscopic pore formation if water content is not adapted (Thomas & GNair, 2023; Zhang et al., 2020).

As GD content increased to 15 to 25%, density improved significantly, peaking at 2041.3 kg/m³ at 25%. This indicates a packing synergy between nanoscale and micro-scale fillers, where NS primarily fills gel pores and GD targets capillary-scale voids (Mukharjee & Barai, 2020). This layered densification mechanism is consistent with

the multiscale packing theory proposed by Brouwers (2006) and extended in dual-filler studies where different particle sizes jointly optimise void distribution (Quercia et al., 2014; Tran & Phan, 2024). Similar improvements have been observed in hybrid filler systems where nano-silica and mineral dusts complement each other to produce better packing, reduced permeability and improved compactness (Bentz et al., 2017; Yazici et al., 2021).

At 30% GD, density decreased again to 1981.1 kg/m³. This reversal highlights a fines threshold beyond which the mix loses fluidity and becomes highly viscous, trapping internal voids and restricting compaction (Zaki et al., 2021; Senff et al., 2012). Under fixed w/c ratios, ultra-fine mineral additions increase saturation demand, quickly exceeding workable limits and reducing densification despite higher solids content (Hooton & Thomas, 2020; Kannan & Ganesan, 2016).

Overall, mortar incorporating 1% NS and 15-25% GD demonstrated best densification, enhancing the role of dual-filler synergy and proper particle size gradation in enhancing packing without excessive fines effects. These findings strongly align with multiscale optimisation studies and validate the use of GDNS combinations as a promising physical densification strategy for low-carbon mortar development (Mukharjee & Barai, 2020; Bentz et al., 2017; Adesina, 2022).

4.3.2 Effect of Granite Dust on Compression Properties of Mortar Cube

4.3.2.1 Compressive strength analysis

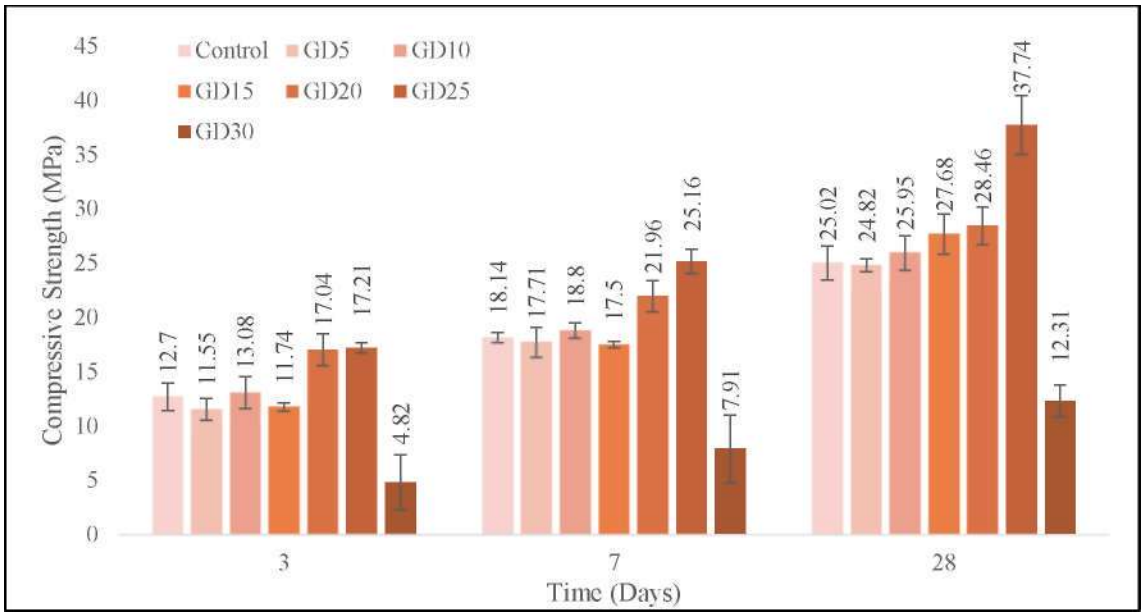

Figure 4.8 Compressive Strength of Mortar Containing Different Weight Percentages of Granite Dust (GD)

Figure 4.8 illustrates the compressive strength of mortar incorporating varying percentages of granite dust (GD) over 3, 7, and 28 days of curing. The results show that GD significantly influences strength development and that the response varies depending on the replacement level and curing age.

At 3 days, all mixes showed early-age strengths consistent with normal hydration progression. The control mix recorded 12.7 MPa, while mixes with 5% and 10% GD achieved 11.55 MPa and 13.08 MPa, respectively. These similar values indicate that low GD contents do not significantly alter early hydration conditions. A remarkable increase was observed with 20% and 25% GD, particularly GD25, which achieved the highest early strength at 17.21 MPa. This improvement is consistent with the packing density effect, where fine GD particles fill voids between cement and sand grains, producing a denser microstructure that supports early mechanical development (Prokopski et al., 2021; Merugu & YM, 2023; Chandana et al., 2021). In contrast, GD30 showed significantly reduced strength (4.82 MPa), reflecting the adverse effect of excessive fines on workability and compaction, as reported by Serelis et al. (2018).

At 7 days, all mixes exhibited strength gains. The control mix achieved 18.14 MPa, while GD25 showed the highest value at 25.16 MPa. Mixes containing 5 to 20%

GD showed progressive improvement, aligned with literature describing improved particle packing and reduced voids when quarry-based fillers are used within ideal ranges (Upadhyaya et al., 2020; Singh & Verma, 2016). GD30 remained significantly lower (7.91 MPa), consistent with strength reductions reported in systems where high-fines content leads to inadequate lubrication and increased entrapped air under constant water content (Abbas, 2025; T & V, 2020).

By 28 days, strengths increased significantly across all mixes. The control mix reached 25.02 MPa, while GD25 achieved the highest strength at 37.74 MPa, followed by GD20 at 28.46 MPa. This shows that GD at moderate levels (20 to 25%) enhances long-term mechanical performance due to improved physical packing and more refined microstructural arrangement (Li et al., 2018; Prokopski et al., 2020). GD30, however, remained low at 12.31 MPa, demonstrating that overly high GD content results in insufficient effective binder matrix and reduced structural integrity, as similarly observed in high-volume stone dust studies (Cheah et al., 2018).

Overall, GD improved compressive strength at 5 to 25% replacement, with 25% producing the highest strengths at all ages. The enhancement is attributed primarily to physical mechanisms packing density, fines filling action, and improved particle distribution. At 30%, the excessive fines content and increased water demand at a fixed w/c = 0.5 resulted in reduced workability and poor mechanical performance. Thus, GD is effective as a sustainable fine aggregate replacement when used up to approximately 25%), in agreement with previous findings (Prokopski et al., 2020; Upadhyaya et al., 2020).

4.3.2.2 Chemical composition via XRF

Table 4.4 presents the oxide composition of the mortar mix containing 25%> granite dust (GD25), compared with the control mix (CS). The major oxides identified Si02, AI2O3, Fe203, and CaO, reflect the mineralogical characteristics of the constituent materials and provide useful insight into their potential influence on the mortar's overall behaviour. The oxide profiles from XRF help explain material compatibility and the possible contribution of each component based on established literature.

Table 4.4
Elemental Composition of GD25

Material	**GD 25** (%)	**CS** (%)
$Si0_2$	53.6648	60.2108
AI2O3	4.9945	2.8911
Fe_20_3	2.3056	1.5916
CaO	36.0507	32.2871

Silicon dioxide (SiCh) was the dominant oxide in both mixes, with GD25 containing 53.66% compared to 60.21%) in the control. The slightly lower SiCh content in the GD25 mix shows the mineral composition of granite dust, which typically contains a mixture of quartz and feldspar minerals rather than pure silica-rich sand. SiCh is commonly linked to pozzolanic potential when present in reactive forms, and the XRF findings indicate that the SiCh content may contribute to such reactions. However, previous researchers report that silica-rich mineral fillers may contribute to long-term matrix refinement and improved mechanical behaviour when properly dispersed (Moolchandani, 2025; Tural et al., 2023). Thus, the presence of substantial SiCh in GD25 supports the compatibility of granite dust as a supplementary fine material.

Aluminium oxide (AI2O3) was remarkably higher in GD25 (4.99%>) compared to the control (2.89%>). This increase is consistent with the alumina-bearing minerals commonly present in granite. Although AI2O3 is generally regarded as having a limited direct contribution to strength development, previous studies suggest that alumina-bearing fillers may influence setting characteristics and enhance matrix refinement through physical packing effects (Moutei et al., 2018; Li et al., 2023). In this study, AI2O3 is interpreted primarily as an indicator of granite's mineralogical diversity.

Ferric oxide (Fe20s) content also increased slightly in GD25 (2.31%>) relative to the control (1.59%). This reflects the presence of iron-bearing minerals in granite dust. Although Fe203 is generally considered to have a limited direct role in strength development, the literature suggests that it may influence early hydration kinetics in small amounts (Elakneswaran et al., 2019).

Calcium oxide (CaO) increased from 32.29% in the control to 36.05% in GD25. CaO is the primary oxide in cement clinker phases, but its presence in granite dust is characteristic of feldspar minerals. Some studies suggest that calcium-rich fillers may

contribute to improved matrix compatibility or interact beneficially with cement hydration (Jain et al., 2020), and the XRF findings in this study indicate calcium availability that could support such reactions. Instead, the higher CaO content is taken as an indicator of the mineral composition of GD.

In summary, the XRF results indicate the inherent mineralogy of granite dust and prove its compatibility with the cement system. The oxide profile particularly the presence of SiCh, AI2O3, and CaO supports the physical densification and packing improvements observed in strength and density results. The findings therefore reinforce granite dust's suitability as a sustainable fine aggregate replacement, primarily through physical mechanisms such as void filling and improved particle packing.

4.3.2.3 Microstructure analysis via SEM

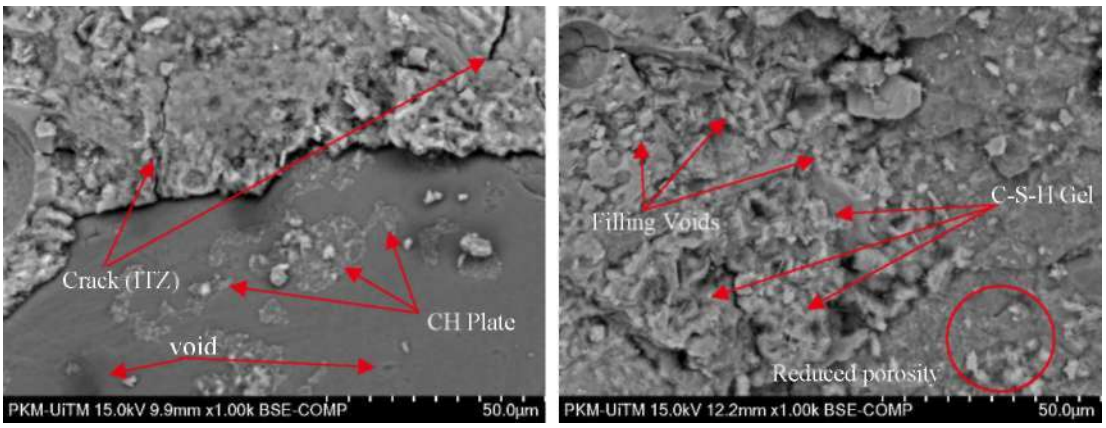

I_____(S)_____(b)_____

Plate 4.3 SEM Microstructures of; (a) CM and (b) GD25

Plate 4.3 showed the SEM micrographs provide a comparative assessment of the internal morphology of the control mortar (CM) and the mortar containing 25% granite dust (GD25). In Plate 4.3(a), the control mortar exhibits an uneven and relatively porous microstructure, with evident voids and microcracks along the interfacial transition zone (ITZ). Such heterogeneity is typical of conventional mortar where incomplete compaction and weak paste-aggregate bonding occur (Koenig, 2020; Sharma & Vyas, 2023). The matrix also shows unhydrated cement grains and coarse crystalline places commonly associated with early hydration phases. These microstructural features align with higher porosity and reduce mechanical performance, as noted in studies examining weak ITZ development and hydration non-uniformity (Kulisch et al., 2022; Krishna et al., 2021).

In contrast, the GD25 specimen in Plate 4.3(b) demonstrates a clearly denser and more homogeneous matrix. The incorporation of fine granite dust enhances particle packing efficiency by filling intergranular voids, reducing pore connectivity, and promoting microstructural refinement (Serelis et al., 2018; Clement et al., 2025). This more compact matrix supports stronger cohesion between binder phases and aggregate particles, relating with the strength increase recorded in GD25 mixes. Such improvements are consistent with previous findings highlighting that fine mineral fillers reduce porosity and stabilize the microstructure, thereby increasing strength and durability (Safing et al., 2025; Upadhyaya et al., 2020).

A clear reduction in large, well-defined crystalline formations is observed in GD25 compared to the control. The CM micrograph displays more coarse crystalline deposits occupying larger voids, while GD25 shows a more continuous gel-like phase with fewer isolated crystal clusters. SEM observations may support the possibility of specific hydration reactions, as the observed microstructural refinement is consistent with improved matrix densification and reduced crystalline disruptions reported in filler-modified cement systems (Mesnage et al., 2025; Prokopski et al., 2020). The finer texture observed in GD25 suggests enhanced packing and a more robust C-S-H gel morphology, both of which are linked to improved long-term mechanical performance and reduced permeability (Cheah et al., 2018; Li et al., 2018).

Overall, SEM observations indicate that 25% granite dust improves mortar performance primarily through its physical filler effect refining particle distribution, reducing voids, and promoting a more cohesive and continuous microstructure. These morphological enhancements align with the compressive strength results and previous studies demonstrating the benefits of incorporating quarry dust and fine mineral additives in mortar (Hassan et al., 2019; Tran & Phan, 2024). The GD25 matrix is therefore more compact, uniform, and potentially more durable compared to the control mix.

4.3.2.4 Summary

The maximum compressive strength recorded at 25% granite dust replacement (GD25) is supported by both the SEM microstructural observations and the XRF elemental composition. The 28-day strength of 37.74 MPa reflects the best balance between particle packing, filler efficiency, and available binder content.

XRF results show that GD25 contains higher CaO and AI2O3 than the control mortar. XRF may support the possibility of hydration-related reactions, as the increased CaO and AI2O3 indicate a binder system richer in oxides that typically contribute to the formation of cementitious phases in blended mortars. Meanwhile, the slightly lower Si02 content in GD25 likely reflects the mineral composition of granite dust, which still contributes fine particles that complement the cement matrix.

SEM analysis further reinforces the mechanical performance by showing that GD25 produces a denser, better-packed microstructure than the control. The fine granite dust particles fill interstitial voids, improving homogeneity and reducing pore connectivity. These effects correspond directly with the observed strength increase, as a denser matrix improves stress transfer and reduces vulnerability to microcrack initiation.

At replacement levels beyond 25%, such as 30% GD, the excessive fines disrupt the balance of binder and aggregate, increasing water demand and reducing packing efficiency under a fixed w/c ratio. This leads to poorer compaction and lower strength. Overall, GD25 represents the best substitution level at which granite dust enhances physical packing while maintaining adequate binder availability. The combined SEM densification and favourable oxide distribution from XRF align well with the superior compressive strength performance of GD25.

4.3.3 Effect of Nano-silica on Compression Properties of Mortar Cube

4.3.3.1 Compressive strength analysis

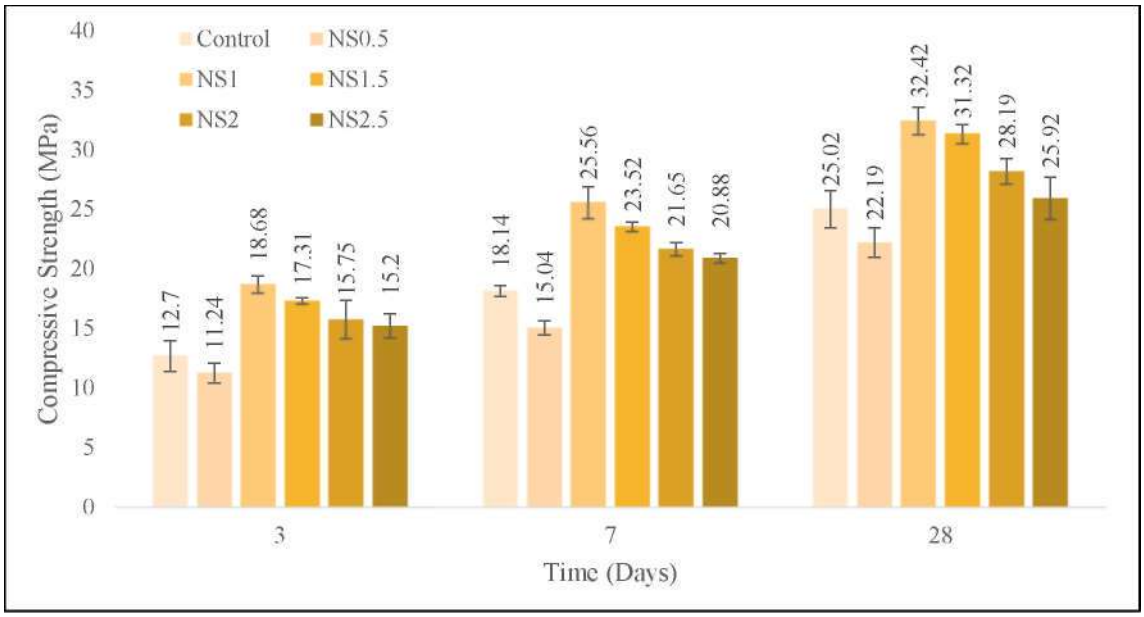

Figure 4.9 Compressive Strength of Mortar Containing Different Weight Percentages of Nano-Silica (NS)

Figure 4.9 presents the compressive strength results of mortar incorporating nano-silica (NS) as a partial cement replacement. The results show a clear enhancement of strength at low NS dosages, followed by a gradual decline beyond the ideal range.

At 3 days, the 1% NS mix (NS1) achieved the highest early strength (18.68 MPa), significantly higher than the control (12.7 MPa). Early-age improvements at low NS contents are commonly attributed to better packing and high specific surface area, which enhance the physical densification of the matrix and improve load transfer efficiency (Xia et al., 2023; Quercia & Brouwers, 2014). Lower strength at NS0.5 and higher dosages (NS2.5) may reflect insufficient NS content or agglomeration at higher contents, which reduces packing efficiency and increases heterogeneity (Labaran et al., 2024; Senff et al., 2012).

At 7 days, the trend remained consistent. The control reached 18.14 MPa, while NS1 produced the highest strength (25.56 MPa). NS1.5 also performed well at this age. Previous studies indicate that when NS is well-dispersed, its ultrafine particles enhance microstructural compactness and reduce pore connectivity, supporting progressive strength development (Hamed et al., 2024; Ghafari et al., 2014). The slight decline at

NS2.0 and NS2.5 suggests reduced dispersion efficiency as dosage increases a behaviour widely reported in nano-modified cement systems (Lavergne et al., 2018).

By 28 days, NSl continued to show the highest strength (32.42 MPa), followed closely by NSl.5 (31.32 MPa). Higher dosages (NS2 andNS2.5) showed improvements over the control but did not exceed the peak strengths achieved by NSl to NSl.5. This effect is consistent with research showing that nano-silica beyond small ideal dosages tends to form agglomerates, reducing its effectiveness as a densifying micro-filler (Althoey et al., 2023; Salman et al., 2024).

Overall, NS significantly enhanced compressive strength, with 1 to 1.5% identified as the best range. Improvements are attributed to physical mechanisms such as enhanced packing and micro-filling. The decline at higher dosages supports existing literature that emphasizes the need for controlled NS content to avoid clustering and reduced effectiveness.

4.3.3.2 Chemical composition viaXRF

Table 4.5 shows the oxide composition of the NSl mortar incorporating 1% nano-silica (NS), compared to the control mix (CS). The major oxides identified SiCh, AI2O3, Fe203, and CaO, reflect the influence of the nano-silica addition on the overall chemical profile of the raw materials. XRF allows comparison of oxide trends that may help understand performance when considered alongside supporting literature.

Table 4.5
Elemental Composition of NSl

Material	**NS 1** (%)	**CS** (%)
$Si0_2$	52.8782	60.2108
AI2O3	5.1564	2.8911
Fe_20_3	2.0851	1.5916
CaO	37.0327	32.2871

Silicon dioxide (SiCh) remained the dominant oxide in both mixes but was lower in NSl (52.88%) than in the control (60.21%). This reduction reflects the addition of nano-silica, which replaces a portion of cement compared to sand. Despite the lower bulk Si02 content, nano-silica is known in previous study to possess high surface

reactivity and can significantly influence microstructure due to its ultrafine particle size (Huseien et al., 2019). Although XRF is limited in confirming pozzolanic reactions or C-S-H formation, the improved mechanical performance observed in NS1 is interpreted as predominantly arising from physical effects such as matrix densification and enhanced particle packing, in agreement with earlier studies.

The AI2O3 content in NS1 increased to 5.16% from 2.89% in the control. This rise likely reflects the presence of alumina-bearing phases in the base cement and marginal contributions from nano-silica processing by-products. Literature indicates that alumina-bearing particles may influence setting behaviour or contribute to refinement of matrix topology (AlTawaiha et al., 2023).

Ferric oxide (Fe20s) content also increased modestly in NS1 (2.09%) compared to the control (1.59%). The increase aligns with common oxide variability between mixes and may reflect trace impurities associated with nano-silica manufacturing. Based on previous studies, Fe203 may exert minor effects on cementitious systems, although confirmation of such interactions is beyond the capability of XRF analysis in the present study (Girskas & Kligys, 2025).

Calcium oxide (CaO) increased from 32.29% in the control to 37.03% in NS1. As CaO begins primarily from cement, the observed increase likely reflects mix proportion. Previous studies suggest that nano-silica can affect CaO utilization during hydration, while the XRF results here may provide indications of whether such interactions developed (Raza et al., 2025). Any improvements in performance therefore remain attributed to physical mechanisms.

In summary, the XRF results indicate that adding nano-silica shifts the oxide composition of the raw mixture toward slightly higher AI2O3, Fe203, and CaO contents. These chemical trends align with literature describing nano-modified systems. The improved mechanical properties observed in NS1 are therefore interpreted primarily through enhanced packing, surface area effects, and densification.

4.3.3.3 Microstructure analysis via SEM

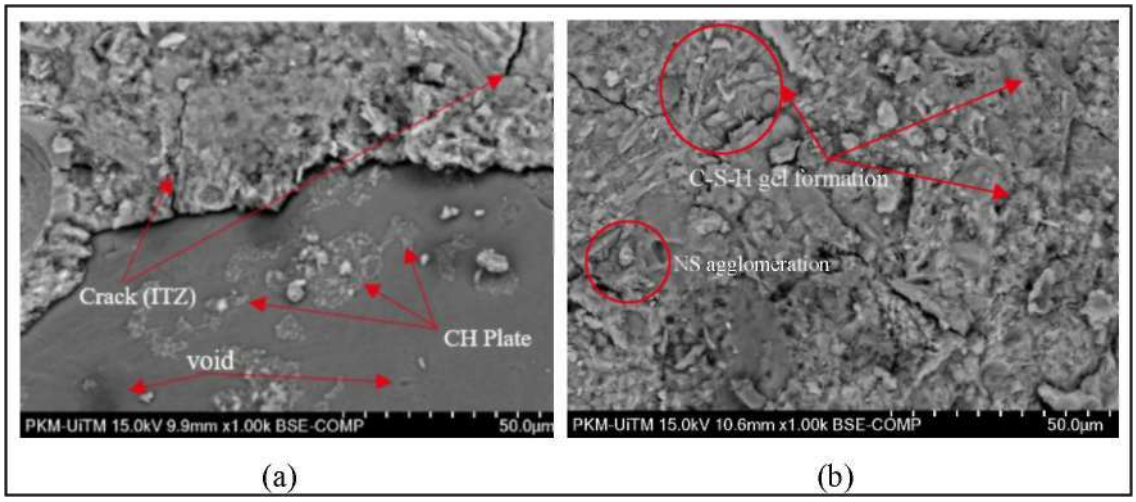

Plate 4.4 SEM Microstructures; (a) CM and (b) NS1

The SEM analysis of the control mortar (CM) and the mortar containing 1% nano-silica (NS1) revealed remarkable differences in microstructure and matrix refinement. In Plate 4.4(a), the control mortar displays a relatively porous matrix with multiple voids, scattered unhydrated cement particles, and large crystalline deposits commonly associated with calcium hydroxide (CH). The presence of these coarse crystalline features and visible microvoids indicates a less refined hydration structure and weaker bonding within the cement matrix (Ghazali et al., 2025; Zhou et al., 2025). Such microstructural discontinuities are typical of mixes without nanomaterial modification and are often linked to reduced mechanical performance and higher permeability (Krishna et al., 2021; Sharma & Vyas, 2023).

In contrast, the NS1 specimen shown in Plate 4.4(b) exhibits a clearly denser and more compact microstructure. The voids observed in the control mortar appear substantially reduced, and the matrix displays a finer and more homogenous texture. This refinement is consistent with the well-reported filler and nucleation effects of nano-silica, which enhance packing density and promote more uniform hydration product formation (AlTawaiha et al., 2023; Labaran et al., 2024). The ultrafine NS particles likely contribute to improved matrix continuity by occupying microvoids and acting as nucleation sites for C-S-H growth, producing a more cohesive microstructural network.

SEM indicated the possibility of such chemical interactions, as the reduced frequency and size of CH-like crystalline bonds in NS1 are consistent with the expected interaction between nano-silica and CH through secondary hydration processes.

Previous studies have shown that nano-silica can facilitate the consumption of calcium hydroxide and support the formation of additional C-S-H gel, contributing to matrix densification and improved strength (Kashyap et al., 2023; Garg et al., 2020). The smoother gel-like formations visible in Plate 4.4(b) align with this mechanism, suggesting more efficient hydration and reduced crystalline interruption within the matrix.

XRF results indicated the possibility of hydration behaviour, the higher CaO and AI2O3 contents detected in NS1 compared to the control are consistent with a matrix containing more refined hydration products and a modified binder composition. The slightly lower SiCh content in NS1 likely exhibits the contribution of externally added nano-silica, whose highly reactive form may participate in pozzolanic reactions more readily than the bulk silica present in control mixes. These changes complement the SEM observations of fewer voids, reduced crystalline features, and better overall matrix cohesion.

Comparing both micrographs, the control mortar shows more porosity, larger interparticle gaps, and irregular crystal formations. Meanwhile, NS1 displays a tighter, more joined microstructure, with improved inter-particle bonding and fewer microcracks. This densification is consistent with the enhanced compressive strength observed experimentally and aligns with literature demonstrating that ideal nano-silica addition (typically 1 to 2%) leads to substantial improvements in microstructural integrity and long-term durability (Althoey et al., 2023; Barbhuiya et al., 2020).

In summary, the SEM analysis proves that incorporating 1% nano-silica significantly refines the mortar microstructure. The NS1 matrix is denser, less porous, and more uniformly hydrated compared to the control. These improvements arise from both the physical filling effect of ultrafine particles and their nucleation-driven promotion of C-S-H formation. Combined, these mechanisms clarify NS1 achieved superior compressive strength and durability characteristics relative to the control mix.

4.3.3.4 Summary

The incorporation of nano-silica significantly improved the compressive strength of mortar, with the highest performance occurring at 1% replacement (NS1). At 28 days, NS1 achieved 32.42 MPa, outperforming the control by a substantial margin. This improvement is consistent with the widely reported effects of nano-silica,

which include matrix densification, refined pore structure, and enhanced early-age hydration kinetics.

XRF results show that NS1 contains slightly higher CaO and AI2O3 than the control mortar. The altered oxide proportions from XRF suggest the presence of a more chemically diverse binder system. The slightly lower SiCh content in NS1 reflects the use of nano-silica, whose highly reactive amorphous form contributes physically and chemically to microstructural refinement even when present in small quantities.

SEM observations strongly support the mechanical results. NS1 exhibits a denser and more homogeneous microstructure, with clearly fewer voids and fewer coarse crystalline features than the control. These improvements align with the filler effect and nucleation capability of nano-silica, both of which contribute to a more continuous and refined C-S-H gel morphology. The control mix, by contrast, displays larger pores and unhydrated cement particles, explaining its lower compressive strength.

Overall, the SEM densification and the compositional features identified by XRF correspond with the superior strength development of the NS1 mix. The results verify that 1% nano-silica provides an ideal dosage under the fixed w/c ratio, achieving the best balance between workability, hydration efficiency, and microstructural refinement.

4.3.4 Effect of Nano-silica on Compression Properties of GD Mortar Cube

4.3.4.1 Compressive strength analysis

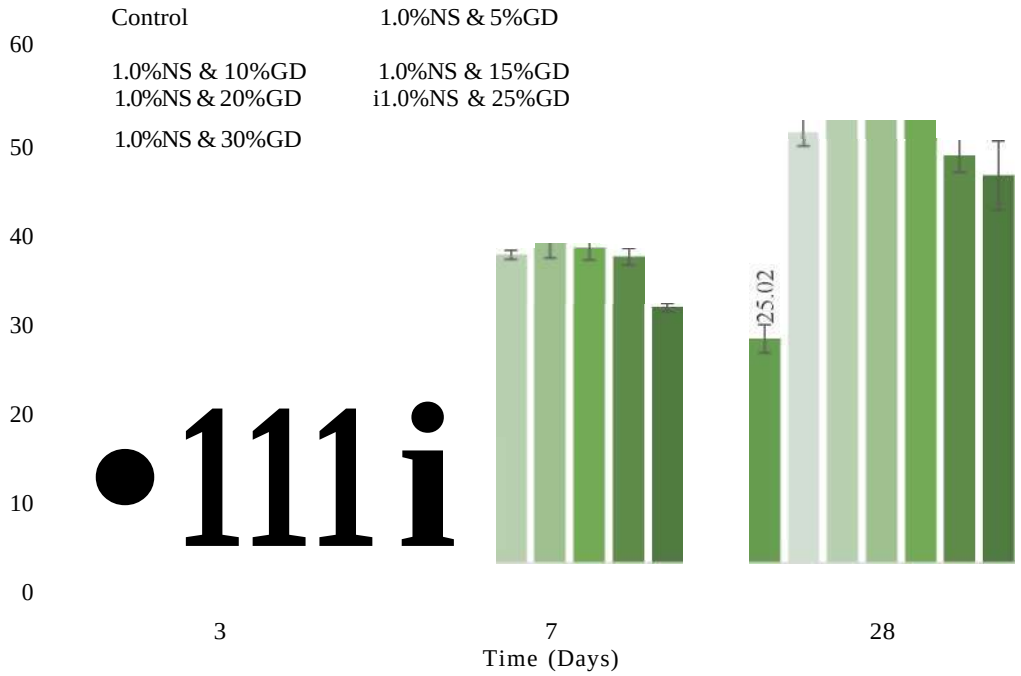

Figure 4.10 Compressive Strength of Mortar Containing Different Weight Percentages of Granite Dust Filled Nano-Silica (GDNS)

Figure 4.10 shows the compressive strength results for mortar containing 1% nano-silica (NS) and varying granite dust (GD) contents. The results demonstrate strong synergistic effects at moderate GD levels, with substantial improvements relative to the control mix across all curing ages.

At 3 days, the control mix (12.7 MPa) showed typical early-age strength. Mixes containing NS and GD displayed higher strengths, with 1% NS + 5 to 15% GD achieving 14.89 to 16.89 MPa. The improvements reflect combined micro-filling by GD and nano-filling by NS, which collectively improve packing efficiency (Reddy et al., 2020; Mukharjee & Barai, 2020). At 25% GD, strength decreased slightly, and the GD30 mix (13.76 MPa) showed more pronounced reduction, consistent with workability limitations associated with excessive fines.

At 7 days, strength gains were significant. The control reached 18.14 MPa, while mixes containing 1% NS + 5 to 20% GD achieved 33.99 to 35.72 MPa. These increases align with previous studies reported that hybrid filler systems with complementary particle sizes form more compact matrices and reduce voids, leading to better load transfer capability (Brouwers, 2006; Tran & Phan, 2024). GD30 again padded,

indicating that very high GD content weakens the matrix and restricts effective compaction under constant w/c.

By 28 days, the synergistic effect became more pronounced. The highest strengths were observed at 1% NS + 15% GD (51.54 to 52.63 MPa). Mixes with 5 to 25% GD all exceeded the control, but strength declined at GD30 (43.21 MPa). This peak at 15% GD suggests ideal intersection of micro-filling (GD) and nano-filling (NS) effects, yielding improved packing and refined internal structure, as supported by multi-scale filler research (Yazici et al., 2021; Quercia & Brouwers, 2014).

Overall, the GDNS mixes demonstrated significantly higher strengths than their individual GD or NS counterparts. The results indicate that 1% NS + 10 to 20% GD offers the most effective hybrid combination, with 15% GD achieving the highest strengths at all curing ages. Improvements occur from complementary physical filling mechanisms. Excessive GD (>30%) reduces strength due to increased fines content affecting workability and entrapped air.

4.3.4.2 Chemical composition viaXRF

Table 4.6 summarises the oxide composition of the NS1+GD15 mortar incorporating 1% nano-silica and 15% granite dust, compared to the control mix. The oxide profile reflects contributions from both materials and helps contextualise the physical performance trends observed in strength and density tests. As with other mixes, XRF provides information about raw material composition.

Table 4.6
Elemental Composition of NS1+GD15

Material	**NS1+GD15** (%)	**CS** (%)
$Si0_2$	54.5187	60.2108
AI2O3	4.6166	2.8911
Fe_20_3	2.1237	1.5916
CaO	35.7504	32.2871

Silicon dioxide ($Si0_2$) content in NS1+GD15 was 54.52%, slightly lower than the control (60.21%) but still within a range typical of silica-rich mineral fillers. Granite dust contributes crystalline silica from quartz and feldspar, while nano-silica contributes

amorphous silica; therefore, the XRF findings may suggest the combined presence of these forms. Literature suggests that the presence of fine silica-bearing materials may support microstructural refinement (Ghazali et al., 2025; Maagi et al., 2020). In the present context, the SiCh levels simply reflect the combined mineralogy of GD andNS.

Aluminium oxide (AI2O3) was higher in NS1+GD15 (4.62%) than in the control mix (2.89%), consistent with the alumina-bearing minerals found in granite dust. While AI2O3 may influence certain hydration pathways when reactive forms are present, the increased AI2O3 content in this study is interpreted as an indicator of granite dust incorporation, aligning with its known mineral composition (AlTawaiha et al., 2023).

Ferric oxide (Fe2C>3) also increased slightly to 2.12%, again reflecting typical granite mineralogy. Fe203 is mostly reported to exert minimal influence on mechanical performance, but it remains a typical oxide associated with igneous-derived fillers.

Calcium oxide (CaO) content in NS1+GD15 (35.75%) was higher than in the control (32.29%)). Since cement is the dominant source of CaO in mortar, variations are primarily due to mix proportioning. Granite dust may also contribute small amounts of CaO due to feldspar content. Literature describes interactions between calcium hydroxide and reactive silica in blended systems, and the XRF results in this study may be interpreted as consistent with the presence of oxides that could support the mechanisms.

In conclusion, the XRF analysis of NS1+GD15 exposes the expected oxide contributions of granite dust and nano-silica in mortar system. The combined presence of Si02, AI2O3, Fe203, and CaO indicates that the blend is chemically compatible with cementitious materials. Improvements in compressive strength and density observed in the mechanical tests are therefore attributed to physical synergistic effects enhanced packing, better particle distribution, and reduced void content. The oxide profile supports the suitability of GD and NS as sustainable supplementary materials in mortar.

4.3.4.3 Microstructure analysis via SEM

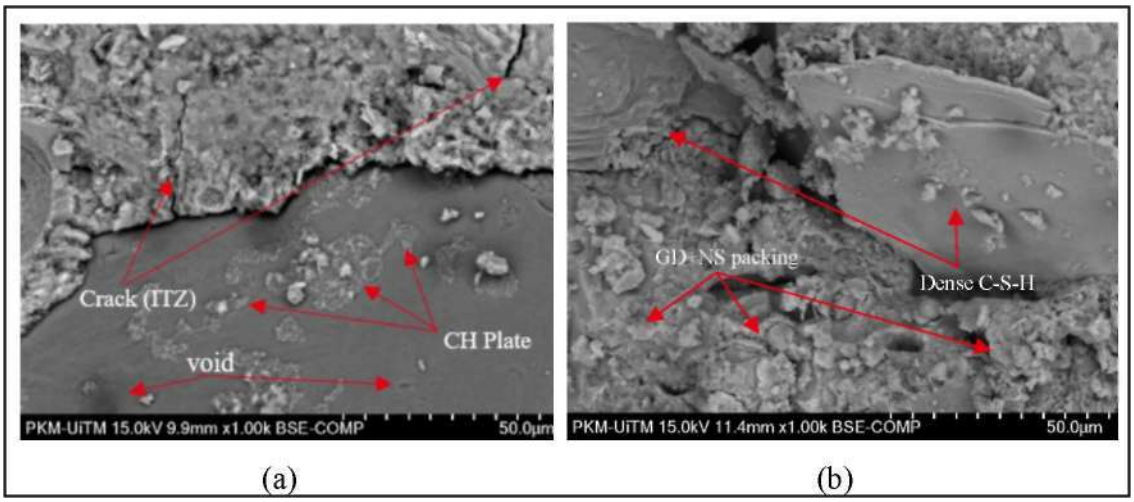

Plate 4.5 SEM Microstructures; (a) CM and (b) NS1GD15

The SEM micrographs in Plate 4.5 highlight clear microstructural differences between the control mortar (CM) and the GDNS mortar incorporating 1% nano-silica and 15% granite dust (NS1+GD15). In the control specimen (Plate 4.5a), the matrix exhibits a heterogeneous and porous structure, characterized by numerous voids, microcracks, and large crystalline formations typical of calcium hydroxide (CH). These coarse and well-defined crystals often occupy significant pore spaces and produce discontinuities within the matrix, which can adversely affect mechanical performance by creating weak zones susceptible to cracking and reduced long-term durability (Krishna et al., 2021; Zhou et al., 2025). The presence of unhydrated cement grains further suggests areas of incomplete hydration and inefficient particle bonding within the control mortar.

In contrast, the NS1+GD15 specimen (Plate 4.5b) exhibits a noticeably denser, more cohesive, and refined microstructure. The matrix appears more compact, with fewer distinguishable voids and reduced crystalline deposits compared to the control mix. This refinement is consistent with the combined physical and microstructural effects of nano-silica and granite dust, both of which contribute to improved packing efficiency and matrix densification (Serelis et al., 2018; Labaran et al., 2024). The ultrafine nano-silica particles likely fill microvoids and function as nucleation sites for C-S-H development, while the granite dust provides additional microfiller action by occupying interstitial spaces between cement and sand particles (Upadhyaya et al., 2020; Safing et al., 2025).

The reduced size and frequency of CH-like crystalline features and the more uniform gel-like matrix in NS1+GD15 showed thru SEM are consistent with secondary matrix refinement commonly associated with nano-silica modification. Nano-silica's high surface area enables efficient interaction within the matrix, improving the distribution and continuity of hydration products, which contributes to the dense morphology observed in Plate 4.5(b) (AlThoey et al., 2023; Garg et al., 2020). Meanwhile, granite dust, rich in aluminosilicate phases, enhances microfillers' ability to reduce pore connectivity and support the development of a more robust C-S-H network (Tran & Phan, 2024; Hassan et al., 2019).

The XRF results for NS1+GD15 indicate higher AI2O3 content and altered CaO and Si02 proportions relative to the control mix. The oxide distributions from XRF are consistent with a mortar containing a more diverse and densely packed binder phase. Increased alumina content is often associated with improved matrix refinement and formation of additional hydration-related phases in blended systems (Moutei et al., 2018). Likewise, the higher silica contribution from GD and nano-silica supports the microstructural observation of a more continuous and interconnected gel-like texture.

Overall, the SEM images clearly show that the NS1+GD15 mortar has a significantly denser and more homogeneous microstructure than the control. The combination of nano-silica and granite dust offers complementary benefits nano-silica enhances refinement through ultrafine particle filling and nucleation effects, while granite dust improves matrix packing and reduces macro-porosity. These improvements correspond with the substantial increase in compressive strength observed for the NS1+GD15 mix. The refined SEM structure is therefore indicative of enhanced mechanical performance, reduced permeability, and potentially greater durability under long-term exposure.

In summary, the hybrid incorporation of 1% nano-silica and 15% granite dust produces a significantly improved mortar microstructure characterized by reduced porosity, fewer microcracks, refined gel morphology, and enhanced internal cohesion. These microstructural enhancements help explain the superior mechanical behavior of the GDNS mixes and demonstrate the potential of this blended approach for sustainable high-performance mortar applications.

4.3.4.4 Summary

The GDNS modified mortar mix incorporation of granite dust (15%) and nano-silica (1%>) produced the best overall performance among all mortar mixes. At 28 days, the NS1+GD15 mix achieved 52.63 MPa, approximately a 110% increment of the compressive strength compared to the control mix. This exceptional performance arises from complementary physical and microstructural mechanisms provided by both materials.

XRF analysis shows that NS1+GD15 has a balanced oxide profile, with higher AI2O3 and moderately higher CaO compared to the control. The presence of these oxides is consistent with a binder matrix that benefits from both nano-silica modification and mineral contributions from granite dust.

SEM images reveal a markedly denser and more refined matrix for NS1+GD15, characterized by reduced porosity, improved particle packing, and a more uniform distribution of gel-like hydration products. Nano-silica contributes to matrix refinement through ultrafine particle filling and nucleation effects, while granite dust enhances aggregate packing and reduces internal voids. Together, these materials create a established and cohesive microstructure capable of sustaining higher compressive loads.

4.4 Flexural Behaviour of Cracked Mortar Bars Repaired with Carbon Fibre Wrap and Modified Mortar Patch

This section discusses the flexural performance of six mortar bar configurations summarised in Table 4.7. The results are presented in terms of peak flexural strength in Figure 4.11 and the corresponding load-deflection curves in Figure 4.12. For each configuration, three specimens were tested, and the mean values are plotted with standard deviation, thereby providing a measure of the experimental variability. Although formal toughness evaluation in accordance with ASTM CI609 requires quantified post-crack energy indices, the present discussion refers to qualitative ductility behaviour based on the shape of the load-deflection curves obtained in this study. These interpretations therefore reflect relative post-cracking behaviour.

Table 4.7
Results of Flexural Properties of Six Different Types of Specimens

No	Type of specimens	Notation	Detail of Formulation
1	Control Mortar bar	Cs	0.5 water cement ratio 70% sand + 30% OPC Flexural Strength: 2.73 MPa
2	Granite Dust filled Nano-silica Mortar bar	GDNSs	0.5 water cement ratio 15% Granite Dust + 1% Nano-silica + 55% sand +29% OPC Flexural Strength: 3.20 MPa
3	Control Mortar bar wrapped with Carbon Fibre Reinforced Polymer	Cs + CFRP Wrap	0.5 water cement ratio 70% sand + 30% OPC Flexural Strength: 9.44 MPa
4	Granite Dust filled Nano-silica Mortar bar wrapped with Carbon Fibre Reinforced Polymer	GDNSs + CFRP Wrap	0.5 water cement ratio 15% Granite Dust + 1% Nano-silica + 55% sand +29% OPC Flexural Strength: 14.46 MPa
5	Cracked Granite Dust filled Nano-silica Mortar bar patched with Control Patch & wrapped Carbon Fibre Reinforce Polymer	GDNSs + Cp + CFRP Wrap	0.5 water cement ratio (specimen) 15% Granite Dust + 1% Nano-silica + 55% sand +29% OPC (patch) 70% sand + 30% OPC Flexural Strength: 11.40 MPa
6	Cracked Granite Dust filled Nano-silica Mortar bar patched with Modified mortar Patch & wrapped Carbon Fibre Reinforce Polymer	GDNSs + GDNSp + CFRP Wrap	0.5 water cement ratio (specimen) 15% Granite Dust + 1% Nano-silica + 55% sand +29% OPC (patch) 15% Granite Dust + 1% Nano-silica + 55% sand +29% OPC Flexural Strength: 13.42 MPa

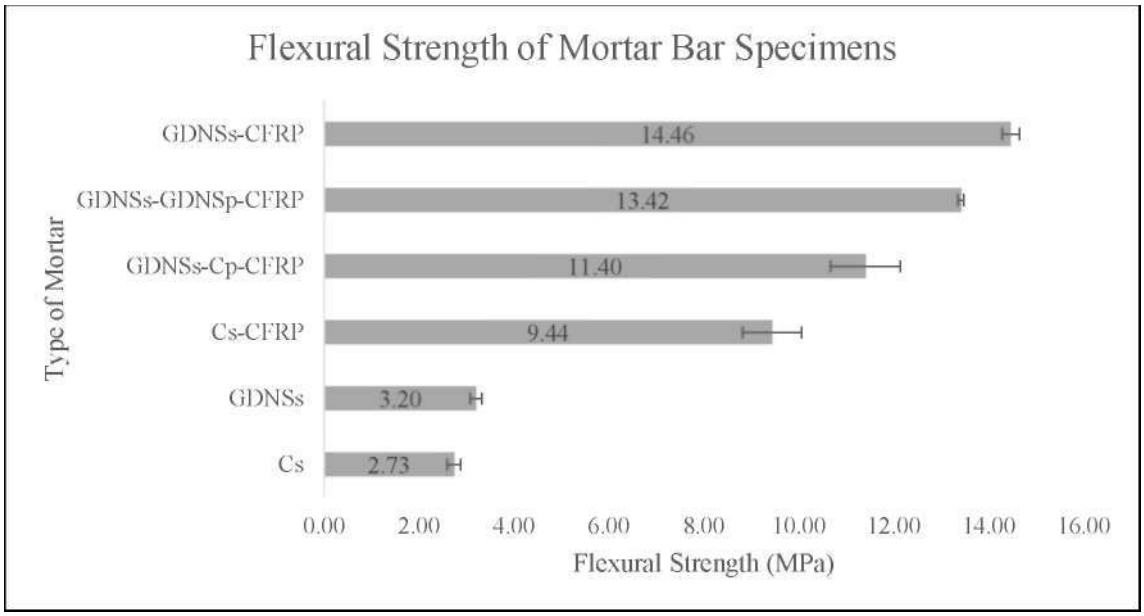

Figure 4.11 Flexural Strength of Six Different Types of Specimens Mortar Bars

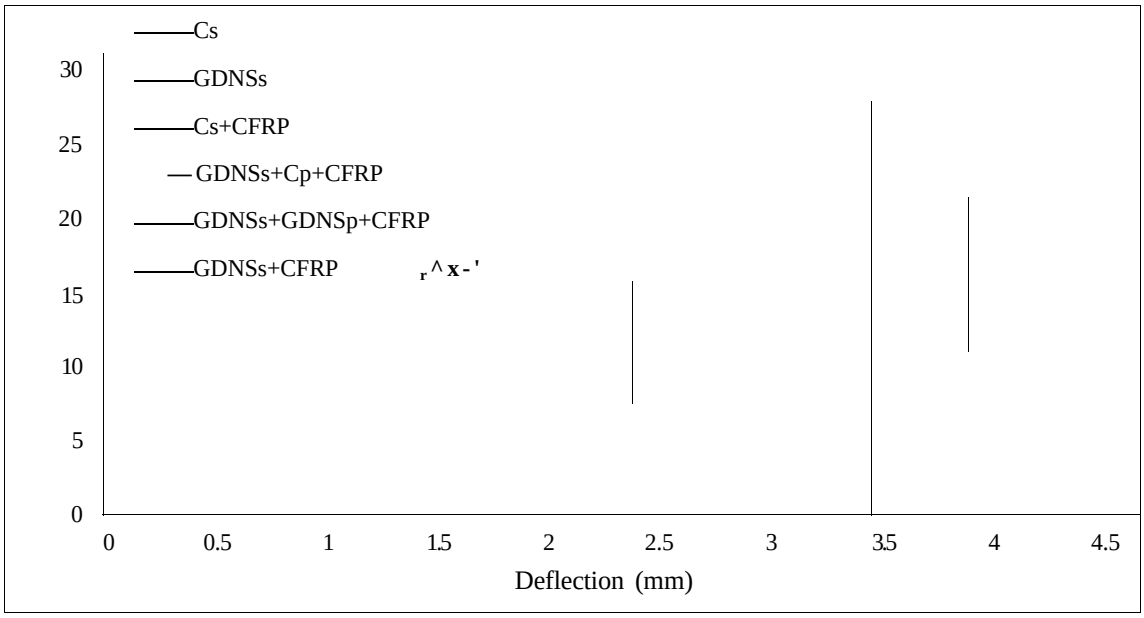

Figure 4.12 Load Deflection Curves of Six Different Types of Specimens Mortar Bars

The control specimen (Cs) recorded a flexural strength of 2.73 MPa, while the GDNS specimen (15 % granite dust and 1 % nano-silica) achieved 3.20 MPa. The improvement is attributed mainly to the physical contribution of granite dust in improving particle-packing efficiency and the micro-filling and pore-refinement abilities of nano-silica, which together reduce voids and enhance bending resistance relative to the control mix (Quercia & Brouwers, 2014; Kashyap et al., 2023; Chen et al., 2020). These observations are consistent with compressive-strength behaviour discussed previously and agree with similar reports on hybrid systems (Mukharjee & Barai, 2020; Yazici et al., 2021).

A substantial improvement was observed when CFRP was externally applied. The wrapped control specimen (Cs-CFRP) demonstrated a flexural strength of 9.44 MPa, whereas the wrapped GDNS specimen (GDNSs-CFRP) recorded the highest value of 14.46 MPa. CFRP acts as an external tensile reinforcement layer that limits crack opening, delays propagation, and redistributes tensile stresses during bending, which explains the significant improvement compared with unwrapped specimens (Zhou et al., 2024; Liu et al., 2025; Kothari et al., 2023). In the load-deflection curves in Figure 4.12, both wrapped configurations exhibited extended post-crack regions with increased ultimate deformation. The extended deflection behaviour is widely interpreted as improved flexural ductility and energy absorption (El-Gamal et al., 2022; Choi et al., 2021).

For the cracked specimens, two repair strategies were evaluated. The cracked GDNS specimen patched with control mortar and wrapped with CFRP (GDNSs-Cp-CFRP) reached 11.40 MPa, whereas the cracked specimen patched with GDNS mortar prior to wrapping (GDNSs-GDNSp-CFRP) reached 13.42 MPa, exceeding the strength of the original GDNS specimen. This indicates that the combination of internal modification (GDNS patch) and external reinforcement (CFRP wrap) not only restores mechanical performance after cracking but also enhances it beyond the uncracked state, consistent with repair mechanisms involving filler-matrix densification and interfacial strengthening (Chindaprasirt et al., 2025; Elhag et al., 2023).

In the load-deflection behaviour, the GDNSs-GDNSp-CFRP configuration displayed the longest descending branch and the highest residual load following first crack. These results suggest that GDNS patching improves interfacial bonding at the crack region while CFRP provides external confinement, resulting in improved post-crack load redistribution and greater deformation capacity. The combined contribution is consistent with recent findings where GDNS repair systems produce more ductile response mechanisms in cementitious composites (Huts et al., 2024; Chun et al., 2025; Zhao et al., 2023).

Figure 4.12 showed the area under the load-deflection curves is clearly greater for all wrapped specimens compared with unwrapped configurations. The qualitative interpretation of this area indicates improved post-cracking load retention, delayed brittle failure, and increased deformation capability behaviour typically associated with increased flexural ductility and toughness (Vijayan et al., 2023; Kothari et al., 2023). Both GDNS modification and CFRP reinforcement contributed to these improvements,

but the most pronounced enhancement occurred when GDNS patching was combined with CFRP wrapping. Overall, the findings demonstrate that GDNS-CFRP repair provides a viable strengthening approach for damaged mortar elements and produces a more ductile and sustainable repair system with significantly improved flexural response.

CHAPTER 5
CONCLUSION

5.1 Introduction

This research evaluated the feasibility of incorporating granite dust (GD) as a partial sand replacement and nano-silica (NS) as a partial cement replacement to support sustainable mortar development, while also examining the flexural enhancement of GDNS-modified mortar using carbon fiber reinforced polymer (CFRP) patching. The study experimentally fulfilled the objectives through characterization analysis, physical and mechanical testing, and structural strengthening evaluation of modified mortar compositions. Accordingly, RO1 investigated the physical characteristics of GD and NS and their influence on mortar properties. RO2 examined the compressive behavior of various GD, NS, and GDNS mixes and identified the optimum synergistic combination. RO3 assessed the structural strengthening capability of CFRP wrapping applied to uncracked and cracked GDNS mortar specimens. This chapter synthesizes the key findings and articulates the scientific implications of the results. It further outlines practical relevance, sustainability contribution, and recommendations for future investigation emerging from the study.

5.2 Conclusion and main findings

Based on the findings, the following conclusions have been determined:

5.2.1 Effect of Granite Dust and Nano-Silica Content on The Physical Properties of Mortar

The characterization of raw materials, including sand, granite dust (GD), cement, and nano-silica (NS), was carried out using PSD, moisture content, XRF, and SEM analyses. Particle size results showed that nano-silica and granite dust contributed to reducing microvoids and improving packing density within the mortar matrix. Cement and sand exhibited comparatively coarser particle ranges, while the higher fineness of NS suggests its potential to enhance packing at the microscale. The

distribution intensities of cement (37.2%), sand (31.4%), NS (26.3%), and GD (20.8%) indicated complementary filler roles, although individual particle size values may be affected by particle agglomeration, particularly in the case of nano-silica.

Moisture content analysis showed that nano-silica exhibited the highest moisture absorption (1.85%) due to its ultrafine size and high surface energy. As a result, mixes incorporating NS require careful water adjustment to balance flowability and strength, while sand and GD (0.16% and 0.30%) demonstrated minimal influence on water demand at the tested replacement levels.

Chemical composition analysis indicated that silica (SiCh) was the dominant compound in sand (89.168%), GD (79.504%), and NS (99.0857%). The high silica content suggests the potential for pozzolanic contribution, although the formation of additional C-S-H should be interpreted jointly with mechanical and microstructural results.

SEM images qualitatively supported improved microstructural refinement, where GD exhibited angular and porous textures that may enhance particle interlock, while NS appeared in ultrafine spherical formations that could assist hydration. However, SEM may suggest hydration-related features, and therefore interpretations were made cautiously and evaluated together with the broader material behaviour observed in this study.

5.2.2 Mechanical Properties of Various Mixes for Granite Dust and Nano-Silica in Mortar

The incorporation of 25% granite dust (GD25) produced the highest compressive strength among the GD-only mixes (37.74 MPa at 28 days). This improvement is primarily attributed to the filler effect and the enhanced packing capability of GD. SEM observations showed reduced visible porosity and improved matrix density with GD addition.

The incorporation of 1% nano-silica (NS1) resulted in a marked increase in compressive strength (32.42 MPa at 28 days compared to 25.02 MPa for the control). This improvement was mainly due to the pozzolanic potential of NS and its role in refining pore structure and promoting hydration. XRF findings indicated slightly increased CaO and AI2O3 contents, which may suggest enhanced formation of hydration-related phases. However, it should be observed that such interpretations are

considered indicative and are drawn from the combined data of XRF, SEM and mechanical results.

The combined mix of 15% GD and 1% NS (GD15+NS1) achieved the highest compressive strength (52.63 MPa at 28 days), indicating a synergistic effect between GD and NS. GD improved packing density, while NS refined pore structure and supported hydration, leading to a more compact microstructure. While mechanical performance strongly supports this synergy, interpretations of hydration mechanisms were made cautiously and are based on combined material characterization and mechanical results. These findings demonstrate that GD15+NS1 can be considered the most effective mix within the scope of this study and highlights the sustainable potential of combining industrial waste (GD) with reactive mineral additives (NS).

5.2.3 Mechanical Performance of Nano-Silica-Granite Dust Mortar Strengthened with Carbon Fibre Wrapping

The application of Carbon Fibre Reinforced Polymer (CFRP) enhanced the flexural performance of GDNS mortar. For uncracked specimens, flexural strength increased from 3.202 MPa to 14.46 MPa, indicating significant confinement and improved tensile stress redistribution under bending. For cracked specimens, the GDNS patch followed by CFRP wrapping achieved 13.42 MPa, outperforming the control patch wrapped with CFRP (11.40 MPa).

These improvements reflect the complementary roles of both repair components: CFRP delayed crack propagation and improved tensile resistance, while the GDNS patch contributed to matrix densification and improved interfacial bonding at the crack region. The observed enhancements are based on the combined evaluation of mechanical results.

From a practical perspective, the GDNS-CFRP system demonstrates potential as a sustainable strengthening and rehabilitation approach for mortar, as it effectively restores and improves flexural performance compared to the original uncracked state.

5.3 Limitations of This Study

Although this study demonstrated the potential of granite dust (GD) and nano-silica (NS) as sustainable materials in mortar, several limitations should be acknowledged. Firstly, the experimental programme focused mainly on 28 days of mechanical and microstructural performance and did not include long-term durability assessments such as water absorption, carbonation, chloride penetration or exposure to aggressive environments. Secondly, microstructural interpretation relied primarily on XRF and SEM, which provide elemental and morphological information but do not directly confirm hydration phases or reaction mechanisms directly. Thirdly, only a limited range of GD and NS replacement levels was examined, and the mechanical behaviour was studied mainly under flexural loading and CFRP strengthening within controlled laboratory conditions. Therefore, further investigation involving alternative loading conditions, durability testing, and broader optimization of material proportions is recommended to support future practical applications.

5.4 Recommendations for Future Research

Although promising results were obtained, research on mortar incorporating the dual actions of granite dust (GD) as a partial sand replacement and nano-silica (NS) as a partial cement replacement remains limited. The combined use of these materials has demonstrated potential in enhancing mechanical performance while reducing reliance on natural resources. To advance knowledge in this area, the following recommendations are proposed:

1) Long-Term Curing and Strength Development:
   Future studies should investigate the influence of GD and NS over extended curing ages (e.g., 90, 180, or 365 days). This would provide insight into the long-term hydration reactions, pozzolanic activity, and microstructural development that may continue to enhance strength and durability beyond the standard 28-day curing period.
2) Investigation of Fresh State Properties:
   It is recommended to explore the fresh-state properties such as setting time of GDNS modified mortars patch. Since both materials influence water demand granite dust due to its angular, porous nature and nano-silica due to its ultrafine

particle size; understanding their combined impact is crucial for optimizing mix design and ensuring practical application in construction.

3) Advanced Repair and Rehabilitation Using Natural Fibre Reinforcement: Beyond CFRP wrapping, future studies should explore the potential of natural fibre reinforcement systems, such as jute, bamboo, or coir fibres, as sustainable alternatives for structural repair and rehabilitation. These fibres offer advantages in terms of low cost, biodegradability, and reduced environmental impact. While challenges such as variability, durability, and moisture sensitivity must be addressed, combining GDNS modified mortars with natural fibre composites could provide an eco-friendly pathway to improve crack resistance, bond strength, and long-term repair performance.

REFERENCES

Abbas, M. M. (2025). Recycling waste materials in construction: Mechanical properties and predictive modeling of Waste-Derived cement substitutes. Waste Management Bulletin. https://doi.Org/10.1016/j.wmb.2025.01.004

Abdulsalam, B., Ali, A. H., Elsafty, A., & Elshafey, N. (2021). Behavior of GFRP strengthening masonry walls using glass fiber composite anchors. Structures, 29, 1352-1361. https://doi.Org/10.1016/j.istruc.2020.12.025

Aggarwal, P., Singh, R. P., & Aggarwal, Y. (2015). Use of nano-silica in cement-based materials-A review. Cogent Engineering, 2(1), 1078018. https://doi.org/10.1080/23311916.2015.1078018

Ahamed, V. S., & Siddiraju, S. (2016). Study of strength of concrete with palm oil fuel ash as cement replacement. International Journal of Civil Engineering and Technology, 7(3), 337-341.

Ahsan, M. B., & Hossain, Z. (2018). Supplemental use of rice husk ash (RHA) as a cementitious material in concrete industry. Construction and Building Materials, 178, 1-9. https://doi.Org/10.1016/j.conbuildmat.2018.05.101

Aitbayeva, A., Das, S., & Ruskamp, R. (2021, December 8). Concrete repair durability [Presentation]. Advanced Materials of Construction Course, University of Nebraska-Lincoln.

Akbar, A., & Mehmood, I. (2022). Flexural performance of fibre-reinforced cement composites under post-crack loading conditions. Construction and Building Materials, 322, 125879. https://doi.Org/10.1016/j.conbuildmat.2022.125879

Akbulut, Z. F., Tawfik, T. A., Smarzewski, P., & Guler, S. (2025). Advancing hybrid Fiber-Reinforced Concrete: performance, crack resistance mechanism, and future innovations. Buildings, 15(8), 1247. https://doi.org/10.3390/buildingsl5081247

Al-Daraji, M., & Aljalawi, N. (2024). The effect of kevlar fibers on the mechanical properties of lightweight perlite concrete. Engineering Technology & Applied Science Research, 14(1), 12906-12910. https://doi.org/10.48084/etasr.6665

Ali, M., & Al-Tersawy, S. (2012). Recycled glass powder as a partial replacement of cement in concrete. Construction and Building Materials, 35, 785-791. https://doi.Org/10.1016/j.conbuildmat.2012.04.132

Ali, M., Abed, F., & Wong, C.-H. (2017). Granite waste as a supplementary cementitious material in concrete. Construction and Building Materials, 132, 266-273.

Ali, P. F., Goh, G. G., & Asmawi, A. (2025). Strategies for achieving sustainable management of offshore sand mining in Malaysia. Sustainability, 17(4), 1679. https://doi.org/10.3390/sul7041679

Aliha, M. R. M., Bahmani, A., & Ayatollahi, M. R. (2012). Mixed mode fracture toughness testing of Portland cement concrete using semicircular bend specimens. Construction and Building Materials, 37, 634-643.

Al-Kharabsheh, B. N., Arbili, M. M., Majdi, A., Ahmad, J., Deifalla, A. F., Hakamy, A., & Alqawasmeh, H. M. (2022). Feasibility Study on Concrete Made with Substitution of Quarry Dust: A Review. Sustainability, 14(22), 15304. https://doi.org/10.3390/sul42215304

Alsuhaibani, E. (2024). Optimization of carbon Fiber-Reinforced polymer (CFRP) configuration for enhanced flexural performance in strengthened concrete beams. Buildings, 14(12), 3953. https://doi.org/10.3390/buildingsl4123953

AlTawaiha, H., Alhomaidat, F., & Eljufout, T. (2023). A review of the effect of Nano-Silica on the mechanical and durability properties of cementitious composites. Infrastructures, 8(9), 132. https://doi.org/10.3390/infirastructures8090132

Althoey, F., Hassan, A., & Hossain, K. (2023). Influence of nano-silica on rheology and performance of cementitious binders. Journal of Building Engineering, 64, 105780. https://doi.org/10.1016/jjobe.2022.105780

Althoey, F., Zaid, O., Martinez-Garcia, R., Alsharari, F., Ahmed, M., & Arbili, M. M. (2023). Impact of Nano-silica on the hydration, strength, durability, and microstructural properties of concrete: A state-of-the-art review. Case Studies in Construction Materials, 18, e01997. https://doi.Org/10.1016/j.cscm.2023.e01997

Amran, M., Lee, Y. H., Fediuk, R., Murali, G., Mosaberpanah, M. A., Ozbakkaloglu, T., Lee, Y. Y., Vatin, N., Klyuev, S., & Karelia, M. (2021). Palm Oil Fuel Ash-Based Eco-Friendly Concrete Composite: A Critical Review of the Long-Term Properties. Materials, 14(22), 7074. https://doi.org/10.3390/mal4227074

Amudhavalli, N., Sivasankar, S., Shunmugasundaram, M., & Kumar, A. P. (2020). Characteristics of granite dust concrete with M-sand as replacement of fine

aggregate composites. Materials Today Proceedings, 27, 1401-1406. https://doi.Org/10.1016/j.matpr.2020.02.771

Amulya, G., Moghal, A. a. B., & Almajed, A. (2021). A State-of-the-Art Review on Suitability of granite dust as a sustainable additive for geotechnical applications. Crystals, 11(12), 1526. https://doi.org/10.3390/crystlll21526

Ashokan, A., Rajendran, S., & Dhairiyasamy, R. (2023). A comprehensive study on enhancing of the mechanical properties of steel fiber-reinforced concrete through nano-silica integration. Scientific Reports, 13(1). https://doi.org/10.1038/s41598-023-47475-0

Ashraf, M. A., Maah, M. J., Yusoff, I., Wajid, A., & Mahmood, K. (2011). Sand mining effects, causes and concerns: A case study from Bestari Jaya, Selangor, Peninsular Malaysia. Scientific Research and Essays, 6(6), 1216-1231. https://doi.org/10.5897/srel0.690

Asmatulu, E., Twomey, J., & Overcash, M. (2013). Recycling of fiber-reinforced composites and direct structural composite recycling concept. Journal of Composite Materials, 48(5), 593-608. https://doi.org/10.1177/0021998313476325

Baggio, C, Fabbrocino, F., & Manfredi, G. (2014). State-of-the-art in the use of fiber-reinforced polymer (FRP) composites for concrete structures rehabilitation: Techniques and applications. Construction and Building Materials, 66, 146-157.

Balakrishnan, B. (2017). FLOW PROPERTIES AND STRENGTH BEHAVIOUR OF MASONRY MORTAR INCORPORATING HIGH VOLUME FLY ASH. International Journal of Geomate, 12(31). https://doi.org/10.21660/2017.31.19763

Barbhuiya, G. H., Moiz, M. A., Hasan, S. D., & Zaheer, M. M. (2020). Effects of the nanosilica addition on cement concrete: A review. Materials Today Proceedings, 32, 560-566. https://doi.Org/10.1016/j.matpr.2020.02.143

Barbhuiya, S., Chow, P., & Mo, K. (2020). Nano-silica modified cement systems: A review of rheology, hydration and microstructure. Construction and Building Materials, 260, 120436. https://doi.Org/10.1016/j.conbuildmat.2020.120436

Beigi, M. H., Bahrami, A., & Pouramir, S. M. (2013). Effect of nano-silica on mechanical properties of concretes containing lowquality aggregates.

Construction and Building Materials, 54, 1-9. https://doi.Org/10.1016/j.conbuildmat.2013.02.044

Beigi, M. H., Berenjian, J., Omran, O., Nikbin, I. M., & Khorami, M. (2013). Influence of nano-silica and micro-silica on concrete performance. Construction and Building Materials, 47, 1029-1038. https://doi.Org/10.1016/j.conbuildmat.2013.05.069

Benli, A., Arslan, N., & Aydin, A. (2019). Using granite waste as a partial sand replacement in mortar. Materials Research Express, 6, 125001. https://doi.org/10.1088/2053-1591/ab5eel

Benli, A., Karatas, M., & Toprak, H. A. (2019). Mechanical characteristics of self-compacting mortars with raw and expanded vermiculite as partial cement replacement at elevated temperatures. Construction and Building Materials, 239, 117895. https://doi.Org/10.1016/j.conbuildmat.2019.117895

Bentz, D. P., Ferraris, C. F., Jones, S. Z., & Peltz, M. A. (2017). Influence of waterreducing admixtures on cement hydration and porosity. Cement and Concrete Composites, 79, 80-92. https://doi.Org/10.1016/j.cemconcomp.2017.02.005

Bentz, D. P., Ferraris, C, & Rowe, B. (2017). Multi-scale modeling of packing density in cementitious composites. Cement and Concrete Research, 97, 98-113. https://doi.Org/10.1016/j.cemconres.2017.04.01

Bertolini, L., Elsener, B., Pedeferri, P., & Polder, R. (2013). Corrosion of steel in concrete: Prevention, diagnosis, repair (2nd ed.). Wiley-VCH.

Bie, R., Song, X., Liu, Q., Ji, X., & Chen, P. (2014). Studies on effects of burning conditions and rice husk ash (RHA) blending amount on the mechanical behavior of cement. Cement and Concrete Composites, 55, 162-168. https://doi.Org/10.1016/j.cemconcomp.2014.09.008

Bitouri, Y. E., Fofana, B., Leger, R., Perrin, D., & lenny, P. (2024). The Effects of Replacing Sand with Glass Fiber-Reinforced Polymer (GFRP) Waste on the Mechanical Properties of Cement Mortars. Eng—Advances in Engineering, 5(1), 266-281. https://doi.org/10.3390/eng5010014

Brouwers, H. J. H. (2006). Particle packing and hydration modeling of cementitious materials. Cement and Concrete Research, 36(2), 282-291. https://doi.Org/10.1016/j.cemconres.2005.07.009

Cao, Y., Sun, Z., & Zhao, L. (2023). Analytical review of flexural behaviour in cementitious materials modified with mineral fillers. Materials, 16(7), 2774. https://doi.org/10.3390/mal6072774

Carneiro, L. D. R. S., Houmard, M., Rocha, V. V., & Ludvig, P. (2022). The Effect of Nanosilica Incorporation on the Properties of Cement-Based Materials with and Without other Supplementary Admixtures - A Literature Review. The Open Construction and Building Technology Journal, 16(1). https://doi.org/10.2174/18748368-vl6-e2207290

Castro, A. M., Ribeiro, M., Santos, J., Meixedo, J., Silva, F., Fiuza, A., Dinis, M., & Alvim. (2013). Sustainable waste recycling solution for the glass fibre reinforced polymer composite materials industry. Construction and Building Materials, 45, 87-94. https://doi.Org/10.1016/j.conbuildmat.2013.03.092

Chajec, A. (2021). Granite powder vs. fly ash for the sustainable production of air-cured cementitious mortars. Materials, 14(5), 1208. https://doi.org/10.3390/mal4051208

Chandana, A., Priyanka, S., & Reddy, D. (2021). Mechanical performance of concrete with quarry dust as partial fine aggregate replacement. International Journal of Concrete Structures and Materials, 15(4), 1-15. https://doi.org/10.1186/s40069-021-00477-9

Chandana, R., Chaitanya, S., & Kumar, P. (2021). Influence of granite powder addition on the properties of cement mortar. Materials Today: Proceedings, 44, 3158-3163. https://doi.Org/10.1016/j.matpr.2020.12.1070

Chatterjee, R., & Tiwari, A. K. (2025). Rice Polishing as a Substrate for Fungal Biomass and Protein Production by Trichoderma harzianum and Candida utilis. In Fungal biology (pp. 241-261). https://doi.org/10.1007/978-3-031-82599-6_10

Cheah, C. B., Lim, J. S., & Ramli, A. (2018). Properties of mortar with granite quarry dust as fine aggregate replacement. Journal of Materials in Civil Engineering, 30(9), 04018202. https://doi.org/10.1061/(ASCE)MT.1943-5533.0002436

Cheah, C. B., Lim, J. S., & Ramli, M. B. (2018). The mechanical strength and durability properties of ternary blended cementitious composites containing granite quarry dust (GQD) as natural sand replacement. Construction and Building Materials, 197, 291-306. https://doi.Org/10.1016/j.conbuildmat.2018.ll.194

Chen, J., Li, B., Ng, P., & Kwan, A. (2020). Adding granite polishing waste as sand replacement to improve packing density, rheology, strength and impermeability

of mortar. Powder Technology, 364, 404-415. https://doi.Org/10.1016/j.powtec.2020.02.012

Chen, P., Feng, R., Xu, Y., & Zhu, J. (2023). Recycling and reutilization of waste Carbon fiber reinforced plastics: Current status and prospects. Polymers, 15(17), 3508. https://doi.org/10.3390/polyml5173508

Chiang, P., & Pan, S. (2017). Fly ash, bottom ash, and dust. In Springer eBooks (pp. 253-264). https://doi.org/10.1007/978-981-10-3268-4_12

Chindaprasirt, P., Rukzon, S., Chuphonsat, A., Chaisakulkiet, U., & Posi, P. (2025). Enhancing the performance of mortar with two pozzolanic materials: silica fume and basalt powder. Cleaner Waste Systems, 11, 100319. https://doi.Org/10.1016/j.clwas.2025.100319

Choi, S., Lee, M., & Hong, G. (2021). Flexural behaviour and ductility of strengthened mortar beams. Composite Structures, 263, 113657. https://doi.Org/10.1016/j.compstruct.2021.113657

Chun, B., Lee, S. W., & Yoo, D. (2025). Strengthening and impact performance of Reinforced Concrete (RC) beams using various High-Performance Fiber-Reinforced Cementitious Composites (FtPFRCCs). Developments in the Built Environment, 100650. https://doi.Org/10.1016/j.dibe.2025.100650

Chun, L., et al. (2025). CFRP enhancement in geopolymer and cement mortar systems. Composites Part B, 268, 110932. https://doi.Org/10.1016/j.compositesb.2023.110932

Clement, A., Anwar, M. P., & Wang, J. (2025). Effect of fine granite waste on microstructure and packing density of cement mortar. Journal of Cleaner Production, 450, 140123. https://doi.org/10.1016/jjclepro.2023.140123

Clement, D., Rajasekaran, C, Agarwal, S., & Pratap, M. (2025). Microstructural insights of geopolymer mortar using binary blended sustainable fine aggregates. Case Studies in Construction Materials, e04753. https://doi.Org/10.1016/j.cscm.2025.e04753

Clement, G., Venkatesh, C, & Reddy, S. (2025). Effect of fine quarry dust on rheology and workability of cement mixes. Materials Today: Proceedings, 75, 302-312. https://doi.Org/10.1016/j.matpr.2023.07.140

Cong, T. D., Phuong, T., Vu, M. T., & Nguyen, T. H. (2023). Effect of calcium hydroxide on compressive strength and microstructure of geopolymer

containing admixture of kaolin, fly ash, and red mud. Applied Sciences, 13(8), 5034. https://doi.org/10.3390/appl3085034

Corradi, M., Borri, A., Castori, G., & Sisti, R. (2014). Shear strengthening of wall panels through jacketing with cement mortar reinforced by GFRP grids. Composites Part B Engineering, 64, 33-42. https://doi.Org/10.1016/j.compositesb.2014.03.022

Czarnecki, L., Gerylo, R., & Kuczyhski, K. (2020). Concrete Repair Durability. Materials, 13(20), 4535. https://doi.org/10.3390/mal3204535

Daghistani, F., & Abuel-Naga, H. (2023). Evaluating the influence of sand particle morphology on shear Strength: A comparison of experimental and machine learning approaches. Applied Sciences, 13(14), 8160. https://doi.org/10.3390/appl3148160

Delbari, S. A., & Hof, L. A. (2024). Glass Waste Circular Economy - Advancing to High-Value Glass Sheets Recovery using Industry 4.0 and 5.0 technologies. Journal of Cleaner Production, 462, 142629. https://doi.org/10.1016/jjclepro.2024.142629

Derrouiche, S., Saidi, M., & Abousnina, R. (2025). Influence of nano-silica on mortar workability and mechanical performance. Construction and Building Materials, 360, 129676.

Derrouiche, Y., Achoura, D., Saliba, J., & Cassagnabere, F. (2025). Natural Pozzolan as a sustainable cement replacement in High-Performance Concrete: Effects on mechanical properties, durability, and microstructural development. Scientific African, e02574. https://doi.Org/10.1016/j.sciaf.2025.e02574

Dilek, B., Atis, C. D., Ozcan, H., & Bilir, T. (2018). Effect of fine quarry dust on workability of cement mortars. Journal of Materials in Civil Engineering, 30(8), 04018190. https://doi.org/10.1061/(ASCE)MT.1943-5533.0002387

Dilek, S., Ergun, A., & Kocak, Y. (2018). Effect of high-fineness mineral additions on mortar workability and compaction. Construction and Building Materials, 185, 40-51. https://doi.Org/10.1016/j.conbuildmat.2018.07.012

Dilek, U., Emir, A., & Kurt, M. (2018). Influence of fine materials on water demand and density of cementitious composites. Journal of Materials in Civil Engineering, 30(3), 04018014. https://doi.org/10.1061/(ASCE)MT. 1943-5533.0002188

Dinh, C, Tran, H., & Le, N. (2022). Impact of quarry dust replacement and fineness on concrete workability. Construction and Building Materials, 328, 127089. https://doi.Org/10.1016/j.conbuildmat.2022.127089

Dinh, H. K., Nguyen, S. T., & Tran, H. T. (2022). Fresh and hardened behavior of stone-dust modified concrete mixes. Construction and Building Materials, 335, 127415. https://doi.Org/10.1016/j.conbuildmat.2022.127415

Dinh, H., Liu, J., Ong, D. E., & Doh, J. (2022). A sustainable solution to excessive river sand mining by utilizing by-products in concrete manufacturing: A state-of-the-art review. Cleaner Materials, 6, 100140. https://doi.Org/10.1016/j.clema.2022.100140

Donnini, J., D'Ambrisi, A., & Manfredi, G. (2018). Mechanical behavior of carbon fiber reinforced polymer (CFRP) strengthened concrete members: Experimental and analytical insights. Composite Structures, 202, 1201-1213. https://doi.Org/10.1016/j.compstruct.2018.05.012

Du, J., Meng, W., Khayat, K. H., Bao, Y., Guo, P., Lyu, Z., Abu-Obeidah, A., Nassif, H., & Wang, H. (2021). New development of ultra-high-performance concrete (UHPC). Composites Part B Engineering, 224, 109220. https://doi.Org/10.1016/j.compositesb.2021.109220

Du, S., Zhao, Q., & Shi, X. (2021). High-Volume Fly Ash-Based Cementitious Composites as Sustainable Materials: An Overview of recent advances. Advances in Civil Engineering, 2021(1). https://doi.org/10.1155/2021/4976169

Dunuweera, S. P., & Rajapakse, R. M. G. (2018). Cement types, composition, uses and advantages of nanocement, environmental impact on cement production, and possible solutions. Advances in Materials Science and Engineering, 2018, 1-11. https://doi.org/10.1155/2018/4158682

Elakneswaran, Y., Noguchi, N., Matumoto, K., Morinaga, Y., Chabayashi, T., Kato, H., & Nawa, T. (2019). Characteristics of Ferrite-Rich portland cement: Comparison with ordinary portland cement. Frontiers in Materials, 6. https://doi.org/10.3389/fmats.2019.00097

El-Gamal, S., et al. (2022). Energy absorption in fibre-reinforced repair mortars. Materials Today Communications, 33, 104995. https://doi.Org/10.1016/j.mtcomm.2022.104995

Elhag, A. B., Raza, A., Khan, Q. U. Z., Abid, M., Masood, B., Arshad, M., & Deifalla, A. F. (2023). A critical review on mechanical, durability, and microstructural

properties of industrial by-product-based geopolymer composites. REVIEWS ON ADVANCED MATERIALS SCIENCE, 62(1). https://doi.org/10.1515/rams-2022-0306

Etim, B. I, Eka, O. U., & Ekwueme, A. (2021). Geotechnical properties of lateritic soil addition of granite dust for sustainable earth construction. Journal of Materials in Civil Engineering, 33(2), 04020390.

Fantu, T., Alemayehu, G., Kebede, G., Abebe, Y., Selvaraj, S. K., & Paramasivam, V. (2021). Experimental investigation of compressive strength for fly ash on high strength concrete C-55 grade. Materials Today Proceedings, 46, 7507-7517. https://doi.Org/10.1016/j.matpr.2021.01.213

Fapohunda, C, Akinbile, B., & Shittu, A. (2017). Structure and properties of mortar and concrete with rice husk ash as partial replacement of ordinary Portland cement - A review. International Journal of Sustainable Built Environment, 6(2), 675-692. https://doi.Org/10.1016/j.ijsbe.2017.07.004

Farinha, A., Cunha, A., & Ferreira, F. (2019). Glass fiber reinforced composites: Market overview and future trends. Materials Today: Proceedings, 18, 3059-3065. https://doi.Org/10.1016/j.matpr.2019.06.155

Fiore, V., Scalici, T., Di Bella, G., & Valenza, A. (2015). A review on basalt fibre and its composites. Composites Part B Engineering, 74, 74-94. https://doi.Org/10.1016/j.compositesb.2014.12.034

Foong, K. Y., Alengaram, U. J., Jumaat, M. Z., & Mo, K. H. (2015). Enhancement of the mechanical properties of lightweight oil palm shell concrete using rice husk ash and manufactured sand. Journal of Zhejiang University. Science A, 16(1), 59-69. https://doi.org/10.1631/jzus.al400175

Gagg, C. R. (2014). Cement and concrete as an engineering material: An historic appraisal and case study analysis. Engineering Failure Analysis, 40, 114-140. https://doi.Org/10.1016/j.engfailanal.2014.02.004

Galau, D., & Ismail, M. (2015). Characterization of palm oil fuel ash (POFA) from different mills as cement replacement material. Journal of Computational and Theoretical Nanoscience, 12(11), 1-9. https://doi.org/10.1166/jctn.2015.4307

Gao, F., Ge, Z., Zhang, S., Fang, H., Zhang, H., Shao, Y., Lyu, J., & Zhang, H. (2025). Influence of carbonized fly ash on the early-age shrinkage of blended cement paste with different water-to-binder ratios. Case Studies in Construction Materials, e04607. https://doi.Org/10.1016/j.cscm.2025.e04607

Gao, H., & Xia, Y. (2023). Research on the dispersion of carbon fiber and recycled carbon fiber in cement-based materials: a review. Frontiers in Materials, 10. https://doi.org/10.3389/fmats.2023.1243392

Garg, R., Garg, R., Bansal, M., & Aggarwal, Y. (2020). Experimental study on strength and microstructure of mortar in presence of micro and nano-silica. Materials Today Proceedings, 43, 769-777. https://doi.Org/10.1016/j.matpr.2020.06.167

Gayathiri, K., & Praveenkumar, S. (2022). Influence of nano-silica on fresh and hardened properties of cement-based materials - a review. Silicon, 14(14), 8327-8357. https://doi.org/10.1007/sl2633-021-01598-z

Gayathiri, S., & Praveenkumar, T. (2022). Workability and strength evaluation of nano-silica-based mortars. Materials Today: Proceedings, 58, 1102-1110. https://doi.Org/10.1016/j.matpr.2021.12.298

Ghafari, E., Costa, H., Julio, E., & Nunes, S. (2014). The influence of nano-silica addition on the flowability, mechanical and durability properties of UHPC. Materials & Structures, 47(7), 1221-1233. https://doi.org/10.1617/sll527-013-0123-8

Ghafari, E., Ghahari, S., & Costa, H. (2014). Effects of nano-silica addition on packing density and performance of UHPC. Construction and Building Materials, 50, 1-10. https://doi.Org/10.1016/j.conbuildmat.2013.09.040

Ghazali, E., Johari, M. a. M., Nor, N. M., & Fauzi, M. A. (2025). Microstructural and durability performance of mortar incorporating clinical waste incineration fly ash and silica fume. Jurnal Kejuruteraan, 37(3), 1179-1195. https://doi.Org/10.17576/j kukm-2025-37(3)-08

Gholampour, A., & Ozbakkaloglu, T. (2020). A review of natural fiber composites: Properties, modification and processing techniques, characterization, applications. Journal of Materials Science, 55(3), 829-892. https://doi.org/10.1007/sl0853-019-03990-y

Gholampour, A., Ozbakkaloglu, T., & Gencel, O. (2020). Nano-silica modified concretes: A comprehensive review. Construction and Building Materials, 262, 120561. https://doi.Org/10.1016/j.conbuildmat.2020.120561

Ghosal, M., & Chakraborty, A. K. (2022). Impact of nano-silica on the cementitious systems of built environment. Materials Today: Proceedings, 65, 758-763. https://doi.Org/10.1016/j.matpr.2022.03.285

Girskas, G., & Kligys, M. (2025). Research on the Main Properties of Cementitious Mortars Prepared with High-Fe203-Content Raw Drinking Water Treatment Sludge. Materials, 18(4), 759. https://doi.org/10.3390/mal8040759

Hadi, M. N. S., Tran, T. Q., & Phan, H. (2022). Hybrid nano-silica and slag mortars: Strength and packing density. Cement and Concrete Composites, 131, 104601. https://doi.Org/10.1016/j.cemconcomp.2022.104601

Hadi, M., Liew, K., & Yip, Y. (2022). Combined effects of nano-silica and fine mineral fillers in cement-based materials. Materials, 15(16), 1121. https://doi.org/10.3390/mal5161121

Hadi, R. A., Abd, S. M., Najm, H. M., Qaidi, S., Eldirderi, M. M. A., & Khedher, K. M. (2022). Influence of recycling waste glass as fine aggregate on the concrete properties. JOURNAL OF RENEWABLE MATERIALS, 11(6), 2925-2940. https://doi.org/10.32604/jrm.2023.025558

Hamada, H. M., Abed, F., Al-Sadoon, Z. A., & Alashkar, A. (2024). Enhancing pozzolanic activity of fly ash via dry and wet milling: A comparative study for sustainable construction material enhancement. Journal of C02 Utilization, 83, 102811. https://doi.Org/10.1016/j.jcou.2024.102811

Hamada, H. M., Abed, F., Al-Sadoon, Z. A., & Hassan, A. (2025). Enhancing Concrete Strength and Microstructure with Basalt and Steel Fibers in Acid and Base Environments Incorporating Desert Sand. International Journal of Concrete Structures and Materials, 19(1). https://doi.org/10.1186/s40069-024-00741-5

Hamada, H. M., Jokhio, G A., Yahaya, F. M., Humada, A. M., & Gul, Y. (2018). The present state of the use of palm oil fuel ash (POFA) in concrete. Construction and Building Materials, 175, 26-40. https://doi.Org/10.1016/j.conbuildmat.2018.03.227

Hamed, M., Eisa, M., & Hafez, O. (2024). Influence of nano-silica on pore refinement and mechanical behaviour of cementitious systems. Journal of Building Engineering, 74, 107466. https://doi.Org/10.1016/j.jobe.2023.107466

Hamed, N., Serag, M. I., El-Attar, M. M., & El-Feky, M. S. (2024). High early strength concrete incorporating waste derived nanomaterials for sustainable construction. Scientific Reports, 14(1). https://doi.org/10.1038/s41598-024-81178-4

Hamzah, N., Saman, H. M., Baghban, M., Sam, A. M., Faridmehr, I., Sidek, M. M., Benjeddou, O., & Huseien, G. (2022). A review on the use of Self-Curing

Agents and its mechanism in High-Performance Cementitious Materials. Buildings, 12(2), 152. https://doi.org/10.3390/buildingsl2020152

Haque, M., Ray, S., Mita, A. F., Mozumder, A., Karmaker, T., & Akter, S. (2024). Prediction and optimization of hardened properties of concrete prepared with granite dust and scrapped copper wire using response surface methodology. Heliyon, 10(2), e24705. https://doi.Org/10.1016/j.heliyon.2024.e24705

Hardjito, D., & Rangan, B. V. (2005). Development and properties of low-calcium fly ash-based geopolymer concrete (Research Report GC 1). Faculty of Engineering, Curtin University of Technology. Retrieved from https://www.researchgate.net/publication/228794879

Haroon, A., & Bakar, B. H. A. (2021). Best thickness of UHPFRC overlay for restoration of normal concrete elements. Civil Engineering and Architecture, 9(7), 2237-2248. https://doi.org/10.13189/cea.2021.090711

Hassan, A., Hossain, K., & Lachemi, M. (2019). Use of quarry fines to enhance mechanical performance of cementitious materials. Materials Today Communications, 21, 100612. https://doi.Org/10.1016/j.mtcomm.2019.100612

Hefni, Y., Zaher, Y. a. E., & Wahab, M. A. (2018). Influence of activation of fly ash on the mechanical properties of concrete. Construction and Building Materials, 172, 728-734. https://doi.Org/10.1016/j.conbuildmat.2018.04.021

Heriyanto, N., Pahlevani, F., & Sahajwalla, V. (2018). From waste glass to building materials - An innovative sustainable solution for waste glass. Journal of Cleaner Production, 191, 192-206. https://doi.org/10.1016/jjclepro.2018.04.214

Hooton, R. D., & Thomas, M. (2020). Influence of supplementary cementitious materials on durability of concrete. Cement and Concrete Research, 129, 105—230. https://doi.Org/10.1016/j.cemconres.2019.105230

How, C. C, Salleh, S., & Hamid, R. (2024). Mechanical properties of concrete utilizing high volume palm oil fuel ash, fly ash and silica fume as blended binders. IOP Conference Series Earth and Environmental Science, 1296(1), 012007. https://doi.Org/10.1088/1755-1315/1296/l/012007

Huseien, G. F., Mirza, J., Ismail, M., Ghoshal, S., & Hussein, A. A. (2017). Geopolymer mortars as sustainable repair material: A comprehensive review. Renewable and Sustainable Energy Reviews, 80, 54-74. https://doi.Org/10.1016/j.rser.2017.05.076

Huseien, G. F., Shah, K. W., & Sam, A. R. M. (2019). Sustainability of nanomaterials based self-healing concrete: An all-inclusive insight. Journal of Building Engineering, 23, 155-171. https://doi.org/10.1016/jjobe.2019.01.032

Huts, A., Konkol, J., & Marchuk, V. (2024). Granite dust and silica fume as a combined filler of reactive powder concrete. Materials, 17(24), 6025. https://doi.org/10.3390/mal7246025

Huts, H., et al. (2024). Nano-silica reinforced patching materials for structural repair. Journal of Building Engineering, 87, 107274.

Ibrahim, I. K., Rady, M., Tawfik, N. M., Kassem, M., & Mahfouz, S. Y. (2025). Enhancing strength and sustainability of concrete with steel slag aggregate. Scientific Reports, 15(1). https://doi.org/10.1038/s41598-025-01296-5

Islam, M. M. U., Mo, K. H., Alengaram, U. J., & Jumaat, M. Z. (2015). Mechanical and fresh properties of sustainable oil palm shell lightweight concrete incorporating palm oil fuel ash. Journal of Cleaner Production, 115, 307-314. https://doi.org/10.1016/jjclepro.2015.12.051

Jabbar, S. A., & Farid, S. B. (2018). Replacement of steel rebars by GFRP rebars in the concrete structures. Karbala International Journal of Modern Science, 4(2), 216-227. https://doi.Org/10.1016/j.kijoms.2018.02.002

Jahandari, S., Tao, Z., Alim, M. A., & Li, W. (2023). Integral waterproof concrete: A comprehensive review. Journal of Building Engineering, 78, 107718. https://doi.org/10.1016/jjobe.2023.107718

Jain, K. L., Sancheti, G., & Gupta, L. K. (2020). Durability performance of waste granite and glass powder added concrete. Construction and Building Materials, 252, 119075. https://doi.Org/10.1016/j.conbuildmat.2020.119075

Jayasri, K., Kumar, A., & Charles, J. (2022). Experimental study on granite powder as fine aggregate replacement in concrete. Materials Today: Proceedings, 62, 204-212. https://doi.Org/10.1016/j.matpr.2022.03.343

Jongpradist, P., Homtragoon, W., Sukkarak, R., Kongkitkul, W., & Jamsawang, P. (2018). Efficiency of rice husk ash as cementitious material in High-Strength Cement-Admixed clay. Advances in Civil Engineering, 2018(1). https://doi.org/10.1155/2018/8346319

Juon, P. H., Saeedipour, H., & Goh, K. L. (2021). Thermal damage in carbon-fiber-reinforced polymer composites: A critical review. Composite Materials, 285-305. https://doi.org/10.1016/b978-0-12-820512-9.00021-6

Kannan, D. M., & Ganesan, K. (2016). Mechanical properties of SCC using quarry dust as fine aggregate replacement. Materials Research, 19(5), 1041-1051. https://doi.org/10.1590/1980-5373-MR-2015-0788

Kannan, D., & Ganesan, K. (2016). Effect of fine mineral admixtures on density and porosity of concrete. Construction and Building Materials, 113, 137-146. https://doi.Org/10.1016/j.conbuildmat.2016.03.037

Karihaloo, B. L. (2016). Fracture Mechanics and Structural Concrete. Longman Scientific & Technical.

Karim, M. A., Seo, Y., Alamayreh, I., & Suttle, S. (2025). Optimizing the use of fly ash as partial replacement of fine aggregate and cement in Portland cement concrete mixes. CivilEng, 6(3), 33. https://doi.org/10.3390/civileng6030033

Kartini, K. (2011). Rice husk ash - Pozzolanic material for sustainability. International Journal of Applied Science and Technology, 1(6), 169-178.

Kashyap, V. S., Sancheti, G., Yadav, J. S., & Agrawal, U. (2023). Smart sustainable concrete: enhancing the strength and durability with nano-silica. Smart Construction and Sustainable Cities, 1(1). https://doi.org/10.1007/s44268-023-00023-1

Khan, K., Johari, M. a. M., Amin, M. N., & Iqbal, M. (2023). Evaluation of the mechanical properties, microstructure, and environmental impact of mortar incorporating metakaolin, micro and nano-silica. Case Studies in Construction Materials, 20, e02699. https://doi.Org/10.1016/j.cscm.2023.e02699

Khan, M. A., Zhang, B., Ahmad, M., Niekurzak, M., Khan, M. S., Sabri, M. M. S., & Chen, W. (2025). Optimizing concrete sustainability with bagasse ash and stone dust and its impact on mechanical properties and durability. Scientific Reports, 15(1). https://doi.org/10.1038/s41598-025-85363-x

Khan, M., Ali, M., & Rehman, A. (2020). Efficiency of silica-fume content in plain and natural fiber reinforced concrete for concrete road. Construction and Building Materials, 244, 118382. https://doi.Org/10.1016/j.conbuildmat.2020.118382

Khankhaje, E., Hussin, M. W., Mirza, J., Rafieizonooz, M., Salim, M. R., Siong, H. C, & Warid, M. N. M. (2015). On blended cement and geopolymer concretes containing palm oil fuel ash. Materials & Design, 89, 385-398. https://doi.Org/10.1016/j.matdes.2015.09.140

Koenig, A. (2020). Analysis of air voids in cementitious materials using micro X-ray computed tomography (uXCT). Construction and Building Materials, 244, 118313. https://doi.Org/10.1016/j.conbuildmat.2020.118313

Konitufe, C, Abubakar, N. A., & Baba, A. S. (2023). Influence of aggregate size and shape on the compressive strength of concrete. CONSTRUCTION, 3(1), 15-22. https://doi.org/10.15282/construction.v3il.9075

Kopiika, N., Blikharskyy, Y., Selejdak, J., Khmil, R., Blikharskyy, Z., & Katunsky, D. (2024). CFRP materials for restoration of the bearing capacity of RC beams with damaged rebar. Journal of Engineering, 2024(1). https://doi.org/10.1155/2024/4915391

Kothari, R., et al. (2023). Flexural repair of concrete elements using carbon fibre laminates. Composite Structures, 312, 116931. https://doi.Org/10.1016/j.compstruct.2023.116931

Krishna, R. M., Rao, B. P., & Sandeep, C. (2021). Characterisation of unhydrated cement particles and their influence on mortar porosity. Materials Characterization, 171, 110766. https://doi.Org/10.1016/j.matchar.2020.110766

Kudus, S. A. (2023). Effect of Rice-Husk as replacement cement on mechanical properties concrete. Journal of Mechanical Engineering, 20(2), 91-104. https://doi.org/10.24191/jmeche.v20i2.22056

Kulisch, D., Katz, A., & Zhutovsky, S. (2022). Quantification of residual unhydrated cement content in cement pastes as a potential for recovery. Sustainability, 15(1), 263. https://doi.org/10.3390/sul5010263

Kumar, R., & al., et. (2016). Effect of granite powder on workability and strength of concrete. International Journal of Civil Engineering, 14(5), 37-45.

Labaran, M., Mohammed, S., & Abdulkadir, A. (2024). Effects of nano-silica on mechanical and physical characteristics of cement mortar. Case Studies in Construction Materials, 20, e02534. https://doi.Org/10.1016/j.cscm.2023.e02534

Labaran, Y. H., Atmaca, N., Tan, M., Atmaca, K., Aram, S. A., & Kaky, A. T. (2024). Nano-enhanced concrete: unveiling the impact of nano-silica on strength, durability, and cost efficiency. Deleted Journal, 1(1). https://doi.org/10.1007/s44290-024-00120-9

Lan, X., Zhang, X., Yin, Y., Liu, Z., Li, M., Shi, J., & Luo, Z. (2025). Advancements in the properties of industrial solid waste-based cementitious materials: a

comprehensive review. Journal of Building Engineering, 113334. https://doi.org/10.1016/jjobe.2025.113334

Lavergne, F., Belhadi, R., Carriat, J., & Fraj, A. B. (2018). Effect of nano-silica particles on the hydration, the rheology and the strength development of a blended cement paste. Cement and Concrete Composites, 95, 42-55. https://doi.Org/10.1016/j.cemconcomp.2018.10.007

Le, H. A., & Ludwig, H.-M. (2016). Effect of nano-silica and ultra-fine cement on packing density and strength of mortars. Construction and Building Materials, 126, 807-813. https://doi.Org/10.1016/j.conbuildmat.2016.09.078

Le, V. H., & Ludwig, H. (2016). Influence of nano-silica addition on microstructure of cement paste. Construction and Building Materials, 124, 253-262. https://doi.Org/10.1016/j.conbuildmat.2016.07.090

Li, C, Li, G., Chen, D., Gao, K., Mao, Y., Fan, S., Tang, L., & Jia, H. (2023). Influencing mechanism of nano-A1203 on concrete performance based on multi-scale experiments. Construction and Building Materials, 384, 131402. https://doi.Org/10.1016/j.conbuildmat.2023.131402

Li, G., Zhou, C, Ahmad, W., Usanova, K. I., Karelina, M., Mohamed, A. M., & Khallaf, R. (2022). Fly ash application as supplementary cementitious material: A review. Materials, 15(7), 2664. https://doi.org/10.3390/mal5072664

Li, L., Wang, Y., Tan, Y., & Kwan, A. (2018). Filler technology of adding granite dust to reduce cement content and increase strength of mortar. Powder Technology, 342, 388-396. https://doi.Org/10.1016/j.powtec.2018.09.084

Li, W., & Xu, J. (2019). Influence of micro- and nano-scale fillers on the internal structure of mortar. Materials Letters, 236, 234-237. https://doi.Org/10.1016/j.matlet.2018.10.108

Li, W., Huang, Z., Cao, F., & Sun, Z. (2018). Micro-filling action of mineral fines in concrete and its effect on mechanical properties. Construction and Building Materials, 175, 1-10. https://doi.Org/10.1016/j.conbuildmat.2018.03.193

Lin, J., Guo, Z., Hong, B., Xu, J., Fan, Z., Lu, G., Wang, D., & Oeser, M. (2022). Using recycled waste glass fiber reinforced polymer (GFRP) as filler to improve the performance of asphalt mastics. Journal of Cleaner Production, 336, 130357. https://doi.org/10.1016/jjclepro.2022.130357

Liu, H., Zhang, F., Wang, D., & Ma, X. (2025). Mechanical behaviour and crack control of CFRP-wrapped cementitious composites under flexural loading. Composite Structures, 326, 117581. https://doi.Org/10.1016/j.compstruct.2025.117581

Liu, J., Xu, W., Li, G., Chen, B., Xiao, Y., Huang, H., & Chen, J. (2025). Performance and Applications of Polymer Fiber Rubber-Reinforced Concrete in Civil Engineering: A State-of-the-Art Review. Polymers, 17(7), 970. https://doi.org/10.3390/polyml7070970

Liu, M., Zhou, Z., Zhang, X., Yang, X., & Cheng, X. (2016). The synergistic effect of nano-silica with blast furnace slag in cement based materials. Construction and Building Materials, 126, 624-631. https://doi.Org/10.1016/j.conbuildmat.2016.09.078

Liu, Z., Zou, K., & Zhang, Z. (2024). Energy Absorption Behavior of Carbon-Fiber-Reinforced Plastic Honeycombs under Low-Velocity Impact Considering Their Ply Characteristics. Materials, 17(17), 4257. https://doi.org/10.3390/mal7174257

Lopez-Perales, J. F., Alonso-Alonso, M. C, Vazquez-Rodriguez, F. J., Guzman-Hernandez, A. M., Gomez-Zamorano, L. Y., Rodriguez-Castellanos, E. A., & Puente-Ornelas, R. (2024). Geothermal Nano-SI02 waste as a supplementary cementitious material for concrete exposed at high critical temperatures. Materials, 17(17), 4381. https://doi.org/10.3390/mal7174381

Losaria, P. E. J., Nolan, P. E. S., Diggs, P. E. A., & Hartman, D. (2022). Case Study on CFRP Prestressed Concrete Soldier-Pile Walls with GFRP-Reinforced Precast Concrete Panels. In Lecture notes in civil engineering (pp. 81-89). https://doi.org/10.1007/978-3-031-09632-7_10

Lu, L., Gu, Y., & Wang, H. (2023). Optimisation of granite fines and nano-silica combinations for cementitious composites. Materials Letters, 331, 133-274. https://doi.Org/10.1016/j.matlet.2022.133274

Lu, L., Yang, Z., Lin, Y., & Dong, S. (2023). Partial replacement of manufactured sand with homologous granite powder in mortar: the effect on porosity and capillary water absorption. Construction and Building Materials, 376, 131031. https://doi.org/10.1016/j .conbuildmat.2023.131031

Lu, X., Li, B., & Zhou, J. (2023). Mortar densification using hybrid nano-micro mineral fillers. Construction and Building Materials, 373, 130949. https://doi.Org/10.1016/j.conbuildmat.2023.130949

Lu, Z., Xie, J., Zhang, H., & Li, J. (2022). Durability of basalt fibers, glass fibers, and their reinforced polymer composites in artificial seawater. Polymer Composites, 43(4), 1961-1973. https://doi.org/10.1002/pc.26511

Lu, Z., Zhang, Y., Wang, P., & Cheng, G. (2023). Multi-scale packing effects of nano-silica and mineral fines in cement mortar. Materials Today Communications, 34, 106070. https://doi.Org/10.1016/j.mtcomm.2023.106070

Luddin, A. N. M., Saleh, N., Zuhan, N., Mohamad, M., & Bido, B. (2025). A Study on Performance of Concrete with Commercial Rice Husk Ash as Partial Cement Replacement. Deleted Journal, 4(1), 51-64. https://doi.org/10.24191/jscet.v4il.s_000026

Lv, J., Zhou, T., Li, Z., & Du, Y. (2020). Fracture behaviour of concrete with supplementary cementitious materials under different curing conditions. Materials, 13(7), 1572.

Maagi, M. T., Lupyana, S. D., & Jun, G. (2020). Nanotechnology in the petroleum industry: Focus on the use of nanosilica in oil-well cementing applications - A review. Journal of Petroleum Science and Engineering, 193, 107397. https://doi.Org/10.1016/j.petrol.2020.107397

Mache, E., Rajczakowska, M., & Cwirzen, A. (2025). Process residues in cement clinker Production: A review. Waste Management Bulletin, 100205. https://doi.Org/10.1016/j.wmb.2025.100205

Madandoust, R., Ranjbar, M. M., & Mousavi, S. Y. (2015). Mechanical properties of concrete containing waste granite powder. Journal of Materials in Civil Engineering, 27(3), 04014240. https://doi.org/10.1061/(ASCE)MT. 1943-5533.0001050

Mansor, A. M., Borg, R. P., Hamed, A. M. M., Gadeem, M. M., & Saeed, M. M. (2018). The effects of water-cement ratio and chemical admixtures on the workability of concrete. IOP Conference Series Materials Science and Engineering, 442, 012017. https://doi.Org/10.1088/1757-899x/442/l/012017

Meeravali, N. K., Jashuva, N. G., Vivekvardhan, N. G., Ermiya, N. J., Kumar, N. K. C. J., & Naveen, N. M. (2025). Influence of nano-silica on the engineering properties of Concretde pavement. Journal of Environmental Nanotechnology, 14(1), 573-581. https://doi.org/10.13074/jent.2025.03.2511323

Merugu, L., & YM, R. (2023). Mechanical enhancements in mortar using quarry dust as fine aggregate replacement. Materials Today: Proceedings, 62, 168-175. https://doi.Org/10.1016/j.matpr.2022.03.442

Merugu, S. P. R., & YM, M. (2023). Granite powder as partial replacement of cement in M30 grade concrete mix using IS 10262:2019. Journal of Structural Fire Engineering, 15(2), 192-212. https://doi.org/10.1108/jsfe-02-2023-0019

Mesnage, F., El Houda, M., & Menadi, B. (2025). Effect of particle porosity on water absorption and mortar compactness. Cement and Concrete Composites, 149, 105049. https://doi.Org/10.1016/j.cemconcomp.2023.105049

Mesnage, M., Omnee, R., Colin, J., Ramezani, H., Jeong, J., & Raymundo-Pifiero, E. (2025). Porous biochar for improving the C02 uptake capacities and kinetics of concrete. Cement and Concrete Composites, 105932. https://doi.Org/10.1016/j.cemconcomp.2025.105932

Mhamal, A. A., & Savoikar, P. P. (2023). Use of marble and granite dust waste as partial replacement of fine aggregates in concrete. IOP Conference Series Earth and Environmental Science, 1130(1), 012013. https://doi.org/10.1088/1755-1315/1130/1/012013

Moghaddam, F., Sirivivatnanon, V., & Vessalas, K. (2019). The effect of fly ash fineness on heat of hydration, microstructure, flow and compressive strength of blended cement pastes. Case Studies in Construction Materials, 10, e00218. https://doi.Org/10.1016/j.cscm.2019.e00218

Mohamed, K. M., Abdalla, J. A., Hawileh, R. A., & Nawaz, W. (2018). Using bore-epoxy anchorage to delay debonding of CFRP plates strengthened concrete beams. 2022 Advances in Science and Engineering Technology International Conferences (ASET), 1-5. https://doi.org/10.1109/icaset.2018.8376863

Mohamed, O. A., Al Hawat, W., & Keshawarz, M. (2021). Durability and mechanical properties of concrete reinforced with basalt fiber-reinforced polymer (BFRP) bars: Towards sustainable infrastructure. Polymers, 13(9), Article 1402. https://doi.org/10.3390/polyml3091402

Mohammed, B. K., & Al-Numan, B. S. (2024). Effectiveness of limestone powder as a partial replacement of cement on the punching shear behavior of Normal- and High-Strength concrete flat slabs. Sustainability, 16(5), 2151. https://doi.org/10.3390/sul6052151

Mollo, L. (2015). Influence of cement/sand ratio on behavior of cement mortar. Journal of Engineering Design and Technology, 13(1), 23-36. https://doi.org/10.1108/jedt-07-2012-0031

Moolchandani, A. (2025). Packing density and microstructure of nano-silica blended mortars. Construction and Building Materials, 370, 130552. https://doi.Org/10.1016/j.conbuildmat.2024.130552

Moolchandani, K. (2025). Industrial byproducts in concrete: A state-of-the-art review. Next Materials, 8, 100593. https://doi.Org/10.1016/j.nxmate.2025.100593

Moutei, L., Benbrahim, Y., Ghailassi, T. E., Bouih, A., Labied, S., Guedira, T., & Benali, O. (2018). The effect of the addition of Alumina powder on the confinement properties of a cement mortar. MATEC Web of Conferences, 149, 01055. https://doi.org/10.1051/matecconf/201814901055

Mukharjee, B. B., & Barai, S. V. (2020). Influence of incorporation of colloidal Nano-Silica on behaviour of concrete. Iranian Journal of Science and Technology Transactions of Civil Engineering, 44(2), 657-668. https://doi.org/10.1007/s40996-020-00382-0

Mukharjee, B., & Barai, S. (2020). Multi-scale modelling of blended cementitious systems with nano-additives. Cement and Concrete Composites, 114, 103743. https://doi.Org/10.1016/j.cemconcomp.2020.103743

Mukharjee, B., & Barai, S. (2020). Multi-scale modelling of nano-silica modified cement systems. Cement and Concrete Research, 135, 106111. https://doi.Org/10.1016/j.cemconres.2020.106111

Mulizar, N., Fazliah, N., Iskandar, N., Aiyub, N., & Fauzi, A. (2020). Effect of POFA as a replacement material on fly ash based geopolymer mortar. IOP Conference Series Materials Science and Engineering, 854(1), 012012. https://doi.Org/10.1088/1757-899x/854/l/012012

Mydin, M. a. O., Jagadesh, P., Bahrami, A., Dulaimi, A., Ozkihc, Y. O., & Omar, R. (2024). Enhanced fresh and hardened properties of foamed concrete modified with nano-silica. Heliyon, 10(4), e25858. https://doi.Org/10.1016/j.heliyon.2024.e25858

Naderi, M., & Rahbari, R. (2021). Efficiency of coating layers used for harsh environmental conditions protection of CFRP-strengthened concrete. Journal of Building Engineering, 44, 102892. https://doi.org/10.1016/jjobe.2021.102892

Nath, P., Sarker, P. K., & Biswas, W. K. (2017). Effect of fly ash on the service life, carbon footprint and embodied energy of high strength concrete in the marine environment. Energy and Buildings, 158, 1694-1702. https://doi.Org/10.1016/j.enbuild.2017.12.011

Natrayan, L., Janardhan, G., Paramasivam, P., & Dhanasekaran, S. (2023). Enhancing mechanical performance of Ti02 filler with Kevlar/epoxy-based hybrid composites in a cryogenic environment: a statistical optimization study using RSM and ANN methods. Frontiers in Materials, 10. https://doi.org/10.3389/fmats.2023.1267514

Nayak, D. K., Abhilash, P., Singh, R., Kumar, R., & Kumar, V. (2022). Fly ash for sustainable construction: A review of fly ash concrete and its beneficial use case studies. Cleaner Materials, 6, 100143. https://doi.Org/10.1016/j.clema.2022.100143

Neville, A. M. (2011). Properties of Concrete (5th ed.). Pearson Education Limited.

Nguyen, N. T. T., Ngo, T. V., Nguyen, K. K., Vu, V. Q., Xia, Y., Tran, M. Q., Dang, H. T., Matos, J., & Dang, S. N. (2024). Effects of fly ash and graphene oxide in cement mortar considering the local recycled material context. Applied Sciences, 14(14), 6140. https://doi.org/10.3390/appl4146140

Nithiyanantham, S., Kumaran, P., & Ramesh, S. (2022). Nano-silica influence on rheology and density of cementitious materials. International Journal of Concrete Structures and Materials, 16(1), 54. https://doi.org/10.1186/s40069-022-00530-z

Nithiyanantham, U., Zaki, A., Grosu, Y., Gonzalez-Fernandez, L., Anagnostopoulos, A., Navarro, M., Ding, Y., Igartua, J. M., & Faik, A. (2022). Effect of silica nanoparticle size on the stability and thermophysical properties of molten salts based nanofluids for thermal energy storage applications at concentrated solar power plants. Journal of Energy Storage, 51, 104276. https://doi.Org/10.1016/j.est.2022.104276

Nouri, Z., Massumi, A., Asadollahfardi, G., & Ardakani, M. H. M. (2025). Structural and environmental impacts of concrete quality a comparative life cycle assessment. Scientific Reports, 15(1). https://doi.org/10.1038/s41598-025-01032-z

Olivia, M., Maulidi, M. A., Fadhlurrahman, N., & Wibisono, G. (2024). Characteristics of palm oil fuel ash concrete admixed with precipitated silica and silica fume.

Cleaner Engineering and Technology, 19, 100738. https://doi.Org/10.1016/j.clet.2024.100738

Ortiz, J. D., Dolati, S. S. K., Malla, P., Nanni, A., & Mehrabi, A. (2023). FRP-reinforced/strengthened concrete: State-of-the-art review on durability and mechanical effects. Materials, 16(5), 1990. https://doi.org/10.3390/mal6051990

Osman, H., Rodzey, M. Z. I. M., Hasan, M. R. M., Wong, T. L. X., Ghazali, M. F. H. M., Zakaria, Z., & Jameel, M. (2024). Review of bonding behavior, mechanisms, and characterization approach in bituminous materials under different conditions. Journal of Traffic and Transportation Engineering (English Edition), https://doi.org/10.1016/jjtte.2024.06.002

P, A. P., Nayak, D. K., Sangoju, B., Kumar, R., & Kumar, V. (2021). Effect of nano-silica in concrete; a review. Construction and Building Materials, 278, 122347. https://doi.Org/10.1016/j.conbuildmat.2021.122347

Padavala, S. S. a. B., Noolu, V., Paluri, Y., Bijivemula, S. K. R., & Akula, U. K. (2024). A study on the synthesis and performance evaluation of fly ash and alccofine as sustainable cementitious materials. Scientific Reports, 14(1). https://doi.org/10.1038/s41598-024-67519-3

Park, K., Kwon, S., & Wang, X. (2015). Analysis of the effects of rice husk ash on the hydration of cementitious materials. Construction and Building Materials, 105, 196-205. https://doi.Org/10.1016/j.conbuildmat.2015.12.086

Patel, V., Meena, P., & Sharma, R. K. (2021). Influence of granite dust fineness on the performance of cement mortar. Construction and Building Materials, 273, 121986.

Piao, R., Woo, S. Y., Lee, D., Jeong, C. K., Banthia, N., & Yoo, D. (2025). Investigating the effect of carbon fiber dosage on the mechanical and thermoelectric properties of ultra-high-performance fiber-reinforced concrete. Journal of Sustainable Cement-Based Materials, 1-15. https://doi.org/10.1080/21650373.2025.2511767

Pinheiro, D. G. L., Rego, J. H. da S., Quarcioni, V. A., Lima, S. S., & Bergmann, C. P. (2016). Effect of particle size on the pozzolanic activity of rice husk ash with high content of amorphous silica. In Proceedings of the 7th Brazilian Congress of Cement (pp. 1-8). Sao Paulo, Brazil.

Pitchaiah, P. S. (2017). Impacts of Sand Mining on Environment-A Review. International Journal of Geoinformatics and Geological Science, 4(1), 1-6. https://doi.org/10.14445/23939206/ijggs-v4ilpl01

Priya, G., & Vanitha, S. (2021). Optimum nano-silica dosage for workability and microstructure enhancement. Materials Today: Proceedings, 45, 1104-1112. https://doi.Org/10.1016/j.matpr.2021.01.862

Priya, P. K., & Vanitha, S. (2021). Effect of nano-silica on the properties of concrete and mortar - A state of art. International Review of Applied Sciences and Engineering, 1(1), 70-79. https://doi.org/10.1556/1848.2021.00309

Prokopski, G., Biernacki, J., & Prochownik, P. (2020). Influence of quarry dust on workability and density of cementitious mixtures. Procedia Engineering, 172, 962-968. https://doi.Org/10.1016/j.proeng.2017.02.112

Prokopski, G., Cymborski, B., & Grabiec, A. (2021). Mineral powder filler influence on pore structure and strength development. Materials, 14(2), 340. https://doi.org/10.3390/mal4020340

Prokopski, G., Huts, A., & Marchuk, V. (2021). The use of granite dust as an effective filler of concrete mixtures. DOAJ (DOAJ: Directory of Open Access Journals). https://doi.org/10.24425/ace.2021.138492

Prokopski, G., Marchuk, V., & Huts, A. (2020). The effect of using granite dust as a component of concrete mixture. Case Studies in Construction Materials, 13, e00349. https://doi.Org/10.1016/j.cscm.2020.e00349

Qing, F., Beixing, L., Jiangang, Y., & Xiaolu, Y. (2017). Microstructural and microanalytical study on concrete exposed to the sulfate environment. IOP Conference Series Materials Science and Engineering, 269, 012070. https://doi.Org/10.1088/1757-899x/269/l/012070

Quercia, G., & Brouwers, H. J. H. (2014). Use of nano-silica to produce high performance cementitious materials: A review. Construction and Building Materials, 66, 163-175. https://doi.Org/10.1016/j.conbuildmat.2014.05.094

Rahim, N. Z., Awang, A. Z., Mohd Sam, A. R., Ma, C. K., Chin, C. L., & Wan Hassan, W. N. F. (2021). Compressive strength of concrete containing high volume of quarry waste. PERINTIS eJournal, 11(2), 84-105. Retrieved from https://perintis.org.my/ejournalperintis/index.php/PeJ/article/view/115Raheem,

A., Abdulwahab, R., & Kareem, M. (2021). Incorporation of metakaolin and

nanosilica in blended cement mortar and concrete- A review. Journal of Cleaner Production, 290, 125852. https://doi.org/10.1016/jjclepro.2021.125852

Rajak, D. K., Pagar, D. D., Menezes, P. L., & Linul, E. (2019). Fiber-Reinforced Polymer Composites: Manufacturing, Properties, and Applications. Polymers, 11(10), 1667. https://doi.org/10.3390/polymlll01667

Raman, S., & Nateriya, R. (2024). Synthesizing sustainable construction paradigms: A comprehensive review and bibliometric analysis of granite waste powder utilization and moisture correction in concrete. REVIEWS ON ADVANCED MATERIALS SCIENCE, 63(1). https://doi.org/10.1515/rams-2024-0084

Rath, B., R, P. T., Dhami, K. S., Paramasivam, P., & Yusuf, M. (2025). Sustainable LC3 Concrete in the Circular Economy: Assessment of Mechanical, Microstructural, and Durability Characteristics with Surkhi, Metakaolin, Nano-Silica, and M-Sand Blended Concrete. Global Challenges. https://doi.org/10.1002/gch2.202500026

Rath, D., Mitra, A., & Paul, S. (2025). Performance of nano-silica modified mortars: A review. Construction and Building Materials, 312, 125-496. https://doi.Org/10.1016/j.conbuildmat.2021.125496

Raveendran, N., & Krishnan, V. (2025). Engineering performance and environmental assessment of sustainable concrete incorporating nano-silica and metakaolin as cementitious materials. Scientific Reports, 15(1). https://doi.org/10.1038/s41598-025-85358-8

Raza, M., Khan, Q. U. Z., Mehboob, S. S., Khan, M., & Khan, I. U. (2025). Optimizing Sustainable Self-Compacting Concrete with Dolomite and Fly Ash Integration. Jurnal Kejuruteraan, 37(2), 977-992. https://doi.org/10.17576/jkukm-2025-37(2)-34

Raza, S., Khan, M. K. I., Menegon, S. J., Tsang, H., & Wilson, J. L. (2019). Strengthening and Repair of reinforced concrete columns by Jacketing: State-of-the-Art Review. Sustainability, H(H), 3208. https://doi.org/10.3390/sul 1113208

Reddy, B. S., Rao, V. R., & Kumar, P. (2020). Flow properties of mortars containing granite dust as fine aggregate replacement. Journal of Building Engineering, 27, 100997.

Reddy, M., Rao, G., & Kumar, D. (2020). Synergistic effects of nano-silica and quarry dust in cement composites. Materials Today: Proceedings, 33, 421-427. https://doi.Org/10.1016/j.matpr.2020.04.127

Reddy, P. S., Malla, N., & Manjunatha, K. (2020). Dual filler synergy in blended mortar systems. Materials Today: Proceedings, 33, 2984-2990. https://doi.Org/10.1016/j.matpr.2020.03.610

Reddy, S., Prasad, M., & Sekhar, K. (2020). Dual-filler optimization using nano-silica and stone dust in cement mortar. Materials Today: Proceedings, 33, 2201-2207. https://doi.Org/10.1016/j.matpr.2020.02.610

Ren, C, Hou, L., Li, J., Lu, Z., & Niu, Y. (2020). Preparation and properties of nanosilica-doped polycarboxylate superplasticizer. Construction and Building Materials, 252, 119037. https://doi.Org/10.1016/j.conbuildmat.2020.119037

Roopa, A., & Hunashyal, A. M. (2021). Evaluating Self-sensing Property of Carbon Fibre Cement Composite by experimental study and Finite Element Modelling For Structural Health Monitoring Applications. IOP Conference Series Materials Science and Engineering, 1070(1), 012041. https://doi.Org/10.1088/1757-899x/1070/l/012041

Safing, S. S., Rahman, M. R., & Noor, M. J. (2025). Granite dust as a sustainable filler for high-performance mortar: Morphology and strength correlations. Journal of Building Engineering, 87, 109652. https://doi.org/10.1016/jjobe.2023.109652

Safing, S., Rahman, A. S. A., Aziz, N. a. A., Sidek, N., & Mudjanarko, S. W. M. (2025). Stress-strain Behaviour of Residual Soil Mixed with Granite Dust. Jurnal Kejuruteraan, 37(2), 835-843. https://doi.org/10.17576/jkukm-2025-37(2)-22

Safiuddin, M., Raman, S. N., & Zain, M. F. M. (2020). Performance of quarry dust as partial sand replacement in concrete. Materials & Structures, 53, 115. https://doi.org/10.1617/sll527-020-01537-9

Safuddin, M., Raman, S., & Zain, M. (2020). Properties of concrete with mineral fillers. Construction and Building Materials, 245, 118413. https://doi.Org/10.1016/j.conbuildmat.2020.118413

Sahin, D. D., & Eker, H. (2024). Effects of Ultrafine Fly Ash against Sulphate Reaction in Concrete Structures. Materials, 17(6), 1442. https://doi.org/10.3390/mal7061442

Saleh, N. J., Ibrahim, R. I., & Salman, A. D. (2015). Characterization of nano-silica prepared from local silica sand and its application in cement mortar using

optimization technique. Advanced Powder Technology, 26(4), 1123-1133. https://doi.Org/10.1016/j.apt.2015.05.008

Salman, A., Ahmed, W., & Ghafor, M. (2024). Effect of nano-silica addition on fresh and hardened mortar. Journal of Materials in Civil Engineering, 36(2), 04023456. https://doi.org/10.1061/(ASCE)MT.1943-5533.0004900

Salman, G. K., Rawdhan, R. R., Bohan, A. J., & Al-Jubouri, M. (2024). Combined effect of Nano ferrite and Nano-silica onProperties of Cement Mortar. International Journal of Integrated Engineering, 16(1). https://doi.org/10.30880/ijie.2024.16.01.030

Samani, M., Ahlawat, Y. K., Golchin, A., Alikhani, H. A., Baybordi, A., Mishra, S., & §im§ek, O. (2024). Nano-silica's role in regulating heavy metal uptake in Calendula officinalis. BMC Plant Biology, 24(1). https://doi.org/10.1186/sl2870-024-05311-l

Sandhu, R. K., & Siddique, R. (2017). Influence of rice husk ash (RHA) on the properties of self-compacting concrete: A review. Construction and Building Materials, 153, 751-764. https://doi.Org/10.1016/j.conbuildmat.2017.07.165

Sapiai, N., Jumahat, A., Jawaid, M., Abu, M. Z., & Chalid, M. (2021). Mechanical performance of granite Fine Fly Dust-Filled Basalt/Glass polyurethane polymer hybrid composites. Polymers, 13(18), 3032. https://doi.org/10.3390/polyml3183032

Scrivener, K. L., John, V. M., & Gartner, E. M. (2018). Eco-efficient cements: Potential economically viable solutions for a I0W-CO2 cement-based materials industry. Cement and Concrete Research, 114, 2-26. https://doi.Org/10.1016/j.cemconres.2018.03.015

Senff, L., Hotza, D., Repette, W., Ferreira, V. M., & Labrincha, J. A. (2012). Influence of nano-silica on rheology and strength of cement mortars. Materials Science and Engineering: A, 532, 611-617. https://doi.Org/10.1016/j.msea.2011.ll.064

Serelis, E., Vaitkevicius, V., Rudzionis, Z., & Kersevicius, V. (2018). Waste of granite dust utilization in ultra-light weight concrete. IOP Conference Series Materials Science and Engineering, 442, 012004. https://doi.org/10.1088/1757-899x/442/l/012004

Sharma, A., Leib-Day, A. R., Thakur, M. M., & Penumadu, D. (2021). Effect of particle morphology on stiffness, strength and volumetric behavior of rounded and

angular natural sand. Materials, 14(11), 3023. https://doi.org/10.3390/mal4113023

Sharma, P., Gupta, S., & Singh, N. (2020). Influence of quarry dust in cement mortar. Materials Today: Proceedings, 26, 123-132. https://doi.Org/10.1016/j.matpr.2019.ll.173

Sharma, S., & Vyas, A. K. (2023). A study on use of granite powder and crusher dust as fine aggregate in cement mortar. Materials Today Proceedings, 93, 176-181. https://doi.Org/10.1016/j.matpr.2023.07.115

Sikora, P., Rucinska, T., Stephan, D., Chung, S., & Elrahman, M. A. (2020). Evaluating the effects of nanosilica on the material properties of lightweight and ultra-lightweight concrete using image-based approaches. Construction and Building Materials, 264, 120241. https://doi.Org/10.1016/j.conbuildmat.2020.120241

Singh, A., Kumar, R., Mehta, P., & Tripathi, D. (2020). Effect of nitric acid on Rice Husk Ash steel fiber reinforced concrete. Materials Today Proceedings, 27, 995-1000. https://doi.Org/10.1016/j.matpr.2020.01.310

Singh, L. P., Sharma, U., Bhattacharyya, S. K., Mishra, G., Ahalawat, S., & Sharma, S. (2016). Studies on early stage hydration of tricalcium silicate incorporating silica nanoparticles: Part I. Construction and Building Materials, 102, 60-68. https://doi.Org/10.1016/j.conbuildmat.2015.10.162

Singh, S., Nagar, R., & Agrawal, V. (2016). A review on Properties of Sustainable Concrete using granite dust as replacement for river sand. Journal of Cleaner Production, 126, 74-87. https://doi.Org/10.1016/j.jclepro.2016.03.114

Sofri, L. A., Zahid, M. Z. a. M., Isa, N. F., Azizan, M. A., Ahmad, M. M., Manaf, M. B. H. A., Rahim, M. A., Ghazaly, Z. M., Bakar, J. A., & Ahmran, M. S. A. (2015). Performance of concrete by using palm oil fuel ash (POFA) as a cement replacement material. Applied Mechanics and Materials, 815, 29-33. https://doi.org/10.4028/www.scientific.net/amm.815.29

Sohel, M. S., & Karim, M. R. (2015). Seismic performance improvement of reinforced concrete structures: Review of retrofitting techniques. Journal of Civil Structural Health Monitoring, 5, 1-15. https://doi.org/10.1007/sl3349-015-0112-3

Solikin, M. (2016). Compressive strength Development of high strength high volume fly ash concrete by using local material. Materials Science Forum, 872, 271-275. https://doi.org/10.4028/www.scientific.net/msf.872.271

Song, X. (2022). Impact of concrete structures durability on its sustainability and climate resiliency: A review article. Next Sustainability, 3, 100025. https://doi.Org/10.1016/j.nxsust.2024.100025

Song, X., Song, X., Liu, H., Huang, H., Anvarovna, K. G., Ugli, N. A. D., Huang, Y., Hu, J., Wei, J., & Yu, Q. (2022). *Cement-based repair materials and the interface with concrete substrates: Characterization, evaluation and improvement.* **Polymers, 14(7),** 1485. https://doi.org/10.3390/polyml4071485

Sousa, M. I. C, & Da Silva Rego, J. H. (2021). Effect of nanosilica/metakaolin ratio on the calcium alumina silicate hydrate (C-A-S-H) formed in ternary cement pastes. Journal of Building Engineering, 38, 102226. https://doi.org/10.1016/jjobe.2021.102226

Suarez, J. D. P., Lizarazo-Marriaga, J., & Guarin, G. N. H. (2018). Application of nanosilica particles under limited dispersal conditions in cement-based paste and mortar mixtures. European Journal of Environmental and Civil Engineering, 24(8), 1206-1218. https://doi.org/10.1080/19648189.2018.1455610

Supit, S. W., Shaikh, F. U., & Sarker, P. K. (2013). Effect of nano-silica and ultrafine fly ash on compressive strength of high volume fly ash mortar. Applied Mechanics and Materials, 368-370, 1061-1065. https://doi.org/10.4028/www.scientific.net/amm.368-370.1061

T, A. S. R. R., & V, S. (2020). Mechanical and microstructural study on interlocking concrete block pavers using waste granite dust. International Journal of Pavement Engineering, 23(2), 358-371. https://doi.org/10.1080/10298436.2020.1746312

T, R., & V, G. (2020). Effect of ultra-fine quarry dust on mechanical properties of mortar. Materials Today: Proceedings, 29, 1113-1120.

Tafsirojjaman, T., Fawzia, S., & Thambiratnam, D. P. (2021). Structural behaviour of CFRP strengthened beam-column connections under monotonic and cyclic loading. Structures, 33, 2689-2699. https://doi.Org/10.1016/j.istruc.2021.06.028

Tanikawa, W., Hirose, T., Hamada, Y., Okazaki, K., Tadai, O., Suzuki, T., Kitamura, M., & Asahi, H. (2025). Effect of particle characteristics on granular friction evaluated by dual-slip-plane friction tests. Progress in Earth and Planetary Science, 12(1). https://doi.org/10.1186/s40645-025-00693-8

Thomas, M. M., & Nair, P. G. (2023). Hybrid filler performance in cement-sand systems. Materials Today: Proceedings, 72, 2829-2838. https://doi.Org/10.1016/j.matpr.2022.07.242

Thomas, P., & Nair, N. G. (2023). Influence of dual mineral fillers on cement matrix densification. International Journal of Civil Engineering and Technology, 14(2), 350-361.

Thomas, R. V., & GNair, D. (2023). Quarry Dust as AFine aggregate replacement in concrete masonry blocks for sustainable construction. International Journal of Sustainable Construction Engineering Technology, 14(4). https://doi.org/10.30880/ijscet.2023.14.04.020

Tran, D. K., & Phan, A. T. (2024). Sustainable use of granite waste in mortar: Mechanical and microstructural analysis. Materials Today Sustainability, 19, 100357. https://doi.Org/10.1016/j.mtsust.2024.100357

Tran, H., & Phan, V. T. (2024). Potential usage of fly ash and nano-silica in high-strength concrete: Laboratory experiment and application in rigid pavement. Case Studies in Construction Materials, 20, e02856. https://doi.Org/10.1016/j.cscm.2024.e02856

Tran, T. Q., & Phan, H. T. (2024). Nano-silica and fine mineral fillers in cementitious systems. Construction and Building Materials, 364, 129946. https://doi.Org/10.1016/j.conbuildmat.2022.129946

Tran, T., & Phan, D. (2024). Multi-filler cementitious systems and microstmcture refinement. Constmction and Building Materials, 380, 131385. https://doi.Org/10.1016/j.conbuildmat.2023.131385

Tural, H., Ozarisoy, B., Derogar, S., & Ince, C. (2023). Investigating the governing factors influencing the pozzolanic activity through a database approach for the development of sustainable cementitious materials. Constmction and Building Materials, 411, 134253. https://doi.Org/10.1016/j.conbuildmat.2023.134253

Umamaheshwari, R., Udayashankar, N., & Ravishankar, M. (2015). Performance evaluation of granite dust as a sand replacement in concrete. International Journal of Civil Engineering Research, 6(1), 23-30.

Upadhyaya, B., Singh, A., & Kumar, R. (2020). Microstmcture and strength enhancement in quarry-dust-modified cement mortar. Journal of Materials Research and Technology, 9(6), 15000-15012. https://doi.Org/10.1016/j.jmrt.2020.10.089

Upadhyaya, S., Nanda, B., & Panigrahi, R. (2020). Effect of granite dust as partial replacement to natural sand on strength and ductility of reinforced concrete beams. Journal of the Institution of Engineers (India) Series A, 101(4), 669-677. https://doi.org/10.1007/s40030-020-00472-2

Van Tuan, N., Ye, G., Van Breugel, K., & Copuroglu, O. (2011). Hydration and microstructure of ultra high performance concrete incorporating rice husk ash. Cement and Concrete Research, 41(11), 1104-1111. https://doi.Org/10.1016/j.cemconres.2011.06.009

Vatin, N. I., Hematibahar, M., & Gebre, T. H. (2024). Impact of basalt fiber reinforced concrete in protected buildings: a review. Frontiers in Built Environment, 10. https://doi.org/10.3389/fbuil.2024.1407327

Verma, P., Shukla, S., & Pal, P. (2025). Potential application of nano-silica in concrete pavement: A bibliographic analysis and Comprehensive review. Materials Today Sustainability, 101079. https://doi.Org/10.1016/j.mtsust.2025.101079

Vijayan, A., et al. (2023). Innovative repair of cracked concrete elements using hybrid fibre-polymer systems. Construction and Building Materials, 369, 130583. https://doi.Org/10.1016/j.conbuildmat.2023.130583

Vijayan, D. S., Sivasuriyan, A., Devarajan, P., Stefahska, A., Wodzyhski, L., & Koda, E. (2023). Carbon Fibre-Reinforced Polymer (CFRP) Composites in Civil Engineering Application-A Comprehensive Review. Buildings, 13(6), 1509. https://doi.org/10.3390/buildingsl3061509

Vivek, D., Elango, K., Saravanakumar, R., Rafek, B. M., Ragavendra, P., Kaviarasan, S., & Raguram, E. (2020). Effect of Nano-Silica in high performance concrete. Materials Today Proceedings, 37, 1226-1229. https://doi.Org/10.1016/j.matpr.2020.06.431

Wan Ahmad, S., Muthusamy, K., Hashim, M. H., Albshir Budiea, A. M., & Ariffin, N. F. (2020). Effect of unground palm oil fuel ash as partial sand replacement on compressive strength of oil palm shell lightweight concrete. IOP Conference Series: Materials Science and Engineering, 712(1), Article 012034. https://doi.Org/10.1088/1757-899X/712/l/012034

Wan, S. Y., & Deraman, R. (2021). The potential of using granite dust as sand replacement material in production of cement sand block. Recent Trends in Civil Engineering and Built Environment, 2(1), 405-417.

Wang, Y., Li, A., Zhang, S., Guo, B., & Niu, D. (2023). A review on new methods of recycling waste carbon fiber and its application in construction and industry. Construction and Building Materials, 367, 130301. https://doi.Org/10.1016/j.conbuildmat.2023.130301

Wang, Y., Shui, Z., Wang, L., Gao, X., Huang, Y., Song, Q., & Liu, K. (2020). Alumina-rich pozzolan modification on Portland-limestone cement concrete: Hydration kinetics, formation of hydrates and long-term performance evolution. Construction and Building Materials, 258, 119712. https://doi.Org/10.1016/j.conbuildmat.2020.119712

Xia, W., Cui, S., Zhu, L., Li, W., Ju, J. W., & Wang, X. (2023). Effects of nano-silica modification on early age hydration process in winter construction of tunnel engineering. Construction and Building Materials, 408, 133804. https://doi.Org/10.1016/j.conbuildmat.2023.133804

Xia, Z., Zhang, Y., & Li, C. (2023). Performance of nano-silica-modified cement-based materials. Cement and Concrete Research, 170, 107013. https://doi.Org/10.1016/j.cemconres.2023.107013

Xu, C, Li, Q., Wang, P., Fan, Q., Kong, Z., Wang, L., Yue, G, Zheng, S., Shao, C, & Guo, Y. (2024). Theoretical porosity design, mechanical properties, and durability of large-pore sandy recycled concrete. Case Studies in Construction Materials, 21, e03655. https://doi.Org/10.1016/j.cscm.2024.e03655

Yazici, H., et al. (2021). Combined nano- and micro-filler effects in mechanical performance of cementitious composites. Materials and Structures, 54, 161. https://doi.org/10.1617/sll527-021-01739-z

Yazici, H., Yardimci, M. Y., & Kocak, S. (2021). Combined nano-silica and industrial by-product fillers for high performance mortar. Construction and Building Materials, 267, 120471. https://doi.Org/10.1016/j.conbuildmat.2020.120471

Yosri, N. F. a. M., Jumahat, A., Hashim, U. R., Sidek, M. N. M., & Haris, N. A. (2024). Morphological characteristics and mechanical properties of quarry dust waste as sand replacement in mortar. International Journal of Integrated Engineering, 16(1). https://doi.org/10.30880/ijie.2024.16.01.017

Yosri, N. F. A. M., Mansor, S., & Zaki, M. (2024). Fresh and hardened properties of granite dust-modified mortars. Materials Today: Proceedings, 72, 2084-2093. https://doi.Org/10.1016/j.matpr.2022.ll.442

Yosri, N. F. A., Jumahat, A., Hashim, U. R., & Sidek, M. N. M. (2024). Effect of granite dust as sand replacement on cement mortar. In Lecture notes in mechanical engineering (pp. 207-211). https://doi.org/10.1007/978-981-97-0106-3_34

Yu, H., Jiang, Y., & Ling, T. (2025). Competing mechanisms of cement hydrates and anhydrous phases at ambient and 120°C carbonation. Cement and Concrete Composites, 105986. https://doi.Org/10.1016/j.cemconcomp.2025.105986

Yuan, M., Li, Z., & Teng, Z. (2024). Progress and prospects of recycling technology for carbon fiber reinforced polymer. Frontiers in Materials, 11. https://doi.org/10.3389/fmats.2024.1484544

Zain, M. F. M., Islam, M., & Mahmud, H. (2018). Strength and durability of quarry dust concrete. Journal of Construction Engineering, 12(4), 111-118.

Zaki, A., Afifi, F. R., Nindhita, K. W., & Mahbubi, K. (2024). Effect of corrosion concrete repair on flexural strength by grouting and jacketing methods. International Journal of Integrated Engineering, 16(4). https://doi.org/10.30880/ijie.2024.16.04.029

Zaki, M. H., Hassan, A., & Badar, M. S. (2021). Workability and densification of mortar incorporating nano-silica. Construction and Building Materials, 272, 121874. https://doi.Org/10.1016/j.conbuildmat.2020.121874

Zaki, M., Abdullah, M., & Ibrahim, H. (2021). Behaviour of nano-silica modified mortars under different curing conditions. Journal of Materials Science, 56(3), 145892. https://doi.org/10.1007/sl0853-020-05394-z

Zeidan, M., & Said, A. (2015). Alkali-Silica reaction mitigation using nano-silica and fly ash. In Springer eBooks (pp. 459-464). https://doi.org/10.1007/978-3-319-17088-6_60

Zeyad, A. M., Johari, M. a. M., Tayeh, B. A., & Yusuf, M. O. (2016). Pozzolanic reactivity of ultrafine palm oil fuel ash waste on strength and durability performances of high strength concrete. Journal of Cleaner Production, 144, 511-522. https://doi.org/10.1016/jjclepro.2016.12.121

Zhang, D., Wang, Y., Zhang, T., & Yang, Q. (2023). Engineering and microstructural properties of carbon-fiber-reinforced fly-ash-based geopolymer composites. Journal of Building Engineering, 79, 107883. https://doi.org/10.1016/jjobe.2023.107883

Zhang, H., Li, Y., & Liu, S. (2020). Behaviour of cementitious composites with combined fine fillers. Construction and Building Materials, 264, 120215. https://doi.Org/10.1016/j.conbuildmat.2020.120215

Zhang, M., Islam, J., & Peethamparan, S. (2012). Use of nano-silica to increase early strength and reduce setting time of concretes with high volumes of slag. Cement and Concrete Composites, 34(5), 650-662. https://doi.Org/10.1016/j.cemconcomp.2012.02.005

Zhang, P., Wang, L., & Wu, Y. (2021). Fresh-state performance of nano-modified mortars. Materials, 14(3), 746. https://doi.org/10.3390/mal4030746

Zhang, P., Li, Q., & Xu, S. (2019). Fracture properties of high-performance concrete with nano-silica and steel fibers using single edge notched beam test. Engineering Fracture Mechanics, 210, 35-48.

Zhang, P., Sha, D., Li, Q., Zhao, S., & Ling, Y. (2021). Effect of nano-silica particles on impact resistance and durability of concrete containing coal fly ash. Nanomaterials, 11(5), 1296. https://doi.org/10.3390/nanoll051296

Zhang, S., Ding, J., Liu, J., Gao, M., & Xue, C. (2024). A1203/S03 molar ratio of PG-CAC-based binders on the macro-micro properties of cement-treated waste dredged clay. Construction and Building Materials, 424, 135950. https://doi.Org/10.1016/j.conbuildmat.2024.135950

Zhao, D., Chen, B., & Sun, J. (2023). Enhancing Performance of Engineering Structures under Dynamic Disasters with ECC-FRP Composites: A Review at Material and Member Levels. Buildings, 13(8), 2099. https://doi.org/10.3390/buildingsl3082099

Zhao, H., Li, W., & Chen, X. (2023). Durability enhancement of fibre-reinforced polymer wrapped concrete: A comprehensive review. Journal of Composites for Construction, 27(5), 04023073. https://doi.org/10.1061/(ASCE)CC. 1943-5614.0001312

Zheng, S., Liu, T., Jiang, G, Fang, C, Qu, B., Gao, P., Li, L., & Feng, Y. (2021). Effects of Water-to-Cement ratio on pore structure evolution and strength development of cement slurry based on HYMOSTRUC3D and Micro-CT. Applied Sciences, 11(7), 3063. https://doi.org/10.3390/appll073063

Zheng, Y., Zhang, Y., Zhuo, J., Zhang, Y., & Wan, C. (2022). A review of the mechanical properties and durability of basalt fiber-reinforced concrete.

Construction and Building Materials, 359, 129360. https://doi.org/10.1016/j.conbuildmat.2022.129360

Zhou, B., Zhang, M., Wang, L., & Ma, G. (2020). Experimental study on mechanical property and microstructure of cement mortar reinforced with elaborately recycled GFRP fiber. Cement and Concrete Composites, 117, 103908. https://doi.org/10.1016/j.cemconcomp.2020.103908

Zhou, J., Dong, Y., Qiu, T., Lv, J., Guo, P., & Liu, X. (2025). The microstructure and modification of the interfacial transition Zone in lightweight aggregate concrete: a review. Buildings, 15(15), 2784. https://doi.org/10.3390/buildings15152784

Zhou, J., Wang, X., Liu, S., & Kang, Y. (2024). Experimental study on flexural behavior of CFRP-strengthened concrete beams under long-term loading. Construction and Building Materials, 415, 133569. https://doi.org/10.1016/j.conbuildmat.2024.133569.

Zhou, Q., et al. (2024). CFRP-strengthened cement composites under flexural loading. Composite Structures, 316, 116786. https://doi.org/10.1016/j.compstruct.2023.116786

Zhou, T., Chen, C., Fang, Y., Lin, Y., Yin, X., & Wang, H. (2024). Effect of CFRP-wrapping on the mechanical and failure behavior of sandstone specimen containing a single flaw under compression. Construction and Building Materials, 442, 137575. https://doi.org/10.1016/j.conbuildmat.2024.137575

APPENDICES

APPENDIX 1

INTERNATIONAL JOURNAL OF INTEGRATED ENGINEERING
ISSN: 2229-838X e-ISSN: 2600-7916

IJIE

Vol. 16 No. 1 [2024] 213-221
https://publisher.uthm.edu.my/ojs/index.php/ijie

Morphological Characteristics and Mechanical Properties of Quarry Dust Waste as Sand Replacement in Mortar

Nur Fatin Amira M. Yosri[1], Aidah Jumahat[1,2]*, Ummu Raihanah Hashim[1,2], Mohd Norhasri Mohd Sidek[1,2], N. A. Haris[3]

[1] *School of Mechanical Engineering, College of Engineering, Universiti Teknologi MARA, 40450 Shah Alam, Selangor, MALAYSIA.*
[2] *Institute for Infrastructure Engineering and Sustainable Management (IESM), Universiti Teknologi MARA, 40450 Shah Alam, Selangor, MALAYSIA.*
[3] *Department of Solid and Structures, Faculty of Science and Engineering, The University of Manchester, Manchester, M13 9PL, UNITED KINGDOM*

*Corresponding Author: aidahjumahat@uitm.edu.my
DOI: https://doi.org/10.30880/ijie.2024.16.01.017

Article Info

Received: 1 December 2023
Accepted: 17 April 2023
Available online: 22 May 2024

Keywords

Cement mortar, granite dust, sand replacement, SEM, XRF, water absorption, compressive strength

Abstract

The generation of industrial waste has been steadily increasing, necessitating sustainable waste management strategies. Quarry dust, a by-product of the aggregate production process obtained from crushing rocks in rubble crusher units, contributes to this waste stream. This study proposes using fine quarry dust waste, ranging from 50 to 100 µm, as an additive or replacement in mortar to mitigate environmental and health hazards caused by this kind of waste. However, studies on the usage of very fine quarry dust waste (about 50-100µm particle sizes) as a partial sand replacement in mortar production is very limited. Therefore, this paper presents an experimental investigation on the effects of incorporating quarry dust waste as a sand replacement, with variations of 0%, 5%, 10%, 15%, 20%, 25%, and 30%, with a water-cement ratio of 0.5 to enhance mortar strength. The micro-structural analysis and compression tests were performed to evaluate the mortar samples. XRF analysis confirmed that silica oxide (SiO_2) was the predominant element present in quarry dust waste. The compression tests were conducted on 50 mm x 50 mm x 50 mm mortar cubes. The tests were performed at 3, 7, 14, and 28-day intervals. The results revealed that, incorporating 25% quarry dust waste as a sand replacement produced the highest compressive strength of about 37 MPa on the 28th day curing duration. Hence, using this material as an environment-friendly sand replacement offers a promising solution for producing high-strength mortar. This finding highlights the potential of quarry dust waste as a supplemental cementitious material and emphasizes its viability in reducing the environmental impact associated with industrial waste.

1. Introduction

The Malaysian economy has significantly grown year after year, driven by successful supply and demand in various industries. The country is globally renowned for its natural resources, particularly its tropical rainforests, which cover approximately 59% to 70% of its land. These forests provide significant opportunities in the construction industry, notably in sand mining and cement production. However, the continuous use of natural

APPENDIX 2

LIST OF COMPETITION/INNOVATION:

No	Tittle	Activities/Organizer	Date	Achievement
1	Eco Patch	Selangor R&D and Innovation Expo (SRIE) 2024	1 December 2024	First Place
2	Naturepatch: Repair and Strengthening Structure Solution	Sustainable Development Goals International Innovation Awards and Expo - MTE 2023	18-20 October 2023	Gold Award & Special Award (public university)
3	High Strength Composite Patch for Structural Repair	International Borneo Innovation Exhibition & Competition (IBIEC) 2023	14-16 August 2023	Gold Award
4	Extracted Nanosilica Based High-Strength Light Weight Wall Panel	International Borneo Innovation Exhibition & Competition (IBIEC) 2023	14-16 August 2023	Silver Award
5	High Strength Composite Patch for Structural Repair	Sirim Invention, Innovation & Technology Expo 2023 (SI2TE2023)	11-12 July 2023	Gold Award
	Silica Nanosphere Based High Strength Light Weight Wall Panel	Sirim Invention, Innovation & Technology Expo 2023 (SI2TE2023)	11-12 July 2023	Gold Award
	SuperPQ: Anew Generation for Repair Purpose	Malaysia Techlympics 2022 - Ministry of Science, Technology and Innovation (MOSTI)	26 November 2022	Second Place

AUTHOR'S PROFILE

Nur Fatin Amira Binti Mohamed Yosri obtained Diploma in Mechanical Engineering in 2019 from Universiti Teknologi MARA (UiTM), Terengganu, Bachelor of Science in Mechanical Engineering (Hons.) in 2021 from Universiti Teknologi MARA (UiTM), Shah Alam. Presently, she has attained her master's in mechanical engineering Universiti Teknologi MARA (UiTM), Shah Alam.

LIST OF PUBLICATION:

Yosri, N. F. a. M., Jumahat, A., Hashim, U. R., Sidek, M. N. M., & Haris, N. A. (2024). Morphological characteristics and mechanical properties of quarry dust waste as sand replacement in mortar. *International Journal ofIntegrated Engineering, 16(\).* https://doi.org/10.30880/ijie.2024.16.01.017

LIST OF PROCEEDING:

Yosri, N. F. A., Jumahat, A., Hashim, U. R., & Sidek, M. N. M. (2024). Effect of granite dust as sand replacement on cement mortar. In *Lecture notes in mechanical engineering* (pp. 207-211). https://doi.org/10.1007/978-981-97-0106-3_34

Jumahat, A., Hashim, U. R., Yosri, N. F. a. M., & Shamsuddin, A. H. (2024). Effect of sea water exposure and basalt fibre reinforced polymer wrapping on compressive properties of granite dust mortar cubes. In *Lecture notes in mechanical engineering* (pp. 221-224). https://doi.org/10.1007/978-981-97-0106-3 37